THE RNA HELICASE DED1 INTEACTS WITH CELL CYCLE COMPONENTS AND OTHER KEY PROTEINS DURING CELLULAR STRESS

By

Sara Brooke Carey

A Dissertation Submitted to the Faculty of the

DEPARTMENT OF MOLECULAR AND CELLULAR BIOLOGY

In Partial Fulfillment of the Requirements

For the Degree of

DOCTOR OF PHILOSOPHY

In the Graduate College of

THE UNIVERSITY OF ARIZONA

2023

THE UNIVERSITY OF ARIZONA
GRADUATE COLLEGE

As members of the Dissertation Committee, we certify that we have read the dissertation prepared by: Sara Carey

titled: The RNA Helicase Ded1 Interacts with Cell Cycle Components and Other Key Proteins During Cellular Stress

and recommend that it be accepted as fulfilling the dissertation requirement for the Degree of Doctor of Philosophy.

Andrew Capaldi — Date: Aug 17, 2023

Ross Buchan
Ross Buchan (Aug 17, 2023 15:26 PDT)
Ross Buchan — Date: Aug 17, 2023

George Sutphin — Date: Aug 10, 2023

Timothy A. Bolger — Date: Aug 14, 2023

Date:

Final approval and acceptance of this dissertation is contingent upon the candidate's submission of the final copies of the dissertation to the Graduate College.

I hereby certify that I have read this dissertation prepared under my direction and recommend that it be accepted as fulfilling the dissertation requirement.

Timothy A. Bolger — Date: Aug 14, 2023

Timothy A. Bolger
Department of Molecular and Cellular Biology

ACKNOWLEDGEMENTS

Graduate school has been something I have dreamed of completing since I started college. Every professor, friend, significant other, colleague, and family member that has helped me through this very long journey is appreciated more than they will ever truly know. There is no way I could possibly list each and every one of those people. There are a few people I would like to specifically acknowledge though.

Firstly, I would like to thank my advisor Dr. Timothy Bolger. I can only assume that is has not always been easy for him to guide me through the struggles of graduate school and life, but he did it with kindness and patience. I have learned so much about being a scientist and a person from you, so thank you from the bottom of my heart.

Labs are a unique place to grow and build as a scientist and I would like to thank the Bolger lab members who have been a pleasure to work with for always being my encouragement when times have been tough. Particularly I would like to thank Telsa, Peyman, David, Akanksha, Ashwin, and Paolo. You all have meant so much to me and have helped me grow tremendously.

As well, I would like to thank my current and former committee members Dr. Ross Buchan, Dr. Andrew Capaldi, Dr. George Sutphin, and Dr. Daniela Zarnescu. You guys never gave up on me and pushed me to make models even when I didn't want to.

I would also love to thank my family for constantly supporting me in my desire to perpetually be a student. Thank you to my siblings and for always showing up when I needed them. Thank you to my nieces and nephews for reminding me to be a kid. Most of all, thank you to my parents Dennis and Barbara Carey for raising me to be a bold woman who follows her dreams. Also, thank you Grandpa for always asking about my work and pretending to understand what I do. Love you guys.

I would also like to thank the friends I've made in Tucson who have become family: Kathleen, Ile, Joey, Aaron, Rachel, David, Akanksha, Nicole, Kamran, Chloe, Scott, Brandon, Aspen, Peyton, and countless others. Without y'all I'd be a mess, not even a hot one. I love you so much.

Lastly, thank you Molly and Serenity for being the best dogs a girl could ask for. Your cuddles and pets really got me through the hard times.

TABLE OF CONTENTS

ABSTRACT

DEAD-box RNA helicases regulate each stage of the RNA life-cycle during gene expression. Ded1 is an essential yeast DEAD-box protein that regulates translation initiation through its effects on mRNA secondary structure and formation of pre-initiation complexes. Ded1 binding to mRNA is not sequence specific, and therefore, it relies on interaction partners for its specificity and regulatory activities during initiation.

Stress conditions require large-scale changes in translation that upregulate certain stress response genes but repress most other nonstress-related genes. The target-of-rapamycin (TOR) pathway is a major regulator of these changes, and we have found that Ded1 is a critical mediator of this stress response. Interestingly, in contrast to its role in promoting translation initiation in pro-growth conditions, Ded1 plays an active role in repressing translation upon TOR inactivation. My work focuses on further characterizing the currently unknown interactions critical for Ded1's repressive function during cellular stress. My results support a physical interaction between Ded1 and Cdc28 in stress conditions that is absent in normal growth conditions, and follow-up results suggest that this interaction may help to coordinate the cell cycle and translation during stress.

Along with this clear connection to Cdc28, I conducted a large-scale screen that also shows connections of Ded1 with ATP transport, stress granule formation, cellular localization, cellular trafficking, and mitochondrial translation. All of these could play a key role in understanding how Ded1 fits into the larger picture of translational regulation during TOR inactivation and each subset seen in the annotated GO terms could be an individual area of study for future understanding of stress responses and translation.

EXPLANATION OF THESIS STRUCTURE

My work focuses on understanding how the DEAD-box RNA helicase Ded1 is able to modulate its function between initiating translation and repressing translation. The initiation aspects of Ded1 have been previously studied and for the most part are generally understood and accepted. However, the relationship between Ded1 and the repression of translation and how ded1-ΔCT is able to overcome growth inhibition are less understood. In all aspects of my work I set out to identify potential co-conspirators of Ded1 and was able to elucidate that Ded1 has a clear and direct connection to the regulation of the cell cycle. The progression of each of these chapters begins as a large data mining screen that ends in the evaluation of direct partners interacting with Ded1. It will be shown that *DED1* has genetic connections to large amounts of proteins varying in function in Chapter 2 and that it has a very clear ability to work with Cdc28 to alter growth patterns in Chapter 3. Put together, my work opens up an unexplored avenue for understanding how translation factors, specifically Ded1, affect quiescence and the cell cycle.

CHAPTER 1: INTRODUCTION

1.1. RNA HELICASES AND THEIR ROLES IN LIFE

RNA metabolism is a process that is essential for all life. The most common processes that RNA is known to be involved in are the various steps of gene expression, including transcription, translation, and splicing (1). These processes require that the RNA involved is folded into specific three-dimensional conformations and associate with proteins and other molecules (2). However, these conformations must also occur in a timely enough manner to assist with the specific process for which they are needed. These necessary conformations are not always the first state the RNA is folded into. In fact, there can be many different kinetically or thermodynamically stable conformations between the first state achieved by RNA and the state needed for function. Through interactions between RNA and different RNA binding proteins, assemblies called ribonucleoproteins (RNP's) are created. These RNP's are needed to carry out the steps of gene expression, and also allow for the stabilization of the RNA molecules to help transition the structure between conformational states until the needed one is formed. This "RNA chaperone" ability of RNP's ensure that a functional conformation is achieved in a timely enough manner to help in the correct process (3).

In vivo these interactions between RNAs and between RNA and RNA binding proteins are mostly facilitated by something called RNA helicases. These ATP dependent helicases are responsible for altering the RNA-RNA and/or RNA-protein interactions formed, thus serving as both RNA and RNP chaperones. RNA helicases consist of superfamilies 1-6 (4,5). Most eukaryotic RNA helicases fall into either superfamily 1 or 2. All members of these superfamilies contain conserved helicase core domains called RecA-like (6). Within superfamily 2 is a large set of RNA helicases referred to as DEAD-box RNA helicases. These helicases consist of a

conserved D-E-A-D amino acid sequence in motif II of their core domain, which is essential for their function. DEAD-box proteins (DEAD-box proteins) are the most abundant subclass of RNA helicases with 26 types in Saccharomyces cerevisiae and 37 in humans (7).

1.2. DEAD-BOX RNA HELICASES

DEAD-box RNA helicases are required for a variety of processes through the cell. These processes included pre-mRNA process, transcription, ribosome biogenesis, nuclear mRNA export, translation initiation, organelle function, and general RNA turnover (8). DEAD-box proteins usually function as an assembly where multiple DEAD-box proteins with varying specificity together with other factors work together to create a functional unit such as the spliceosome or translational machinery. Most DEAD-box proteins have similar enough sequences within their core domains and the structures that have been solved show enough conservation that the assumption is that all DEAD-box proteins would have similar structures (9). This is true regarding the conserved helicase core but is differential between different DEAD-box proteins and what exists of their crystal structures.

The conserved helicase core of DEAD-box proteins consists of two RecA-like domains that are where RNA and ATP have known binding sites (10, 11). Within this core there are also three functional categories for binding ATP, RNA, and the interaction between these two binding regions. The ATP binding portion of this core can be described as a binding cleft (12). As for the portion of the core responsible for binding RNA, the affinity of the core is for the sugar-phosphate backbone of RNA (up to 5 nucleotides), causing this affinity to lack sequence specificity in binding. As well the binding affinity for RNA is greatly increased by ATP and drops substantially following ATP hydrolysis (14,15). This core is preceded and followed by a

less structured N-terminal and C-terminal region, respectively. These two sections are not as well conserved between DEAD-box proteins and are where the specificity of DEAD-box proteins is established.

DEAD-box proteins separate RNA duplexes in a manner that is unique from that of DNA helicases. DEAD-box proteins use local strand separation that is independent of unwinding polarity (61). Local strand separation entails that the DEAD-box protein binds directly to a single strand of the RNA duplex (or to ssRNA in an RNA-protein complex) and through conformational changes causes the bound RNA to crimp or bend. This allows for a few of the base pairs to separate which can result in the destabilization of the duplex resulting in the rest of the base pairs dissociating (14,16). Interestingly, the binding of the ATP is sufficient for this unwinding, and it is not until RNA release is needed that the ATP must be hydrolyzed (13), making continued hydrolysis only necessary for repetitive unwinding. Due to this type of local strand separation unwinding, the ability of DEAD-box proteins to unwind RNA duplexes decreases as the size and/or stability of the duplex increases. In-vivo most RNA duplexes that must be separated are 10-12 base pairs long, making the ability of DEAD-box proteins good enough to act in this capacity (9). Further evidence to support that DEAD-box proteins are the preferred method for this type of unwinding is that for most of the DEAD-box proteins studied, a single stranded portion of RNA adjacent to the duplex increases the unwinding activity of DEAD-box proteins.

Along with unwinding RNA duplexes, there are some DEAD-box proteins that are also responsible for protein disassociation from mRNPs. This action of protein disassociation is ATP-driven and is independent of RNA structure. This would mean that the removal of proteins from RNA by use of DEAD-box proteins is enzymatically unique and not merely just a result of the previously described duplex unwinding (17). Taken together DEAD-box proteins are a unique

subset of RNA remolding enzymes that should be further evaluated for the various roles in a multitude of complex processes.

1.3. DED1 - DEAD-BOX RNA HELICASE

One unique subset of the DEAD-box RNA helicase family is the Ded1/DDX3 subfamily that is conserved from yeast to humans. This subfamily has high sequence conservation within the helicase core domain while N-terminal domain and C-terminal domain less so (18). Every eukaryote that has been sequenced to date has been shown to have at least one member of the Ded1/DDX3 subfamily. This, along with their known connection to various diseases, cancer, and viral infection, have made them into one of the most well studied subfamilies of DEAD-box helicases. Although there exist a DDX3X and DDX3Y that are encoded on the X and Y chromosomes respectively, it is primarily the human ortholog of *DDX3X* has been studied for its connection to disease. Although there are mutations in *DDX3Y*, these have primarily been linked to fertility issues (19). DDX3X has been shown to be involved intimately in medulloblastoma cancer. It has been found to be the second most frequently mutated gene in this cancer just after beta-catenin (20, 21). Throughout this cancer type, there have been numerous variants of *DDX3X* found. It is still debated if the mutations have an oncogenic effect or tumor suppression effect. Regardless of this, some of these effects must be related to protein translation (18, 22, 23). Uncontrolled cellular growth is the most defining feature of cancer, thus making it intriguing that DDX3X's role in translation has also been connected to cell cycle progression and stress response (24, 25).

S. cerevisiae contains two Ded1/DDX3 subfamily proteins. *DED1* is the essential of these two and *DBP1* is the non-essential (26, 27). *DED1* (*Definition of Essential Domain 1*) cleverly

received its title by being one of the first proteins discovered in *S. cerevisiae* where the disruption of the Open Reading Frame (ORF) resulted in lethality (28). Since its discovery it has served as a useful tool in studying the biochemical activities of DEAD-box proteins (18). On a more basic level, Ded1 is a 604 amino acid long polypeptide and has a molecular weight of about 65kDa. The helicase core shows a large conservation of amino acids while both terminal ends of the protein are unique. These terminal ends are both considered low complexity domains and although they have not been resolved in crystal structure, are predicted to be mostly disordered. These terminal ends are where it is thought the most can be learned about Ded1 and its roles in various functions. Through various interactions with distinct factors on either of the terminal ends, studies have shown that Ded1's effects of initiating translation can be modulated or even reversed. (29, 30). Research has shown that Ded1's functions stretch beyond just helicase activity but also can include RNP remodeling, AMP sensing, and strand annealing activity (31, 32, 33). The aforementioned functions are primarily molecular in nature and are more clearly understood. I will focus my study on are Ded1's role in cellular processes that alter its function such as cell cycle progression and quiescence.

Ded1 has a clearly defined role in translation initiation. For instance, when catalytically mutated versions of *ded1* were studied it was seen that there was an increase in non-translating 80S monosomes, a decrease in polysomes, and overall, a reduction in protein synthesis demonstrating a lack of translation initiation. (26, 27). Physical interactions of Ded1 further solidify this role in translation initiation. Ded1 has been shown to interact with eIF4F complex (27, 34, 35). The complex of eIF4F contains eIF4G, the cap binding protein of eIF4E and eIF4A, also a DEAD-box protein. This entire complex forms on the capped portion of the mRNA and is what allows for recruitment of the 43S preinitiation complex (PIC) and then forms the 48S PIC.

Ded1 has been found to contribute to PIC assembly formation through interactions between its NTD and eIF4E and eIF4A as well as its CTD with eIF4G. Removing any of the interactions of Ded1 with the 5'UTR portion of the mRNA alters ability of cells to initiate translation (69,70). All of this must occur before the mRNA can even begin to be scanned for the AUG start-site. At this point Ded1 can facilitate the unwinding of any secondary RNA duplexes that may be preventing the continuation of start site scanning. (34, 30, 36). Although this interaction is key for the initiation of translation, studies have also shown it might be key for a specific function of repression of translation through Ded1 and its potential to bind to other proteins. Previous evidence has shown that a lack of activity of Ded1 through various methods causes the scanning PIC to stall at near-cognate bases, initiating at these locations instead of the main ORF AUG (37). This feature provides more evidence that Ded1 is more than just a stimulator of translation, but a gatekeeper that controls start site selection and timing.

As previously discussed, when looking at the binding affinities of Ded1, it was detailed that Ded1 only has a general specification for RNA backbone; however, studies have shown that some mRNAs are more affected by *ded1* mutants than others. Specifically, there are about 600 mRNAs in yeast that are dependent on Ded1 activity (38). These mRNAs typically have a longer, more structured 5'UTR. It is believed that this larger, more complex structure makes these mRNAs more in need of assistance unwinding duplexes in their 5'UTR structure. It is possible that this increased need for Ded1 could be a result of a general increase in DEAD-box helicase activity in general. However, when the other important DEAD-box helicase translation initiation factor eIF4A was evaluated in similar ways, these same mRNAs were not identified (36). These results have led to the conclusion that these DEAD-box helicases operate together in the creation of the eIF4F complex, but after PIC assembly they act in different capacities and

have important functional differences between their helicase activity, Ded1 specifically having the activity needed to unwind 5'UTRs and structured duplexes within the 5'UTR and eIF4A not. Although the mechanisms behind the initiation of translation and the helicase activity of Ded1 are better understood, there are supported observations in the field that Ded1 may play an active role in translation repression as well. It is known that during specific types of stress like sodium azide treatment or glucose deprivation Ded1 and other translation factors join into aggregates of stalled mRNPs known as stress granules (34, 39). When Ded1 is overexpressed, it is seen that these aggregates form more readily and growth defects occur due to translation repression. This model is referred to as the "gatekeeper" model for Ded1. In this model Ded1 acts as it normally does, forming an mRNP with the early factors of translation initiation, but it is somehow stalled at this stage. The only way to remove these stalled mRNPs would be to hydrolyze ATP. If this ATPase function does not occur, specific domains of Ded1 are able to self-aggregate and form stress granules, stalling translation in its tracks (34). Since the C-terminal portion of Ded1 is essential for its binding to eIF4G, it could be postulated that this is the key component for self-aggregation and stalling. However, studies of different mutants have not been able to create a clear link between Ded1 overexpression, translation repression, and stress granule creation. This means that the model for how Ded1 driven translational repression is executed likely requires revision.

Taking this along with previous work showing that repression can occur without these stalled mRNPs aggregates, it is most likely that the change in Ded1 function occurs before this initial 48S PIC step in translation initiation. This means that is also likely independent of its ability to cause stress granules to form (40). All of this leaves open a key question of how stress

can alter Ded1's ability to initiate translation so that it is able to now inhibit translation, independent of already known systems of inhibition like stress granules.

1.4. TOR SIGNALING PATHWAY

Cells must be able to take a large array of inputs about nutrient availability and potential stress conditions and synthesize those inputs into clear cellular responses. Being able to adapt to the environment of a cell and determine when growth and proliferation are necessary versus when a cell should remain dormant are essential decisions that can alter the success of each individual cell. The ability to do these things is also what keeps a cell from growing without cause and therefore becoming cancerous. One of the main hubs for determining these fates of cells is the Target of Rapamycin signaling pathway (TOR), named after its phenotype of being rendered inactive when in contact with the drug rapamycin. There are complexes of TOR. TOR Complex 1 (TORC1) and TOR Complex 2 (TORC2) are both made of similar components, but each specializes in its own unique set of inputs and outputs for the cell. TORC2 is rapamycin insensitive and is responsible for the regulation of the cytoskeleton and cell polarity (41). TORC1 is responsive to rapamycin and consists of the following components: Lst8, Kog1, Tco89, and TOR1/TOR2. TORC1 is a singling hub that can sense nutrients and then control growth (42). When rapamycin is introduced into the system it is able to inhibit TORC1 by forming a complex with FKBP which does not normally have a function with TORC1 (43). This complex of rapamycin and FKBP bind to TOR and inhibit it.

With TORC1 being the main hub for nutrient sensing in eukaryotic cells, it has the ability to regulate growth and metabolism by altering the expression of hundreds to thousands of genes using a combination of transcription, translational, posttranscriptional, and posttranslational

mechanisms (41, 44-48). It has already been established that TORC1, during stress, downregulates global translation and protein synthesis while simultaneously upregulating stress response genes as a means to conserve cellular materials and promote cell survival (49-53). This overall process is completed by two methods that alter translation initiation. The most well conserved of these methods is the phosphorylation of eukaryotic initiation factor 2 alpha (eIF2α) which then inhibits the 48S PIC assembly. More specifically, after treatment with rapamycin in *S. cerevisiae*, eIF2α is phosphorylated at Ser51 by Gcn2 (54). Phosphorylated eIF2α can now act as a competitor for GDP bound eIF2α with its guanine exchange factor. This competition leads to the eventual decrease in GTP recycling for eIF2α and eventual decrease in ternary complex production and thus PIC assembly and translation initiation. In terms of non-drug induced stress, this same process occurs when Gcn2 activity is altered due to uncharged tRNA abundance increasing as amino acids become scarce. This function of Gcn2 is directly related to TORC1 signaling due to the phosphorylation event that occurs at Ser577 when amino acids become scarce (44). The aforementioned method accounts for how global translation is reduced during times of nutrient deprivation or stress, but at the same time as this downregulation, very specific upregulation of survival genes is occurring. One of the most understood examples of this type of upregulation of stress response genes is *GCN4*, a transcription factor for amino acid biosynthesis (50, 55, 56). In normal growth conditions *GCN4* is expressed at low levels since a regulatory uORF is more commonly translated. However, when nutrients become scarce and the above mechanisms are implemented by the cell the small ribosomal subunit can spend more time scanning along the transcript for *GCN4* where the ORF is found and translated in much higher quantities making it an increased protein during stress conditions.

The second mechanism that works to alter translation initiation is in mammals and involves eIF4E binding proteins (4E-BPs) interacting with eIF4E and repressing translation (49, 51, 52, 57). In normal conditions 4E-BPs are phosphorylated by TORC1, which reduces their affinity for binding with eIF4E and allows for translation to occur naturally. However, during TORC1 stress, such as nutrient deprivation, these 4E-BPs become rapidly dephosphorylated and begin to bind to eIF4E. This binding limits available eIF4E for eIF4G to bind to, thus resulting in the downregulation of translation. Although there are a couple of genes in *S. cerevisiae*, *EAP1* and *CAF20*, that seem to contain similar motifs as those of canonical 4E-BPs, there has not been substantial evidence to validate the claim that they act the same way as 4E-BPs (27, 58, 59).

Although it has long been known that TORC1 is directly involved in the repression of translation through these methods, recent evidence from this lab has shown that Ded1 has an active role in the response to translational control during TORC1 inactivation. When assessing *ded1* mutants that lack the ability to receive signals from TORC1 a global reduction of translation is not seen to the same degree as with Ded1. In addition, alterations in degradation of eIF4G and Ded1 were observed, showing that Ded1 must have its C-terminal domain fully intact to respond to TORC1 and stop translation effectively to conserve resources (60). Overall, this data suggested that a major mechanism of Ded1 function during stress is to dissociate eIF4G from translation complexes and promote its degradation, thus reducing general translation in these conditions.

Other studies have shown that the presence of a C- terminus is fundamental for Ded1's function. When this low complexity domain is removed from Ded1, even with overexpression, the cells were suppressed during times of oxidative stress. This alteration from the previously seen ability of *ded1-ΔCT* cells to essentially ignore stress implies that outside of interaction with

the eIF4G mediated stress response, Ded1 has a unique stress response mechanism that is most likely connected to the C-terminus being able to oligomerize with itself (71).

1.5. CELL CYCLE

One of the most fundamental biological processes in for life is the cell cycle due to its contribution to the growing and reproduction of organisms. The cell cycle is a tightly regulated sequences of events that leads to the duplication of one mother cell to two identical daughter cells. In this process, not only is the genetic material duplicated, but all proteins and essential organelles are copied as well. This means that not only is it important to understand the transcriptional and proteomic levels associated with the cell cycle, but it is also important to understand how translation is affected during each phase.

The cell cycle consists of two major phases: interphase where the cell is able to grow and carry out its normal function, and mitosis where the cell actually goes through division. Interphase is composed of three subphases: Growth 1 (G1), Synthesis (S), and Growth 2 (G2). Each sub phase is controlled by a series of cyclins and cyclin dependent kinases. In *S. cerevisiae*, there is a master regulator kinase known as Cdc28. It is most homologous to Cdk1 in humans. This kinase, through binding with different partners, is able to facilitate the movement of the cell into different stages of the cell cycle. For instance, if Cdc28 interacts with Clb5 and/or Clb6, this promotes the movement of the cell from G1 into S (63). Once completing interphase, cells continue through mitosis, which is a rapid process and cannot be stopped once started (64). When cells lose the ability to regulate when they should progress to the next phase and when they should stall various disease can occur, most famously uncontrolled growth or cancer (65). Another interesting component of the cell cycle is something known as quiescence or Growth 0 (G0) phase. This phase is often referred to as a dormant state that cells enter into, with the

capacity to exit from, when resources are scarce, or division is not needed (66). It is vital for cells to be able to orchestrate the switch in and out of this state as necessary, and when this mechanism is disrupted cell's fates are poor. Most often G0 is depicted as a state that occurs from G1, but some studies have shown that this state can also occur from G2 phase (67). The basic requirement for this state to occur is for the cell to not meet a threshold or checkpoint for continuing on to the next phase. This could be that genetic material has not been properly organized, organelles have not been copied, or something else has occurred that would cause the division to result in death of one or more of the daughter cells (63).

Interestingly TOR has a known connection to the cell cycle. It has been shown that an inactivation of TOR due to environmental changes for the cell causes a signaling cascade that facilitates the shuttling of cells from G1 into G0 when checkpoints are not met. This same signaling has been shown to work in blocking the transition of cells from G2 to M. This allows the conclusion to be made that obviously enough the cell cycle is directly affected by stress responses in the cell (68).

CHAPTER 2: UNBIASED SYNTHETIC GENETIC ARRAY TO IDENTIFY ESSENTIAL COMPONENENTS THAT MODULATE THE DED1 RESPONSE TO RAPAMYCIN

2.1. EXPLANATION OF PAPER

The connection between Ded1 and its ability to modulate the initiation and repression of translation in respect to changes in the extracellular environment was heavily theorized to be controlled by some form of protein partner. Although other options for control do exist, such as posttranslational modifications, previous work within the lab had ruled out the few phosphorylation sites present on Ded1 that were known to be altered in TOR mediated stress. In an effort to look beyond these modifications, an unbiased synthetic genetic array was completed to establish if and what non-essential proteins had the ability to modulate Ded1's ability to respond to stress. This screen was completed by comparing wild-type cells to a *ded1* mutant lacking the C-terminal domain. Each strain was crossed with the complete yeast library of non-essential gene knockouts. From here, growth was evaluated in the absence and presence of rapamycin to detect which combinations altered known phenotypes of *ded1-ΔCT*. These results were then compiled to create an array of potential protein partners capable of assisting with the modulation of Ded1's effect in TOR mediated stress. Paper to follow in Appendix A.

CHAPTER 3: DED1 PHYSICALLY INTERACTS WITH A KEY COMPONENT OF THE CELL CYCLE ALTERING ITS GENERAL RESPONSE TO RAPAMYCIN TREATMENT

3.1. INTRODUCTION TO PROJECT

Previous work in the lab had established that although posttranslational modifications were not out of the question as to what could be modulating the role of Ded1 from initiating translation to repressing translation, as no functional changes were seen when previous post-translational modifications were tested, other approaches for altering protein function should be addressed as well. Since it has previously been established that interactions with initiation factors modulate the ability of translation to occur (71), it could be concluded that an interaction between Ded1 and some unknown protein could be what is causing this shift in functionality. To attempt to elucidate what protein could potentially be changing this function or possibly what other functions and processes are affected by Ded1 a physical interaction screen was conducted to evaluate novel proteins interacting with Ded1 during TOR inactivation or stress.

3.2. RESULTS

IP-MS of Ded1 identifies cell cycle regulatory protein interactions under rapamycin stress

A Ded1 immunoprecipitation (IP) and mass spectrometry (MS) analysis was conducted on cellular samples to assess if any Ded1-interacting protein changed significantly in relative abundance during a treatment of rapamycin, and therefore TOR inactivation. *S. cerevisiae* cells containing a singular copy of *DED1* tagged with *GFP* were initially grown in YPD overnight.

These cultures were then back diluted and grown to a concentration of about 0.5 OD_{600}. From here an untreated control sample was collected and processed to isolate cellular content and keep proteins within them from being naturally broken down. The initial culture was then treated with 200 ng/ml of rapamycin, and samples were taken from it after 30 minutes, 1 hour, 2 hours, and 4 hours of rapamycin treatment. These samples were processed just as the untreated sample was.

The lysates from each time point were then put through a rigorous co-immunoprecipitation assay prep. This preparation consisted of first conjugating magnetic Dynabeads to an anti-GFP antibody. This conjugated Dynabead would then be able to interact with and isolate any protein or molecule tagged with GFP. The Ded1 C-terminal tag allowed the conjugated Dynabead to bind Ded1, isolating it from the lysate sample. While Ded1 is being pulled out from the lysate, any proteins interacting directly with Ded1 are also isolated from the solution as well. These coimmunoprecipitation samples were then run on an SDS-PAGE gel, silver stained, and assessed for changes in protein bands at different time points. At 2 hours of rapamycin treatment, bands were repeatedly seen appearing that did not occur in other time points (Figure 1). On this gel, other bands can be identified besides those of just Ded1 (as labeled on the figure) and the portion that was cut out for evaluation. The top most band on the gel, based on molecular weight (?) is likely eIF4G, a known initiation factor and known interactor of Ded1. As well, it can be seen that there is a band just under that labeled as Ded1-GFP, which is more than likely IgG heavy chain. It is also interesting to note that by 4 hours of rapamycin treatment, the bands that have previously arisen in the gel seem to be completely gone. In further analysis done in the lab, it was determined that these components are present at lower levels leading up to the 2-hour mark and then decrease in abundance after the 2-hour mark. Further study of the mechanism behind this ramping up and ramping down of abundance is required. The

initial speculation is that the factors present in the portion of the gel that was analyzed are localizing together in the cell, causing a build-up, and then the subsequent reduction is a result of different stages of the stress response, and these components are either degraded or localization is altered, severing the interaction with Ded1.

The portion of the gel in the 2-hour sample that showed these bands was excised along with a corresponding section of the gel in the untreated time point. These sections were processed through standard mass spectrometry protocols and a list of proteins were generated from this analysis that changed in relative spectral abundance (Table 1). Strikingly, six of the nine proteins identified in all replicates were cell cycle-related (Cdc28, Clb3, Clb4, Cdc3, Cdc11, and Cdc12). Due to the predominance of the cell cycle factors seen in this assay, these factors were followed as the focus for the continuing work.

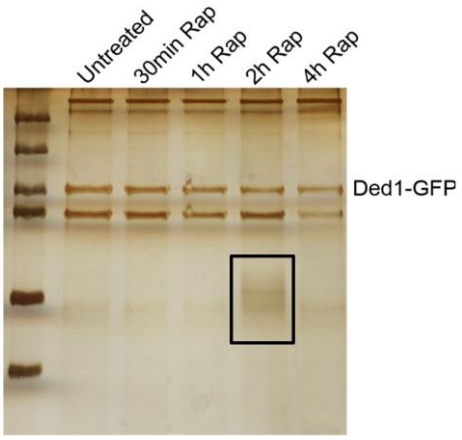

Figure 1: Co-IP of DED1-GFP over a rapamycin treatment time course visualized using silver stain. A strain containing *DED1-GFP* was grown in rich media and then subjected to rapamycin (200ng/ml) treatment for 30 minutes, 1 hour, 2 hours, and 4 hours. A co-IP was then performed by pulling down the GFP tag to see how association of proteins changed with Ded1 as duration of stress was increased. Box shows appearance of new proteins associating with Ded1-GFP during rapamycin treatment after 2 hours.

Protein	Function	Spectral Count (Untreated)	Spectral Count (2 hours Rapamycin)
Cdc3	Component of septin ring required for cytokinesis	0	3
Cdc11	Component of septin ring required for cytokinesis	0	5
Cdc12	Component of septin ring required for cytokinesis	0	8
Cdc28	Cyclin- dependent kinase known as master regulator	0	6
Clb3	G2/M transition	0	4
Clb4	G2/M transition	0	2
Pab1	Poly(A) binding protein	0	6
Ssb2*	Ribosome associated cytoplasmic ATPase	2	4
Tef4*	Translation elongation factor	1	4
Sup45*	Polypeptide release factor in translation termination	5	10
Trp3*	Indole-3-glycerol-phosphate synthase	1	4
Rpt3*	ATPase of the 26s proteasome	2	7
Sam1*	S-adenosylmethionine synthetase	0	2
Tuf1	Mitochondrial Translation elongation factor	2	0
Vma2	Domain of vacuolar H+-ATPase	4	9

Table 1: List of proteins followed up from the initial mass spectrometry analysis: Listed are the names of proteins from mass spectrometry analysis with their known functions and spectral counts from the analysis. *This protein was not found in all replicates; specifically, only found in the first round of experimentation.

Verification of relevant proteins from initial mass spectrometry screening

Identified proteins from the previous mass spectrometry analysis were directly tested for co-affinity with Ded1 to verify that these interactions were not merely artifacts of the co-immunoprecipitation process. Due to technical constraints such as protein abundance in the cell, only Cdc28, Cdc12, and Clb3 from the GFP-tag library were analyzed. GFP-tagged Tbf1, a nuclear and nucleolar factor involved in snoRNA production and telomerase regulation, was also included as a negative control to account for the possibility that this co-affinity might just be a result of the techniques and antibodies used. Tbf1 has no previously reported interaction with Ded1 according to the Saccharomyces Genome Database but is of roughly equal abundance to Ded1 in the cell making it a strong negative control for non-specific binding due to abundance and size.

Cultures were grown in YPD overnight and then back-diluted the next day. These cultures were then allowed to grow to an OD_{600} of 0.3-0.5. Samples were then either treated with rapamycin for 2 hours or remained untreated. Using common immunoprecipitation methods, Cdc28, Cdc12, Clb3, and Tbf1 were pulled down by the GFP tag present on the C-terminus of each and isolates from each lysate were directly blotted for Ded1 with a specific polyclonal antibody. Also, a strain of Cdc28-GFP with a mutant of *ded1* lacking the C-terminal domain, important for Ded1's role in translational repression (60), was analyzed the same way (Figure 2). It was seen that with rapamycin treatment the cell cycle factors analyzed had a strong interaction with Ded1, but without rapamycin no interaction was present. Additionally, when the C-terminal domain of Ded1 was removed, which in normal circumstances causes the continued growth of cells under rapamycin treatment, the interaction of Cdc28 was lost, consistent this being a real, and almost certainly, functional physical interaction.

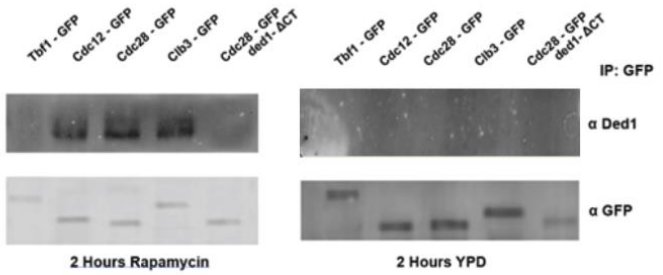

Figure 2: Co-IP of GFP tagged cell cycle proteins after 2 hours of rapamycin treatment to validate proteins identified from mass spectrometry. Five strains (*TBF1-GFP*, *CDC12-GFP*, *CDC28-GFP*, *CLB3-GFP*, and *CDC28-GFP ded1-ΔCT*) were grown in rich media and then either treated with rapamycin (200ng/ml) treatment for 2 hours or allowed to remain untreated. A Co-IP was then performed by pulling down the GFP tag to enrich for proteins physically interacting with the respective protein. Samples were run on an SDS-PAGE gel and visualized using a GFP primary antibody and a Ded1 primary antibody.

Assessing the role of Ded1 versus Cdc28 in growth defects

Due to the fact that *ded1-ΔCT* cells continue to grow during rapamycin treatment while the interaction with Cdc28 is lost, it was determined that Cdc28 function versus Ded1 function needed to be analyzed during rapamycin treatment. I hypothesized that the C-terminal domain of Ded1 is responsible for the downregulation of growth in cells due to an ability to interact with Cdc28 and inhibit it. Therefore, when it is removed as in *ded1-ΔCT*, these cells are able to overcome the inhibition and remain growing. To assess this, a strain with a *cdc28-as1* allele was utilized that would allow the tuning of Cdc28 function. This variant is known as a "bump and hole" variant. This variant has a modification in the ATP binding site of the kinase, Cdc28 in this instance, that does not alter the normal function of the kinase but allows for an inhibitor to competitively bind to the active site rendering the kinase inactive (62).

A *cdc28-as1* strain containing wild-type *DED1* and a *cdc28-as1* strain containing *ded1-ΔCT* were grown overnight. These strains were then back-diluted the next morning and either treated with rapamycin, the *cdc28-as1* inhibitor, both inhibitors, or left untreated (Figure 3 and 4). Growth of the strains without rapamycin and without inhibitor were rather unremarkable, growing similarly to one another. In addition, when *cdc28-as1* with and without *ded1-ΔCT* was treated with inhibitor in YPD, growth was diminished as would be expected. However, when looking at the results for growth in rapamycin, the growth of *cdc28-as1 ded1-ΔCT* with inhibitor was still greater than just *cdc28-as1* with inhibitor. Taken together, this supports that the growth advantages seen in the *ded1-ΔCT* strains are not simply a result of altered Cdc28 function but are clearly somewhat dependent directly on Ded1 function or Ded1's ability to function properly with another protein or pathway. Additionally, the effect of Cdc28 inhibition is substantially greater in the *ded1-ΔCT* cells, suggesting that Ded1 may be affecting Cdc28 activity.

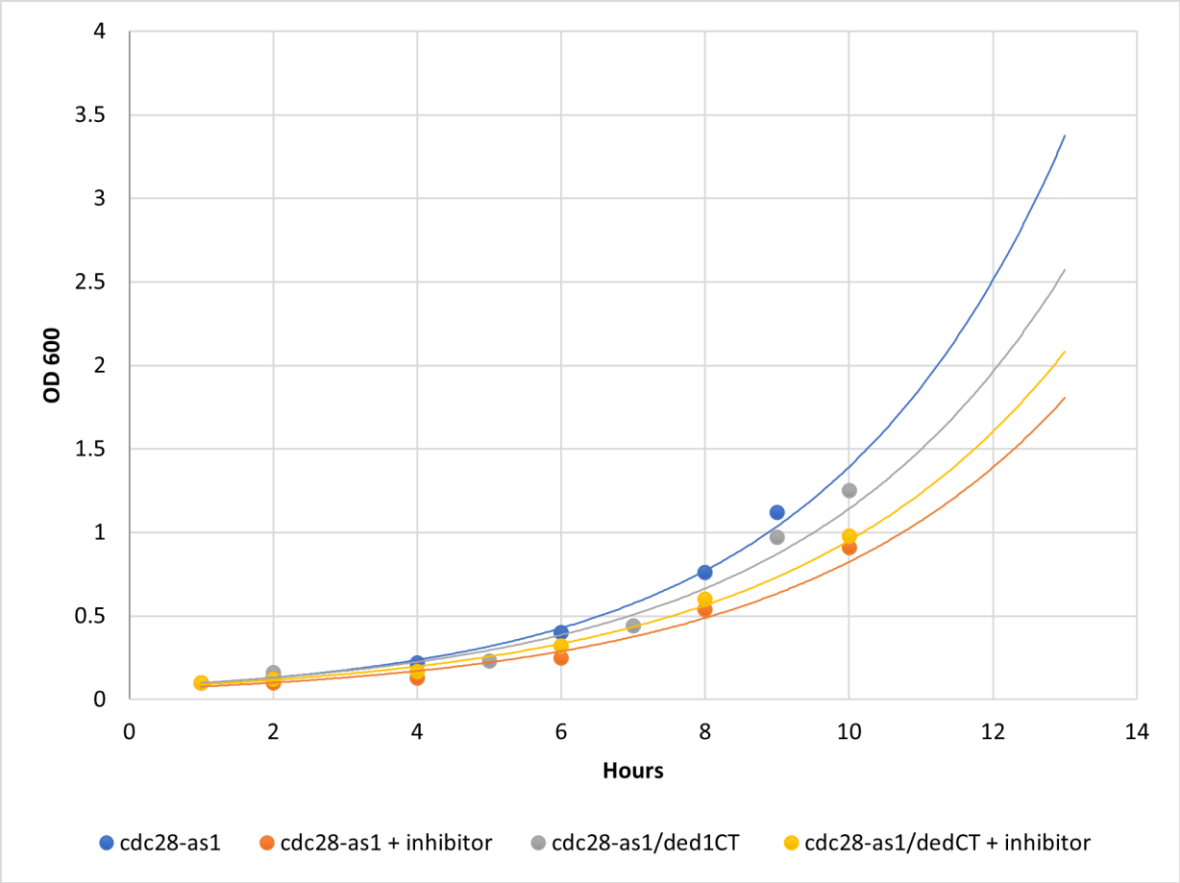

Figure 3: Liquid growth data shows no significant change in growth of individual strains. Wild-type *DED1* or *ded1-ΔCT* with *cdc28-as1* (PPI sensitive version of *CDC28*) cells were grown to mid-log in nutrient rich media, then diluted to 0.1 OD600. These samples were then treated with rapamycin (200ng/ml) and either treated with PPI inhibitor (300nM) and OD was recorded for 12 hours.

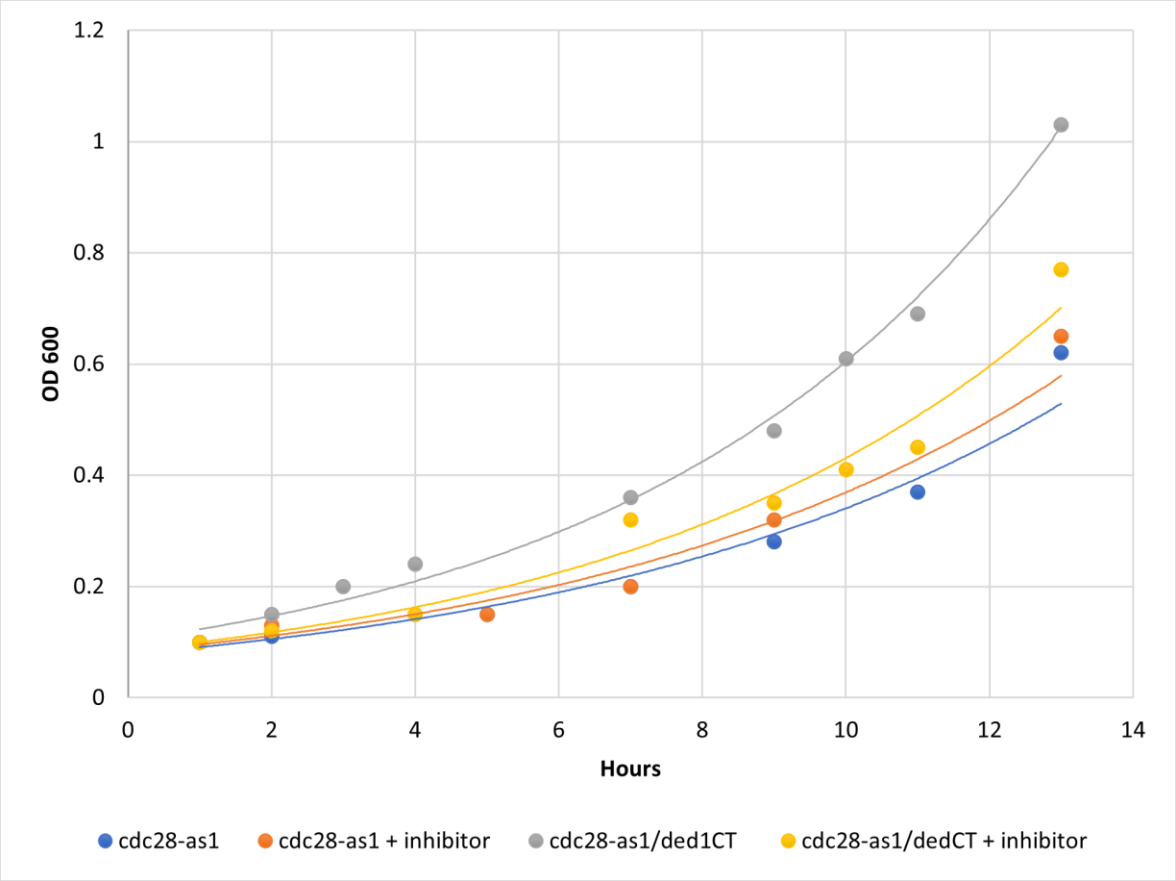

Figure 5: Liquid growth data shows resistance to rapamycin is diminished but maintained when Cdc28 is inhibited. Wild-type *DED1* or *ded1-ΔCT* with *cdc28-as1* (PPI sensitive version of *CDC28*) cells were grown to mid-log in nutrient rich media, then diluted to 0.1 OD600. These samples were then treated with rapamycin (200ng/ml) and either treated with PPI inhibitor (300nM) and OD was recorded for 12 hours.

Analysis of cell cycle progression using flow cytometry

Given the data above, it is logical to suggest that the reason Ded1 has an effect that is correlated to Cdc28's function is because there is some link to the progression of the cell cycle. To determine where this link is, flow cytometry was performed on wild-type cells and *ded1-ΔCT*. Standard Sytox Green protocols were followed (see Appendix B), and cells were plotted for fluorescence versus forward scatter. The signal distribution was plotted, and the cells were assigned to cell cycle phases.

When wild-type and *ded1-ΔCT* cells were evaluated, there was a normal distribution of cells between the various phases of the cell cycle with the majority of cells being in G2, and there was little difference between strains (Figure 6). However, when treated with rapamycin for 2 hours, in wild-type samples, a sub-population of cells developed that exhibit lower GFP signal and higher forward scatter than the typical populations (Figure 7, red cells/peaks). These characteristics are consistent with cells that are arrested in the cell cycle and stalled in G0 as well as a G2 quiescent state (72). The lower GFP fluorescence, representing DNA content, is likely a result of DNA being compressed into heterochromatic, dormant state. This compression would not allow Sytox Green to intercalate into the DNA making it appear as though these groups of cells have less DNA. Likewise, the increased forward scatter is likely because arrested cells are larger than cycling cells on average due to the inability to divide. Strikingly, the arrested cell populations are greatly reduced in *ded1-ΔCT* cells (Figure 7, red peaks). This would imply that cells with wild-type Ded1 are able to enter a quiescent state when treated with rapamycin protecting them from stress, and that when the C-terminal portion of Ded1 is removed, making cells resistant to rapamycin, they lose this ability to become dormant. Ultimately, this would indicate that Ded1 plays a key role in directing cells, through interaction with TOR, into a

dormant state protecting them from stress. However, the *ded1-ΔCT* cells still show increased G1 following rapamycin treatment compared to untreated cells, consistent with these cells still being partially sensitive to rapamycin, indicating that effects of other pathways are still present.

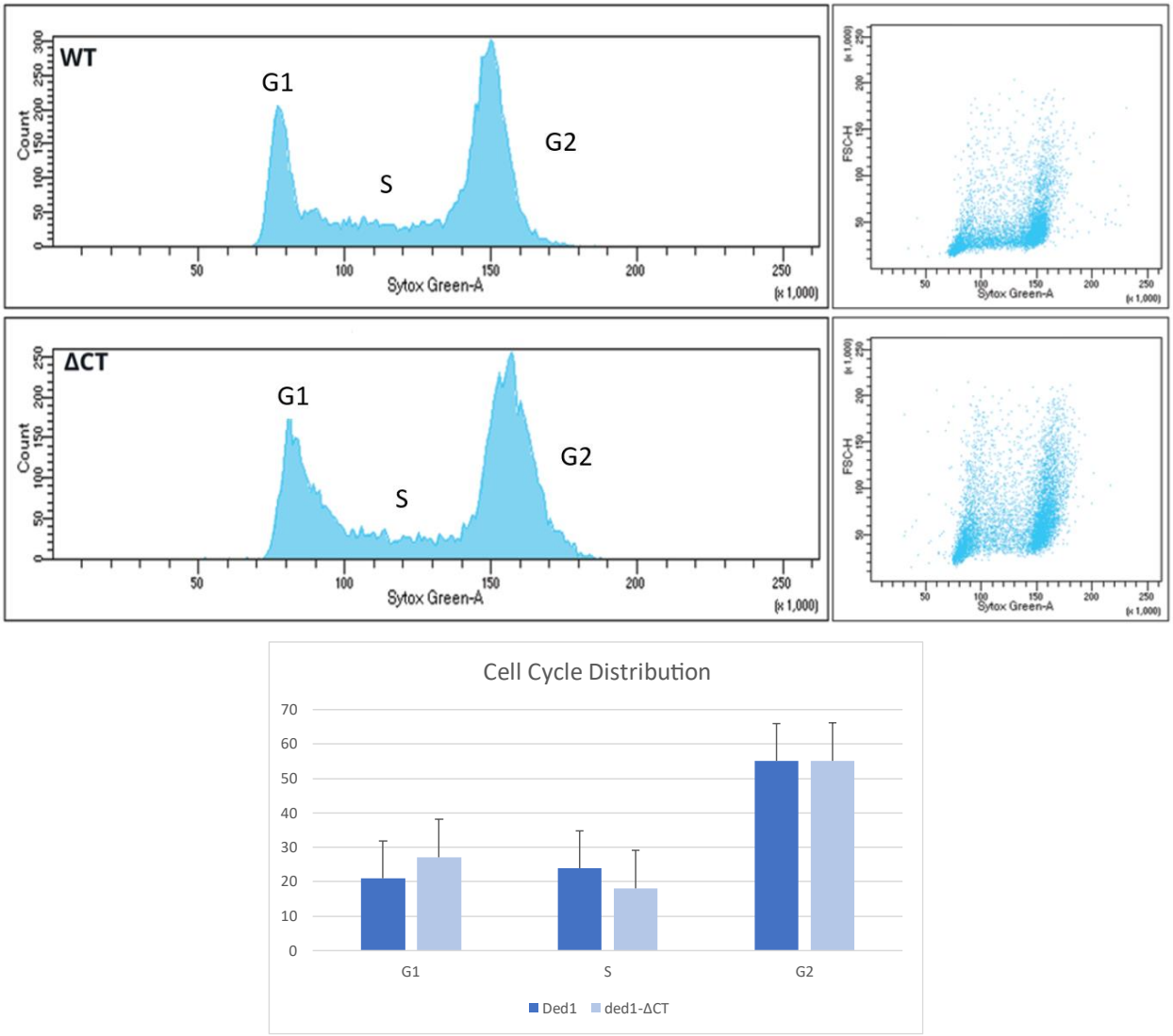

Figure 6: WT and ded1- ΔCT show no significant difference in cell cycle distributions under normal growth conditions. (Top) Wild-type *DED1* or *ded1-ΔCT* cells were grown to mid-log and then collected, fixed, and processed using standard Sytox Green protocols. Using flow cytometry cells were evaluated for DNA content and therefore cell cycle stage. (Bottom) Graphical representation for percentages of cells out of 10,000 in each cell cycle phase represented.

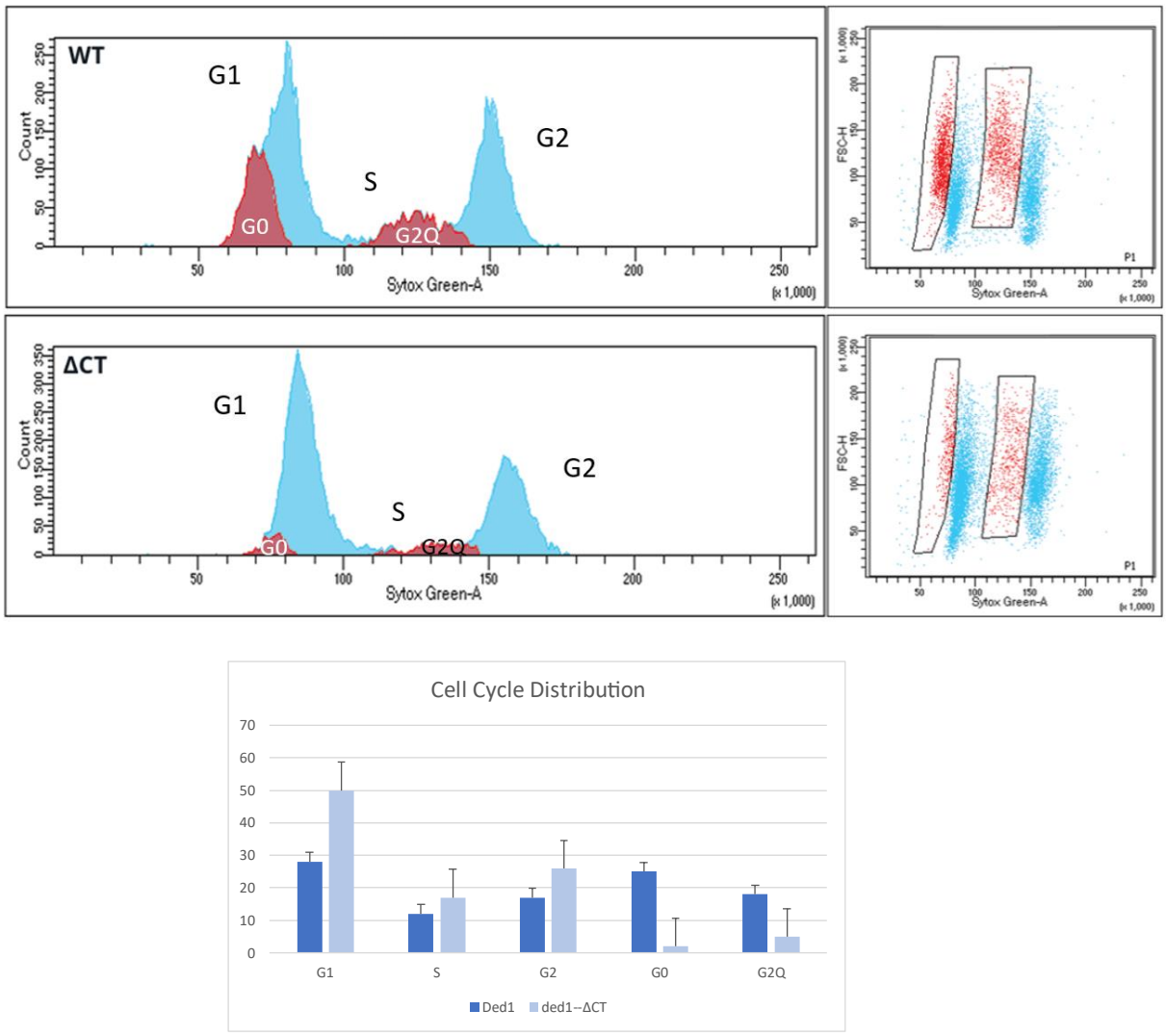

Figure 7: WT and ded1- ΔCT show significant difference in cell cycle distributions under rapamycin treatment. (Top) Wild-type *DED1* or *ded1-ΔCT* cells were grown to mid-log then treated with rapamycin (200ng/ml) for 2 hours. These cells were then collected, fixed, and processed using standard Sytox Green protocols. Using flow cytometry cells were evaluated for DNA content and therefore cell cycle stage. (Bottom) Graphical representation for percentages of cells out of 10,000 in each cell cycle phase represented.

3.3. CONCLUSIONS

Although work on this project is not completed it can be seen from these data that Ded1 interacts with key regulators of the cell cycle, such as Cdc28. This interaction seems to be directly related to Ded1's ability to repress translation, due to the fact that without the C-terminus present on Ded1 these cells lose their connection to the cell cycle factor Cdc28, and they lose their ability to respond to stress and continue to grow even in rapamycin treatment. From preliminary experimentation, ongoing in the lab, it also becoming clear that these changes seen in Ded1 activity are independent of its role in stress granules.

Cdc28 is arguably one of the most studied and important cell cycle regulators of yeast cell cycle progression. When cells encounter stress, Cdc28 signals cells to halt their growth and progression through the cell cycle to preserve resources and to hopefully survive the stress. However, when Cdc28 is partially inhibited through use of a competitive active site inhibitor, it does not fully suppress the rapamycin resistance seen in *ded1-ΔCT* cells. This change between these two growth curves is consistent with Ded1 (through its C-terminus) regulating the response of Cdc28 during rapamycin treatment and/or stress. The shifts in cell cycle phase in *ded1-ΔCT* cells are also consistent with this interpretation. Therefore, without the interaction with Ded1, Cdc28 is unable to completely repress growth. This could also indicate a feedback loop wherein translation itself is not repressed, as previous work in the lab has shown that growth and translation continue during rapamycin treatment in *ded1-ΔCT* cells.

CHAPTER 4: FUTURE DIRECTIONS AND DISCUSSION

4.1. UNBIASED SYNTHETIC GENETIC ARRAY TO IDENTIFY ESSENTIAL COMPONENTS THAT MODULATE THE DED1 RESPONSE TO RAPAMYCIN

Presently the work described within this section provides a huge array of potential targets for further examination. When looking only at the synthetic enhancers of *ded1-ΔCT* (i.e., the double mutant had increased rapamycin-resistance), there were specific trends of proteins that were identified. As mentioned within the paper, there were a large number of ribosomal related proteins. This makes sense with the known function of Ded1 in translation, but it is something that should be further explored. Although one might expect that deletion of ribosomal proteins would cause a decrease in growth and fitness, it is important to keep in mind that each ribosomal mutant in this study is one of a set of paralogs rather than deleting those that are the bare essentials for translation to occur. It is possible that this positive genetic interaction that is seen is a result of that particular paralog being responsible for translating specific proteins that inhibit growth during stress or rapamycin treatment, and therefore the deletion of such paralog would enhance *ded1-ΔCT*.

This area of interactions yielded a result for hydrolase activity as well. This activity is known to be involved in the regulation of cell wall integrity during sporulation and cytokinesis. Collectively my work suggests that Ded1 may contribute to the progression of the cell cycle due to its interactions with various components of both the stress response pathway and cell cycle. Taken together, it is possible that the genetic interactions seen with hydrolases during rapamycin treatment are foreshadowing the ability of Ded1 to assist in the regulation of these transitions. For instance, it could be possible that Ded1 is regulated to assist in the translation of these

hydrolases during times of stress, while its effect on these transcripts is suppressed in pro-growth conditions through the action of other factors. This would mean that Ded1 has the ability to actively regulate, with help of known factors and sequestration processes, the entire progression of cells from G2/M and through meiosis.

Moreover, there are distinct connections to Ded1 and a variety of stress response pathways. The screen showed Ded1 interacting with various downstream targets of TOR, which would imply it is an integral part of the cascade that alters the cellular landscape for stress responses. Notably some of the key interactions are MAPK pathway regulators, transcriptional responses to oxidative stress, protein glycosylation, membrane trafficking, and aerobic respiration. If Ded1 can be modulated by a subset of proteins from each of these categories it could likely be the key in the transduction of stress signals from the outside environment of the cell. The fastest way to change the landscape of the cell and the response that is currently being propagated would be to alter the availability of proteins. Although transcription can change this landscape it would be at a much slower pace. If translation can be directly enhanced or repressed due to their ability to help the cell overcome stress, the cell does not need to wait for the eventual changing of available transcripts.

Likewise, when looking at suppressors of *ded1-ΔCT* (i.e. decreased growth on rapamycin), it is shown that pathways such as mitochondrial translation and amino acid metabolism are identified. When stress occurs in cells, it is not unlikely that these processes must be altered to allow the cell to survive. For example, if mitochondrial translation and function is not altered during these times of stress, significant resources will be put towards the production of ATP, and stockpiles of precious nutrients will be utilized before the cell has access to more. If

a cell is allowed to also use these nutrients continually to produce an abundance of amino acids when translation in bulk should be halted, how are they to survive? It is therefore highly likely that Ded1 is a direct recipient of TOR signaling and used as a means to regulate the ability of cells alter their landscape and allow for proper allocation of resources that would yield eventual cell survival.

The initial screen of my project yielded hundreds of "hits" that seem overwhelming when considering an overall model, but I believe these hits give insight into the translatome of transcripts that are especially sensitive to Ded1 function (Figure 8). Usually this is discussed as a transcript that requires a specific factor to be translated or it is positively regulated by a translation factor. While some of the hits present within this study show just that, I do think there are a subset of hits that show the opposite. Some of the hits seen in this screen likely rely on Ded1 to be adequately and accurately shut off during stress conditions or rapamycin treatment (Figure 8, left). This category would be suppressors of the rapamycin resistance of *ded1-ΔCT*, including the hits in amino acid metabolism and mitochondrial translation. Some hits in the enhancer category, such as genes involved in stress responses and negative regulators of the MAPK pathway, might also repress some of these same genes in parallel. Furthermore, Ded1 may also up-regulate translation of some transcripts, such as stress-induced genes, following rapamycin treatment, and other enhancers may represent these targets (Figure 8, right). I would even postulate that the transcripts that seem to positively enhance the resistance to rapamycin would show a greater binding affinity to Ded1 during stress than in wild-type conditions. Other enhancers, such as the ribosomal proteins, may also positively regulate these same transcripts.

To better understand these processes, it would be a perfect opportunity to utilize ribosome profiling techniques. By evaluating what transcripts are being actively being translated during

stress with wild-type *DED1* and then comparing it to translation changes in *ded1-ΔCT*, many things could be discovered. It is possible that during this analysis it could be seen that when Ded1 is not present in its fully functional role, such as in *ded1-ΔCT*, there is a group of transcripts that are still being actively translated that allow for the production of growth components. These components could include amino acid regulators, cell cycle factors, mitochondrial translation components, and even cell trafficking components. If these proteins are not being downregulated during times of stress but are allowed to remain functioning, cells would be allowed to grow, as seen in previous data, and this would significantly hurt cell survival. Of course, evaluations of these would need to be done by comparison of various conditions. Much like the initial SGA described in my work, it would need to be looked at not only in times of stress or rapamycin treatment but also would need to be looked at in times of normal growth conditions to eliminate the possibilities of false interactors being identified. This work opens many avenues for further exploration and shows many components of cellular activities that are more than likely modulated by Ded1 directly or semi-directly.

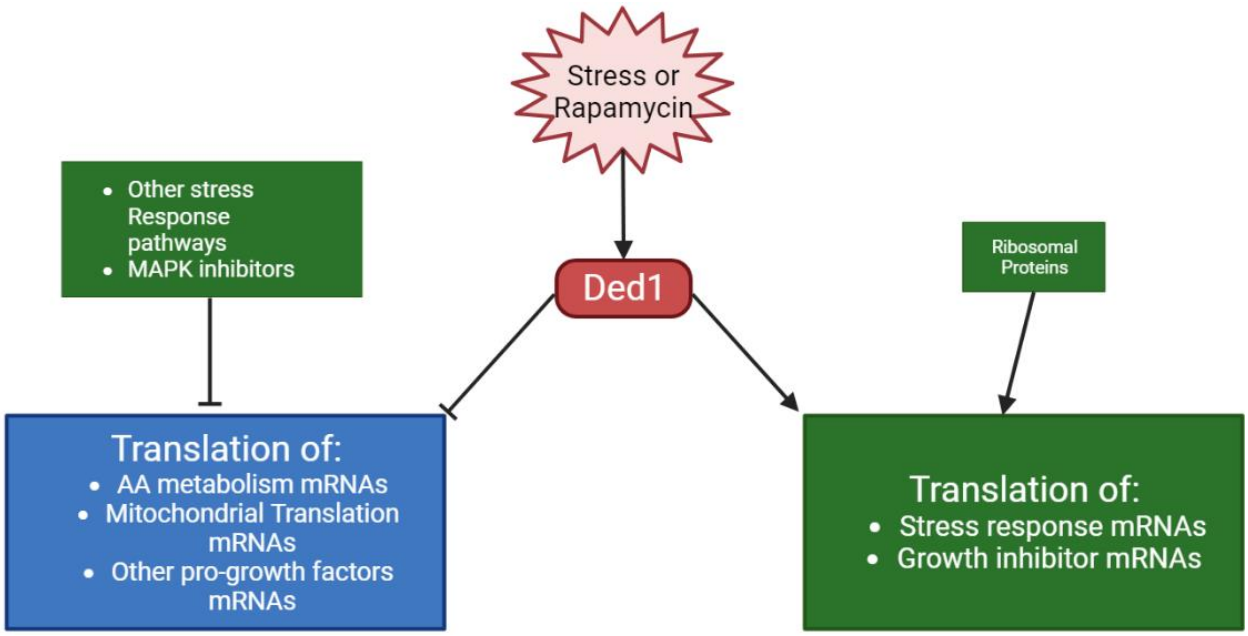

Figure 8: Enhancers and suppressors of ded1-ΔCT in rapamycin. Proposed connectivity of suppressors (blue) and enhancers (green) of *ded1-ΔCT* activity and how they relate to stress and Ded1 as shown through the Synthetic Genetic Array. Listed categories of mRNAs represent potential translational targets of Ded1, while the above boxes list other factors/pathways acting in parallel.

4.2. DED1 PHYSICALLY INTERACTS WITH A KEY COMPONENT OF THE CELL CYCLE ALTERING ITS GENERAL RESPONSE TO RAPAMYCIN TREATMENT

Although it is clear Cdc28 and Ded1 have a distinct physical interaction, how these two proteins interact is not clearly understood. Ded1 and Cdc28 have a clear interaction during rapamycin treatment that is lost when the only available copy of *DED1* is *ded1-ΔCT*. This would indicate that the interaction of Cdc28 and Ded1 in rapamycin is dependent on the C-terminal domain of Ded1, either by direct interaction there or through a protein partner that is lost when the C-terminal domain is lost. The initial thought was that Cdc28 might have the ability to directly interact with Ded1 and possibly phosphorylate the C-terminal portion of Ded1. Motif analysis shows that this portion of Ded1 does not contain any canonically known Cdc28 phosphorylation sites. The only portion of Ded1 that has a relatively acceptable phosphorylation site for Cdc28 is in the conserved helicase core. This would mean, however, that all DEAD-box proteins would likely have the ability to be Cdc28 targets, but this has not been reported in the phosphoproteome datasets for Cdc28. For that matter, these datasets do not include Ded1 as a potential target either. One of the first experiments that could be done from here to evaluate direct connection between these two proteins is an *in vitro* binding assay. Both Cdc28 and Ded1 could be mixed together in solution, given approximately 2 hours to interact (timing taken from previous assays), and then a direct analysis could be done to determine if these two proteins did in fact interact by evaluating size exclusion. If the direct connection of these two proteins alone could not be validated, it would leave the possibility of some sort of "linker" protein partner.

To determine what this protein partner is further studies would need to be completed. For example, a similar study to what was done in my work could be completed. This time, instead of looking at Ded1 interactions gained during rapamycin treatment, Cdc28 interactions would be

evaluated. For this to work, the section of the gel that is analyzed would have to be expanded to beyond just the singular portion, and instead a full lane would need to be analyzed for Cdc28 in rapamycin and in YPD. This data would need to be available for Ded1 as well, so the study would need to be repeated to include the full lane and not just the previously tested portion. If it is true that there is some sort of "linker" protein partner that is responsible for the interaction between Cdc28 and Ded1, this "linker" protein would be identified in both studies. Now, it is possible that multiple proteins could be discovered that do not contribute to this interaction, but further validation could be completed to understand which proteins contribute to this interaction and which are superfluous.

From the analysis that I have done, the ability of *ded1-ΔCT* to continue to grow during rapamycin treatment is to some degree independent of the master regulator of the cell cycle in *S. cerevisiae*, Cdc28. This means that Ded1 is acting in other parallel capacities to affect the growth of cells. What exactly this means for the cell cycle is unknown, but I think that it does hint at the potential for Ded1 to be more directly linked to stress signaling than previously thought. Although my lab has demonstrated that Ded1 is an active participant in the stress response of TOR, this is not something that is well understood. It is possible that somehow TOR is able to directly affect Ded1 through an unidentified posttranslational modification that allows Ded1 to signal to stop growth through interacting with Cdc28 as well as other factors, and that is why when *ded1-ΔCT* is examined during Cdc28 inhibition, there is still an unaccounted-for resistance to rapamycin. This would still be consistent with Ded1 regulating Cdc28 function. The Ded1 posttranslational modification could be phosphorylation, like has been predicted before, but just not in the known locations already tested. Phospho-tag gels could be run on Ded1 and mutants during rapamycin treatment to evaluate any novel locations of phosphorylation. As well, it could

be other forms of posttranslational modifications, though I would postulate that due to Ded1 and TOR's interactome, phosphorylation is the most likely candidate. This does not completely rule out the potential for other modifications being important in the reactions seen, but it would help to establish a starting point for evaluation of these types of modifications.

When examining the interaction between Ded1 and Cdc28, it seems less likely to me that this interaction is a result of Ded1 simply upregulating or downregulating translation. Rather, I hypothesize that Ded1 regulates Cdc28 to control the cell cycle. Given the interaction of Ded1 with septin ring components (Table 1), the localization of Ded1 may contribute to its physical interaction with Cdc28 and ultimately with its potential role in Cdc28 regulation (Figure 9A). Furthermore, at the bud neck of a growing yeast cell, there is a large amount of translation that must occur to make sure that the accurate amount and types of proteins are present, so Ded1 may be present to facilitate this translation even in pro-growth conditions. When stress occurs, it would be essential for cells to halt their growth and stage in the cell cycle quickly, so Ded1 would be pre-positioned to act on Cdc28. I theorize that the low-complexity domain of the C-terminus of Ded1 causes oligomerization and phase separation, pulling Cdc28 into an aggregate, possibly along with other translation factors such as eIF4G1 (Figure 9A, right). This aggregation would likely be transient as seen in Figure 1, possibly due to degradation of the factors involved, but it would also be independent of known stress granule formation as seen in preliminary work in the lab. Ultimately this model suggests that the interaction of Ded1 and Cdc28 and Ded1's ability to modulate Cdc28 function is highly regulated by the specific conditions induced by TOR inhibition.

Although connections of Ded1 and Cdc28 have been seen through biochemical analysis it is not completely clear if this interaction is something that is long-lasting enough to be seen

through time-lapse microscopy as suggested by the model above. Using tagged versions of these proteins and multiple hours long microscopy video tracking, it would be incredibly useful to follow their movement throughout the cell before, during, and after rapamycin treatment to see how their interactions evolve and how their localization and shuttling is altered.

While my primary model involves Ded1 directly affecting Cdc28 function, Ded1 is known to be a key regulator of translation, and it is possible that Ded1's function in translation is affected by Cdc28. Cdc28 may be affecting whether Ded1 activates or represses translation or affecting how Ded1 interacts with different subsets of mRNAs (Figure 9B). Therefore, how the polysome profiles of cells change as Cdc28-as1 is inactivated with and without rapamycin should be evaluated. This should also be compared to how cells containing *ded1-ΔCT* and *cdc28-as1* also change during the same forms of inhibition and stress. It is seen that growth of *ded1-ΔCT* cells during rapamycin is not wholly dependent on Cdc28, but how this affects bulk translation has not been evaluated.

Furthermore, it is seen that *ded1-ΔCT* cells lack the full ability to transition cells into quiescence during rapamycin treatment. This has not been exhaustively examined, and other techniques such as cell morphology and protein profiles should be done to confirm if these cells are in quiescence. However, assuming that this is indeed the case, this effect is not well understood and has only been preliminarily evaluated in conjunction with Cdc28 inactivation. It would be of value to look at these cell cycle profiles using flow cytometry when Cdc28 is inactivated, and with *cdc28-as1* it is possible to evaluate these profiles as Cdc28 is progressively downregulated by use of increasing concentrations of inhibitor. From preliminary work that has been done, I would predict that the effect of *ded1-ΔCT* on quiescence is lost in the inhibited

cdc28-as1 cells. This result would suggest that Ded1's effect on the cell cycle is mediated through Cdc28.

Ultimately, the work done to solidify the interaction of Ded1 and Cdc28 as a physical interaction during rapamycin treatment that is lost in *ded1-ΔCT* is some of the most compelling evidence present to validate that Ded1 is a key component of cellular stress response, and it needs to be followed up. Ded1 is an essential translation initiation factor, but I would argue that Ded1 has the potential to also be considered as an essential stress response protein able to affect processes far beyond just translation.

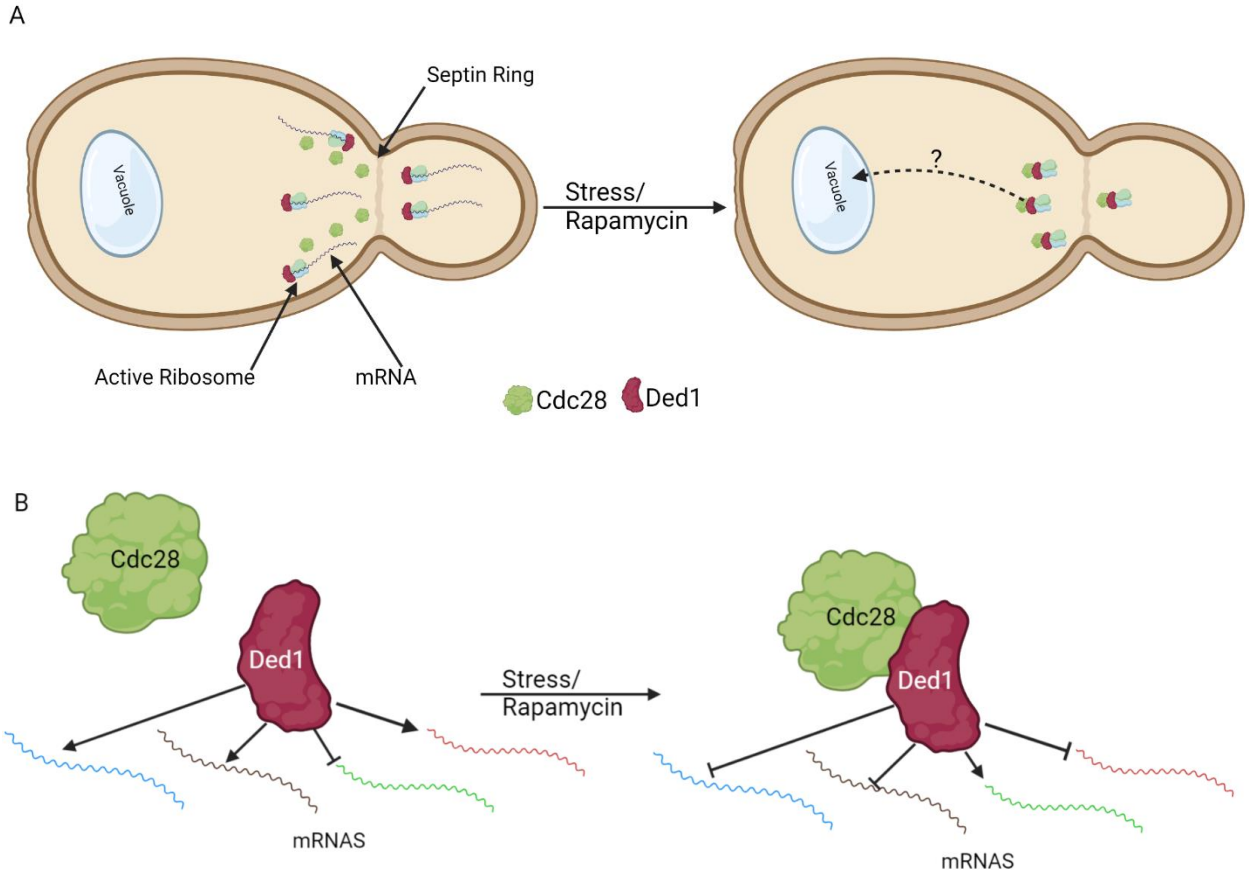

Figure 9: Interaction of Cdc28 and Ded1during stress or rapamycin treatment alters localization and activity. (A) Repression of Cdc28 by Ded1. Left to right: Active translation is halted, and ribosomes are disassembled from mRNA when cell is introduced to stress/rapamycin causing a change in localization to occur, allowing for direct interaction with Ded1 and Cdc28. Cdc28 is then repressed and sequestered by Ded1 (with other translation factors), and the proteins may then be subsequently degraded in the vacuole. (B) Regulation of Ded1 by Cdc28. In pro-growth conditions (left), Ded1 generally promotes translation initiation on mRNAs, perhaps with some exceptions. In stress/rapamycin, Cdc28 binds Ded1, altering its activity to repress translation of many mRNAs, except those encoding stress-response genes.

APPENDIX A

A synthetic genetic array screen for interactions with the RNA helicase *DED1* during cell stress in budding yeast

Sara B. Carey, Hannah M. List, Ashwin Siby, Paolo Guerra, and Timothy A. Bolger

PO Box 210106, Department of Molecular and Cellular Biology, University of Arizona, Tucson, AZ 85716, USA.

Corresponding author: tbolger@email.arizona.edu

Running Title: A synthetic genetic array with *ded1-ΔCT*

Keywords: yeast, helicase, translation, stress, rapamycin

Abstract:

During cellular stress it is essential for cells to alter their gene expression to adapt and survive. Gene expression is regulated at multiple levels, but translation regulation is both a method for rapid changes to the proteome and, as one of the most energy-intensive cellular processes, a way to efficiently re-direct cellular resources during stress conditions. Despite this ideal positioning, many of the specifics of how translation is regulated, positively or negatively, during various types of cellular stress remain poorly understood. To further assess this regulation, we examined the essential translation factor Ded1, an RNA helicase that has been previously shown to play important roles in the translational response to cellular stress. In particular, *ded1* mutants display an increased resistance to growth inhibition and translation repression induced by the TOR pathway inhibitor, rapamycin, suggesting that normal stress responses are partially defective in these mutants. To gain further insight into Ded1 translational regulation during stress, synthetic genetic array analysis was conducted in the presence of rapamycin with a *ded1* mutant and a library of non-essential genes in *S. cerevisiae* to identify positive and negative genetic interactions in an unbiased manner. Here we report the results of this screen and subsequent network mapping and GO-term analysis. Hundreds of candidate interactions were identified, which fell into expected categories, such as ribosomal proteins and amino acid biosynthesis, as well as unexpected ones, including membrane trafficking, sporulation, and protein glycosylation. Therefore, these results provide several specific directions for further comprehensive studies.

Introduction:

During adverse extracellular conditions, such as nutrient deprivation or oxidative stress, cells must re-orient their gene expression profiles to slow growth, conserve resources, and respond to the stressor (Pakos-Zebrucka et al. 2016; Saxton and Sabatini 2017). Translation is both highly energy-intensive and a direct determinant of the cellular proteome; thus, it is a natural point of regulation in stress responses (Crawford and Pavitt 2019; Liu and Qian 2014). Indeed, translation undergoes massive reprogramming during stress, wherein bulk translation is repressed, but translation of select "stress-response" mRNAs is upregulated (Gerashchenko et al. 2012; Ingolia et al. 2009). However, the mechanisms underlying this specificity remain incompletely understood.

In budding yeast, *DED1* encodes an essential RNA helicase of the DEAD-box protein family, which are critical for modulating RNA-RNA and RNA-protein interactions throughout gene expression (Valentini and Linder 2021). Its human ortholog, DDX3X, has been implicated in multiple cancers, including frequent mutations in medulloblastoma, and DDX3X mutations also cause an autism-like cognitive disorder (Mo et al. 2021; Northcott et al. 2012; Snijders Blok et al. 2015; Tang et al. 2021). The primary function of Ded1 is thought to be in translation initiation. In normal, pro-growth conditions, Ded1 promotes initiation by unwinding secondary structure in the 5' UTR of mRNAs and stimulating pre-initiation complex assembly (Gupta et al. 2018; Sen et al. 2015; Sharma and Jankowsky 2014). Furthermore, *ded1* mutation preferentially affects mRNAs with structured 5' UTRs and increases the utilization of alternative translation initiation sites in target mRNAs (Guenther et al. 2018; Sen et al. 2015).

Interestingly, Ded1 also plays roles in repressing translation. *DED1* overexpression inhibits translation and cell growth, and Ded1 affects the formation of stress granules, stress-

dependent, cytoplasmic accumulations of RNA and proteins (Aryanpur et al. 2022; Beckham et al. 2008; Hilliker et al. 2011). Notably, we recently showed that Ded1 mediates the translational response to TOR inactivation (Aryanpur et al. 2019). Specifically, a *ded1* mutant lacking its C-terminal region (*ded1-ΔCT*) was resistant to growth inhibition and translation repression caused by the TOR inhibitor rapamycin. The C-terminal region of Ded1 interacts with the scaffolding factor eIF4G1, and further analysis suggested that eIF4G1 mediates the effects of Ded1 in these conditions (Aryanpur et al. 2019; Hilliker et al. 2011). We proposed a model wherein Ded1 represses translation during TOR inactivation by promoting eIF4G1 dissociation from translation complexes and its subsequent degradation. How this mechanism is regulated and which downstream processes are affected remains unknown, however.

To begin to address these questions, we conducted a synthetic genetic array (SGA) screen with the *ded1-ΔCT* mutant, taking advantage of its resistance to rapamycin-mediated growth inhibition to identify both positive and negative synthetic interactions from the yeast deletion library of non-essential genes (Tong et al. 2001). This screen identified a large number of synthetic interactions with associated GO-terms that include translation, vesicle trafficking, amino acid metabolism, and signal transduction. These hits likely represent upstream regulators, direct interactions, and downstream targets of Ded1 as well as related processes. Compelling candidates will be examined in future studies.

Methods & Materials:

Screen Design

The yeast strain used in this SGA screen is TBY174 (*MATα his3Δ1 leu2Δ0 ura3Δ0 can1Δ0::P_{GAL1}-T_{ADH1}-P_{MFA1}-spHIS5 lyp1Δ0 ded1-ΔCT::Hygro*), which was constructed from the strain Y15583-13.2b from a previous study using similar techniques (Singh et al. 2009). The C-terminal portion of DED1 was removed from Y15583-13.2b and replaced with a hygromycin resistance cassette using the plasmid pUG75 as a template (protocol adapted from (Hegemann and Heick 2011)). The resulting strain was verified using PCR amplification, growth assays, and western blotting. This "query strain" (TBY174) was then used in a standard synthetic genetic array protocol (Singh et al. 2009; Tong and Boone 2006). The yeast knockout library is commercially available and contains approximately 5,000 non-essential gene knockout strains (Horizon Discovery). These strains were constructed using a G418 resistance cassette (Giaever et al. 2002). The mating type of the strains used are MATa allowing them to be mated to the query strain directly.

The screen procedure can be summarized as: re-array of the knockout library, mating of query strain to the library, selection of zygotes, sporulation, selection of haploids, and growth analysis. To re-array the library, the 96-well plates of the library stock were pinned using a RoToR HDA Pinning robot (Singer) to a 384-well format compatible with the robot. These plates contained solid YPD (10 g/L yeast extract, 20 g/L peptone, 20 g/L agar, 200 µl/L 10N NaOH, 2% glucose) + G418 (200 mg/L) media to maintain selection, and yeast were grown for 48 hours at 30°C. To prepare for mating, the query strain was simultaneously grown in liquid culture for 24 hours, plated to a 384-well format, and allowed to grow for an additional 24 hours at 30°C. The

query strain was then replica plated to 14 fresh plates containing YPD. Next, the re-arrayed knockout library plates were replica plated directly on top of the query strain and allowed to grow for 24 hours at 30°C. To select for zygotes, the mated strains were replica plated to new plates containing YPD + G418 + hygromycin (200 mg/L) and allowed to grow for 48 hours at 30°C. For efficient sporulation, the zygote plates were replica plated to plates containing sporulation media (20 g/L agar, 10 g/L potassium acetate, 1 g/L yeast extract, 0.5 g/L glucose, and 0.1 g/L amino acid sporulation supplement; supplement consisted of 2 g histidine, 10 g leucine, 2 g lysine, and 2 g uracil) and allowed to grow for 5 days at 22°C.

Following the sporulation period, the desired double knockout (DKO) haploid strains were isolated using a progression of three different selections. First, MATa sporulated strains were selected by replica plating onto Singer-compatible plates containing SD media (20 g/L agar, 20 g/L glucose, 1.7 g/L yeast nitrogen base without ammonium sulfate and amino acids, 1 g/L monosodium glutamic acid, and 2 g/L amino acid supplement; supplement consisted of 1.2 g adenine, 1.8 g isoleucine, 3.6 g leucine, 1.2 g methionine, 3.0 g phenylalanine, 1.2 g tryptophan, 1.8 g tyrosine, 1.2 g uracil, 9 g valine, 1.5 g aspartic acid, 1.5 g glutamic acid, 1.5 g threonine, 1.5 g serine, and 1.5 g proline) lacking histidine, arginine, and lysine + canavanine (50 mg/L) + thialysine (50 mg/L) and grown for 48 hours at 30°C (MATa cells are selected via *spHIS5* expression by the MATa-specific *MFA1* promoter while canavanine and thialysine select against unsporulated diploids). After 48 hours these plates were replica plated onto fresh plates containing the same media as before and grown for 24 hours at 30°C in order to generate "tighter" spots for subsequent steps. Second, for selection of the knockout library gene deletion, the MATa strains were replica plated onto plates containing SD – His/Arg/Lys + canavanine + thialysine + G418 and grown for 48 hours at 30°C. Third, for selection of the *ded1-ΔCT*

mutation, strains were replica plated onto plates containing SD – His/Arg/Lys + canavanine + thialysine + G418 + hygromycin and grown for 48 hours at 30°C. Growth on the final set of plates generated the DKO strains used for phenotypic screening.

Phenotype Scoring

After generation of the double knockout strains, the strains were tested for growth fitness on media containing rapamycin. Both the single-mutant *ded1-ΔCT* query strain and some library deletion strains are resistant or sensitive to rapamycin (see Figure 1B, Supplemental Table S4, and (Aryanpur et al. 2019)). Therefore, DKO strains were scored by normalizing growth to that of the single-mutant parent strains via a multiplicative method (Baryshnikova et al. 2010). Fitness was assessed for each of the following on YPD and YPD + rapamycin (200 ng/mL) media: Y15583-13.2b (as a wild-type control), *ded1-ΔCT* query strain, single knockout library strains, and DKO strains. While still plated in a 384-well format, YPD plates were grown for 2 days and YPD + rapamycin plates were grown for 5 days at 30°C. Plates were scanned using a flat-bed scanner (Epson) and colony size was analyzed via SGA Tools (http://sgatools.ccbr.utoronto.ca), taking into account all four strains/controls in both conditions (Wagih et al. 2013). SGA Tools calculated fitness as the number of pixels contained in each spot for each strain. Then, using the single knockout in both conditions, the query strain in both conditions, and the wild-type control in both conditions as parameters for comparison, a normalized score was generated that represented the "interaction score" for the DKO strain on a scale from 0 to 2. This score thus provides a quantitative measure of the synthetic interaction between the *ded-ΔCT* allele and the library deletion for rapamycin-dependent growth, where 0 represents no growth of the double mutant, which is an extremely negative synthetic interaction (synthetic-lethal), 1 represents the expected growth given no interaction, and 2 represents much

better growth on rapamycin than expected for the double mutant, a highly positive synthetic interaction (for technical reasons, the actual maximum was 1.961 rather than 2.00).

Classification and Verification of Hits

To determine cut-offs for further analysis of the hits, the interaction scores for all 4,799 DKO strains were analyzed via Graphpad Prism. The score distribution had a mean of 1.007 and a standard deviation of 0.534. Cut-offs were established at 1.0 and 1.5 standard deviations above and below the mean wherein interaction scores below the lower cut-off (0.473 or 0.205, respectively) were analyzed as negative / suppressor interaction hits and scores above the upper cut-off (1.542 or 1.809) were analyzed as positive / enhancer hits. The 1.5 standard deviation cut-off, which yielded 529 suppressor and 544 enhancer hits, was used for most subsequent analysis; however, the 1.0 standard deviation cut-off, which yielded 763 suppressor and 780 enhancer hits, was used for generating lists of SGD-annotated phenotypes.

To experimentally verify the phenotypes, single and double mutants from a selected number of hits were isolated from the screen strains and individually tested via serial dilution growth assays on YPD and YPD + rapamycin plates at 30°C as previously described (Aryanpur et al. 2017). In addition, the list of hits includes a number of genes that were expected based on previous studies (e.g. translation factors).

Network Maps and GO-Term Analysis

Network maps were generated with the hits (1.5 standard deviation cut-off) using STRING (https://string-db.org/) (Snel et al. 2000; Szklarczyk et al. 2021). STRING was then used to perform k-means clustering on the hits, where nodes (genes) were clustered into a predetermined number of clusters such that each node is related more strongly to other nodes

within the same cluster than to nodes within other clusters. The gap statistic method was used to determine that five clusters should be used for each of the two datasets (suppressors and enhancers) (Tibshirani et al. 2001). We then used STRING to associate GO-terms that are significantly enriched within each of the clusters. GO-terms were ranked for each cluster based on the "strength" feature in the STRING analysis, where strength is defined as $\log_{10}$ of the ratio between the number of proteins in the hits that are annotated with a specific GO-term and the number of proteins that would be expected to be annotated with this term in a random network of the same size. GO-term lists were manually curated by eliminating redundant or vague terms (e.g. "cytoplasm"), and up to 10 GO-terms are shown. Complete lists of all significantly enriched GO-terms are included in the Supplemental Tables.

For the GO-term analysis of annotated hits (Table 3 and Supplemental Tables S4 and S5), the hits (1.0 standard deviation cut-off) were examined for a previously annotated phenotype of rapamycin (sirolimus) resistance or sensitivity using the "YeastMine" feature of the *Saccharomyces* Genome Database (SGD). Four categories of hits were thus generated: suppressors (negative synthetic interactions with *ded1-ΔCT*) with a previously annotated rapamycin sensitivity (203 hits), suppressors with annotated rapamycin resistance (54), enhancers with rapamycin sensitivity (78), and enhancers with rapamycin resistance (60). Note that only about one-quarter of the hits were annotated for a rapamycin phenotype in SGD; thus, three of the four categories were too small for effective network mapping. Instead, overrepresented GO-terms (biological process complete) were generated for each category using PANTHER (pantherdb.org) via Fisher's exact test (Mi et al. 2021). GO-terms with less than 4 associated genes were deleted and then were curated as above with the 8 most-enriched terms shown in Table 3 (complete list in Supplemental Table S5).

Results & Discussion:

We crossed a *ded1-ΔCT* mutant to a knockout library of non-essential genes and assessed the resulting 4,799 double mutants for their growth on rapamycin-containing media. We then assigned each pair a synthetic interaction score (from 0 to 2, with 1 representing no interaction) after normalizing for growth on rapamycin of both single mutant parent strains, where a low score indicates that the double mutant grew less well on rapamycin than expected based on the single mutant phenotypes (a negative synthetic interaction), and a high score indicates that the double mutant grew better than expected (a positive synthetic interaction). The interaction scores were distributed across the range of possible scores with an overall mean of 1.007 (Figure 1A). A large number of mutants showed strong synthetic interactions with 266 scoring at the lowest value possible and 453 at the highest, respectively. Cut-offs for candidate hits were established as any mutants with an interaction score more than 1.0 or 1.5 standard deviations from the mean, depending on the downstream analysis (Figure 1A, Supplemental Table S1).

Results were verified by individually testing growth of selected hits. In Figure 1B, three examples are shown. The *fis1-null ded1-ΔCT* and *hsp30-null ded1-ΔCT* double mutants both grew significantly better on rapamycin than the *fis1-null* and *hsp30-null* mutants alone (positive interactions), while the *sbp1-null ded1-ΔCT* double mutant grew similarly to the *sbp1-null* mutant alone (and more poorly than the *ded1-ΔCT* single mutant), indicating a negative interaction. Thus, the growth assays agreed with the results from the screen, although we also found that some strongly negative interactions were also synthetic lethal or synthetic sick in the absence of rapamycin (data not shown). Further supporting the validity of the screen, genes expected to interact were also obtained, including yeast FKBP1 (*FPR1*) and numerous genes involved in translation (*GCN2*, ribosomal genes, etc.). It should be noted, however, that a small

but significant number of the strains in the deletion collection have been shown to have off-target mutations or other defects (Giaever and Nislow 2014); therefore individual hits should be interpreted with caution.

To organize the large number of hits from the screen, we conducted protein network analysis using STRING (Snel et al. 2000; Szklarczyk et al. 2021). An interaction network was built with all the genes showing strongly negative synthetic interactions with *ded1-ΔCT* ("suppressors") in the presence of rapamycin (529 genes with interaction score more than 1.5 standard deviations from the mean), and this network was then partitioned into 5 groups by *k*-means clustering (Figure 2A). A similar network was built and clustered for the 544 genes showing strongly positive synthetic interactions ("enhancers", Figure 2B). These clusters were then analyzed for Gene Ontology (GO) terms that are enriched in these subsets in order to determine which cellular processes and pathways interact with Ded1 most strongly during stress conditions.

Negative interactors / suppressors of ded1-ΔCT

Tables 1 and 2 show the most enriched GO-terms in each cluster (up to 10), following curation to remove highly similar terms (for complete lists of GO-terms, see Supplemental Tables S2 and S3). Suppressor cluster 1 included a substantial number of genes involved in amino acid metabolism, including multiple genes involved in synthesis of several different amino acids (arginine, isoleucine, serine, etc.) as well as synthesis of complex carboxylic acids (Table 1). Amino acid synthesis pathways are often upregulated in nutrient-poor conditions, so these genes may represent downstream targets regulated by Ded1, although amino acid availability also regulates TOR activity upstream (Crawford and Pavitt 2019; Saxton and

Sabatini 2017). Cluster 1 also included eight genes involved in mitochondrial translation, which may affect energy production for translation. Suppressor cluster 2 yielded a number of GO terms that are related to membrane-mediated trafficking, including phosphatidylinositol signaling, intralumenal vesicle formation, endosomal transport, and vacuole regulation. These genes could be regulating Ded1 activity through its degradation along with its binding partner eIF4G1 during cell stress (Aryanpur et al. 2019; Kelly and Bedwell 2015), or they could be cross-talk from TOR-dependent regulation of autophagy and endosomal trafficking (Hatakeyama et al. 2019; Saxton and Sabatini 2017; Strahl and Thorner 2007). Cluster 2 also included eight genes involved in ATP export, which may again reflect an effect on energy production.

Suppressor cluster 3 was largely focused on translation (Table 1), including 19 ribosomal proteins and at least 10 additional translation factors. Other aspects of translation were also represented, including ribosome biogenesis and non-coding RNA processing, which mostly consisted of tRNA processing genes (Supplemental Table S2). These are likely affecting the ability of Ded1 to regulate translation. Three protein chaperones that act co-translationally as well as three heme transport genes were also present in this cluster. Suppressor cluster 4 yielded relatively few GO terms, including the regulation of conjugation (mating) as well as carbohydrate metabolism. We have observed that *ded1-ΔCT* mutants have somewhat delayed sporulation compared to wild-type cells (data not shown), so these interactions are consistent with a Ded1 function in yeast mating/sporulation. Suppressor cluster 5 included a more diverse set of terms, including sucrose catabolism, peptidyl-histidine modification, double-strand break repair, and several terms related to chromatin remodeling and transcription. Alterations in chromatin state and/or transcription are of course part of stress responses and could represent upstream regulation or downstream targets of Ded1 activity following TOR inactivation

(Crawford and Pavitt 2019; Saxton and Sabatini 2017). The three peptidyl-histidine modification genes all target translation factors for modification (ribosomal proteins and elongation factors), which may explain their genetic interaction with Ded1 (Al-Hadid et al. 2016; Uthman et al. 2013).

Positive interactors / enhancers of ded1-ΔCT

Despite a similar number of hits, the enhancer clusters yielded fewer GO terms than the suppressors, suggesting a more diverse set of genes overall (Table 2 and Supplemental Table S3). Enhancer cluster 1 included a number of ribosomal and ribosomal-related proteins, showing that alterations in different proteins involved in translation have the potential to either synergize or antagonize Ded1 function during cell stress. Enhancer cluster 2 only yielded one significant GO-term, for hydrolase activity. These hydrolases are all involved in cell wall regulation during both sporulation and cytokinesis following mitosis. Their link to Ded1 is unclear but may be through sporulation and/or changes to the cell cycle during stress.

Enhancer cluster 3 gave the largest number of GO-terms for the enhancers overall with particular enrichment for signal transduction genes, particularly the MAPK pathway. Notably, several of these (e.g. *PTC2*, *SDP1*, *PTP2*) are phosphatases that negatively regulate the MAPK pathway (Martin et al. 2005); therefore, their deletion would tend to increase growth and might synergize with increased growth in the *ded1-ΔCT* mutant in rapamycin. Other GO-terms in this cluster included transcriptional responses to oxidative stress, which fits well with Ded1 function in stress, and protein glycosylation, which has unclear links to Ded1. Only one GO-term, aerobic respiration, was associated with enhancer cluster 4. This may again be due to energy requirements during stress. Finally, enhancer cluster 5 included several GO-terms associated

with membrane trafficking, similar to suppressor cluster 2, although with a more specific focus on vesicle trafficking, specifically. The relationship to Ded1 function is unclear, although these interactions may be due to TOR-dependent changes in membrane trafficking that affect Ded1 activity during stress.

Annotation of hits by rapamycin-dependent phenotype

In theory, the positive synthetic interactions / enhancers in this screen could be generated either by synergistic effects of a rapamycin-resistant mutation and the rapamycin-resistant *ded1-ΔCT* allele (a resistant enhancer phenotype), or by suppression of a rapamycin-sensitive mutation by *ded1-ΔCT* (a sensitive enhancer phenotype). Likewise, negative synthetic interactions / suppressors could be due to suppression of *ded1-ΔCT* rapamycin resistance by a rapamycin-sensitive mutation (sensitive suppressor), or by suppression by a rapamycin-resistant mutation (resistant suppressor). To attempt to assign hits to these various categories, we mined the phenotypes of the *Saccharomyces* Genome Database for those genes with mutations annotated as resistant or sensitive to rapamycin, and then we correlated these with the genes in our screen with an interaction score more than 1.0 standard deviation from the mean. Only a minority of the hits were annotated for a rapamycin-dependent phenotype (138 enhancers and 257 suppressors), so we were not able to conduct in-depth network analyses for these subsets. Nonetheless, we generated enriched GO-terms for each of the four subsets, which are summarized in Table 3 (for complete lists, see Supplemental Tables S4 and S5). The resistant enhancers subset included GO-terms for regulation of GTPase activity, regulation of transcription, ribosomal biogenesis, and response to stress. The sensitive enhancers subset included transcription elongation, phosphatase activity, membrane trafficking, translation, and DNA repair. The sensitive suppressors subset included the largest number of annotated hits (203) and yielded the largest number of GO-terms,

including intralumenal vesicle formation, other membrane trafficking terms, ATP export, TOR signaling, and DNA maintenance. By contrast, the resistant suppressors subset was the smallest with 54 genes, and GO-terms included transcription regulation, ubiquitination, and ion homeostasis. Overall, the GO-terms in this analysis largely corresponded to the terms from the cluster analysis above, with several new terms such as GTPase activity and ubiquitination. However, this division into subcategories may be useful in designing follow-up experiments to directly examine these interactions with Ded1.

In this screen, we obtained a large number of potential interactions with the *ded1-ΔCT* mutant. Many of these fell into categories that would be predicted by the known functions of Ded1 during cellular stress, including ribosomal proteins and translation factors, amino acid biosynthesis genes, and transcription and chromatin remodeling factors. Some of these, such as ribosomal proteins, translation factors, and amino acid regulators, likely function together with Ded1 and/or in parallel to effect immediate translational reprogramming during stress. Likewise, mutations affecting other gene expression processes (e.g. transcription and chromatin remodeling) can presumably also indirectly affect translation through mRNA transcript abundance. Interestingly, ribosomal proteins were identified as both enhancers and suppressors of *ded1-ΔCT*, perhaps reflecting the complexity of ribosome composition and function.

Several more categories of hits have more tangential links to the stress function of Ded1, including genes involved in membrane trafficking, signal transduction, mitochondrial / energy production genes, and sporulation genes. Stress regulation, and TOR signaling in particular, are strongly linked to changes in autophagy and other membrane trafficking processes (Saxton and Sabatini 2017), so it is not entirely surprising that genetic interactions between Ded1 and membrane trafficking components were observed. Likewise, Ded1 has been suggested

previously to have a role in the regulation of sporulation (Guenther et al. 2018), making hits in sporulation genes also highly plausible. Notably, the identified hits in the MAPK cascade are largely negative regulators of that pathway (Supplemental Table S3), so null mutants of these factors might be expected to enhance stress-resistant growth. Follow-up experiments to explore the links between Ded1 and these processes could lead to better understanding of the coordination and regulation of cellular stress responses.

Lastly, some hits were in unexpected categories, such as cell wall hydrolases, protein glycosylation, and GTPase activity. As with other hits, hits in this category could represent upstream regulators of Ded1 (GTPases), cross-talk between cellular processes (cell wall regulation or protein glycosylation), or possibly mRNAs that are translationally targeted by Ded1 (any). Future work may be able to elucidate these interactions with Ded1 and how they contribute to stress or other cellular responses.

Data Availability Statement:

Strains and plasmids are available upon request. The supplemental tables contain complete lists of all data and analysis from the screen, including interaction scores for all genes (Supplemental Table S1), SGD-annotated phenotypes (S4), and complete lists of GO-terms (S2, S3, and S5).

Acknowledgments:

We would like to thank the University of Arizona's Functional Genomics Core facility for support on and the use of the Singer RoToR HDA pinning robot along with essential reagents and training. We would also like to thank members of the Bolger laboratory, past and present, for discussions and suggestions on the screen results and the manuscript.

Conflict of Interest:

The authors declare they have no conflicts of interest in this study.

Funder Information:

This work was supported by a grant from the National Institutes of Health to T.A.B. (1R01-GM136827).

Literature Cited:

Al-Hadid Q, Roy K, Chanfreau G, Clarke SG. 2016. Methylation of yeast ribosomal protein rpl3 promotes translational elongation fidelity. RNA. 22(4):489-498.

Aryanpur PP, Mittelmeier TM, Bolger TA. 2022. The rna helicase ded1 regulates translation and granule formation during multiple phases of cellular stress responses. Mol Cell Biol. 42(1):e0024421.

Aryanpur PP, Regan CA, Collins JM, Mittelmeier TM, Renner DM, Vergara AM, Brown NP, Bolger TA. 2017. Gle1 regulates rna binding of the dead-box helicase ded1 in its complex role in translation initiation. Mol Cell Biol.

Aryanpur PP, Renner DM, Rodela E, Mittelmeier TM, Byrd A, Bolger TA. 2019. The dead-box rna helicase ded1 has a role in the translational response to torc1 inhibition. Mol Biol Cell. 30(17):2171-2184.

Baryshnikova A, Costanzo M, Kim Y, Ding H, Koh J, Toufighi K, Youn JY, Ou J, San Luis BJ, Bandyopadhyay S et al. 2010. Quantitative analysis of fitness and genetic interactions in yeast on a genome scale. Nat Methods. 7(12):1017-1024.

Beckham C, Hilliker A, Cziko AM, Noueiry A, Ramaswami M, Parker R. 2008. The dead-box rna helicase ded1p affects and accumulates in saccharomyces cerevisiae p-bodies. Mol Biol Cell. 19(3):984-993.

Crawford RA, Pavitt GD. 2019. Translational regulation in response to stress in saccharomyces cerevisiae. Yeast. 36(1):5-21.

Gerashchenko MV, Lobanov AV, Gladyshev VN. 2012. Genome-wide ribosome profiling reveals complex translational regulation in response to oxidative stress. Proc Natl Acad Sci U S A. 109(43):17394-17399.

Giaever G, Chu AM, Ni L, Connelly C, Riles L, Veronneau S, Dow S, Lucau-Danila A, Anderson K, Andre B et al. 2002. Functional profiling of the saccharomyces cerevisiae genome. Nature. 418(6896):387-391.

Giaever G, Nislow C. 2014. The yeast deletion collection: A decade of functional genomics. Genetics. 197(2):451-465.

Guenther UP, Weinberg DE, Zubradt MM, Tedeschi FA, Stawicki BN, Zagore LL, Brar GA, Licatalosi DD, Bartel DP, Weissman JS et al. 2018. The helicase ded1p controls use of near-cognate translation initiation codons in 5' utrs. Nature. 559(7712):130-134.

Gupta N, Lorsch JR, Hinnebusch AG. 2018. Yeast ded1 promotes 48s translation pre-initiation complex assembly in an mrna-specific and eif4f-dependent manner. Elife. 7.

Hatakeyama R, Peli-Gulli MP, Hu Z, Jaquenoud M, Garcia Osuna GM, Sardu A, Dengjel J, De Virgilio C. 2019. Spatially distinct pools of torc1 balance protein homeostasis. Mol Cell. 73(2):325-338 e328.

Hegemann JH, Heick SB. 2011. Delete and repeat: A comprehensive toolkit for sequential gene knockout in the budding yeast saccharomyces cerevisiae. Methods Mol Biol. 765:189-206.

Hilliker A, Gao Z, Jankowsky E, Parker R. 2011. The dead-box protein ded1 modulates translation by the formation and resolution of an eif4f-mrna complex. Mol Cell. 43(6):962-972.

Ingolia NT, Ghaemmaghami S, Newman JR, Weissman JS. 2009. Genome-wide analysis in vivo of translation with nucleotide resolution using ribosome profiling. Science. 324(5924):218-223.

Kelly SP, Bedwell DM. 2015. Both the autophagy and proteasomal pathways facilitate the ubp3p-dependent depletion of a subset of translation and rna turnover factors during nitrogen starvation in saccharomyces cerevisiae. RNA. 21(5):898-910.

Liu B, Qian SB. 2014. Translational reprogramming in cellular stress response. Wiley Interdiscip Rev RNA. 5(3):301-315.

Martin H, Flandez M, Nombela C, Molina M. 2005. Protein phosphatases in mapk signalling: We keep learning from yeast. Mol Microbiol. 58(1):6-16.

Mi H, Ebert D, Muruganujan A, Mills C, Albou LP, Mushayamaha T, Thomas PD. 2021. Panther version 16: A revised family classification, tree-based classification tool, enhancer regions and extensive api. Nucleic Acids Res. 49(D1):D394-D403.

Mo J, Liang H, Su C, Li P, Chen J, Zhang B. 2021. Ddx3x: Structure, physiologic functions and cancer. Mol Cancer. 20(1):38.

Northcott PA, Jones DT, Kool M, Robinson GW, Gilbertson RJ, Cho YJ, Pomeroy SL, Korshunov A, Lichter P, Taylor MD et al. 2012. Medulloblastomics: The end of the beginning. Nat Rev Cancer. 12(12):818-834.

Pakos-Zebrucka K, Koryga I, Mnich K, Ljujic M, Samali A, Gorman AM. 2016. The integrated stress response. EMBO Rep. 17(10):1374-1395.

Saxton RA, Sabatini DM. 2017. Mtor signaling in growth, metabolism, and disease. Cell. 168(6):960-976.

Sen ND, Zhou F, Ingolia NT, Hinnebusch AG. 2015. Genome-wide analysis of translational efficiency reveals distinct but overlapping functions of yeast dead-box rna helicases ded1 and eif4a. Genome Res. 25(8):1196-1205.

Sharma D, Jankowsky E. 2014. The ded1/ddx3 subfamily of dead-box rna helicases. Crit Rev Biochem Mol Biol. 49(4):343-360.

Singh I, Pass R, Togay SO, Rodgers JW, Hartman JLt. 2009. Stringent mating-type-regulated auxotrophy increases the accuracy of systematic genetic interaction screens with saccharomyces cerevisiae mutant arrays. Genetics. 181(1):289-300.

Snel B, Lehmann G, Bork P, Huynen MA. 2000. String: A web-server to retrieve and display the repeatedly occurring neighbourhood of a gene. Nucleic Acids Res. 28(18):3442-3444.

Snijders Blok L, Madsen E, Juusola J, Gilissen C, Baralle D, Reijnders MR, Venselaar H, Helsmoortel C, Cho MT, Hoischen A et al. 2015. Mutations in ddx3x are a common cause of unexplained intellectual disability with gender-specific effects on wnt signaling. American journal of human genetics. 97(2):343-352.

Strahl T, Thorner J. 2007. Synthesis and function of membrane phosphoinositides in budding yeast, saccharomyces cerevisiae. Biochim Biophys Acta. 1771(3):353-404.

Szklarczyk D, Gable AL, Nastou KC, Lyon D, Kirsch R, Pyysalo S, Doncheva NT, Legeay M, Fang T, Bork P et al. 2021. The string database in 2021: Customizable protein-protein networks, and functional characterization of user-uploaded gene/measurement sets. Nucleic Acids Res. 49(D1):D605-D612.

Tang L, Levy T, Guillory S, Halpern D, Zweifach J, Giserman-Kiss I, Foss-Feig JH, Frank Y, Lozano R, Belani P et al. 2021. Prospective and detailed behavioral phenotyping in ddx3x syndrome. Mol Autism. 12(1):36.

Tibshirani R, Walther G, Hastie T. 2001. Estimating the number of clusters in a data set via the gap statistic. Journal of the Royal Statistical Society: Series B (Statistical Methodology). 63(Part 2):411-423.

Tong AH, Boone C. 2006. Synthetic genetic array analysis in saccharomyces cerevisiae. Methods Mol Biol. 313:171-192.

Tong AH, Evangelista M, Parsons AB, Xu H, Bader GD, Page N, Robinson M, Raghibizadeh S, Hogue CW, Bussey H et al. 2001. Systematic genetic analysis with ordered arrays of yeast deletion mutants. Science. 294(5550):2364-2368.

Uthman S, Bar C, Scheidt V, Liu S, ten Have S, Giorgini F, Stark MJ, Schaffrath R. 2013. The amidation step of diphthamide biosynthesis in yeast requires dph6, a gene identified through mining the dph1-dph5 interaction network. PLoS Genet. 9(2):e1003334.

Valentini M, Linder P. 2021. Happy birthday: 30 years of rna helicases. Methods Mol Biol. 2209:17-34.

Wagih O, Usaj M, Baryshnikova A, VanderSluis B, Kuzmin E, Costanzo M, Myers CL, Andrews BJ, Boone CM, Parts L. 2013. Sgatools: One-stop analysis and visualization of array-based genetic interaction screens. Nucleic Acids Res. 41(Web Server issue):W591-596.

Tables and Figures:

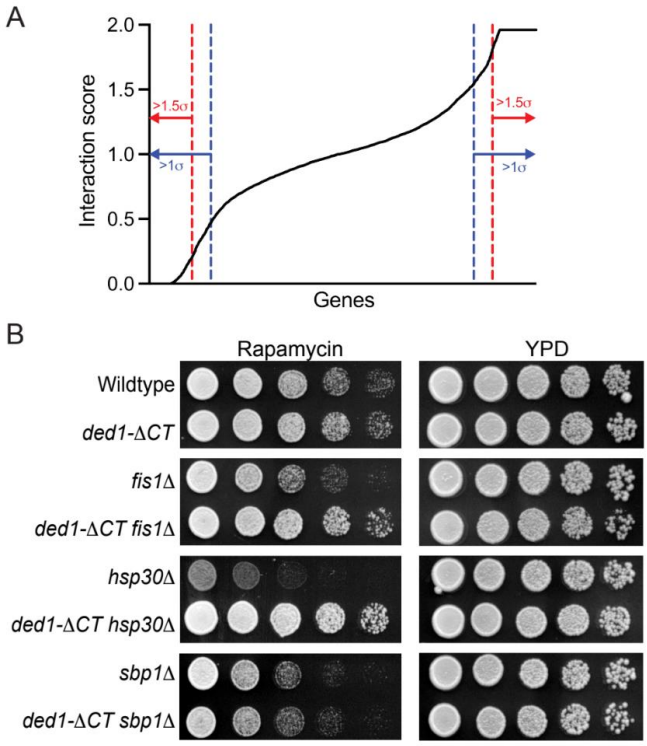

Figure 1: Identification of genetic interactions with *ded1-ΔCT* following rapamycin treatment. (A) The synthetic interaction scores with *ded1-ΔCT* for growth on rapamycin for all genes tested (4799) are shown in ascending order. Dashed blue lines represent 1 standard deviation from the mean score, and dashed red lines represent 1.5 standard deviations. Genes falling outside of these thresholds were considered "hits" and used for further analysis. (B) Growth of single (*fis1Δ*, *hsp30Δ*, and *sbp1Δ*) and *ded1-ΔCT* double mutants for three representative hits on rich media (YPD) and rich media plus rapamycin are shown. Five-fold serial dilutions were grown at 30°C for 2 (YPD) or 4 (Rapamycin) days. Synthetic interactions were observed consistent with the screen results.

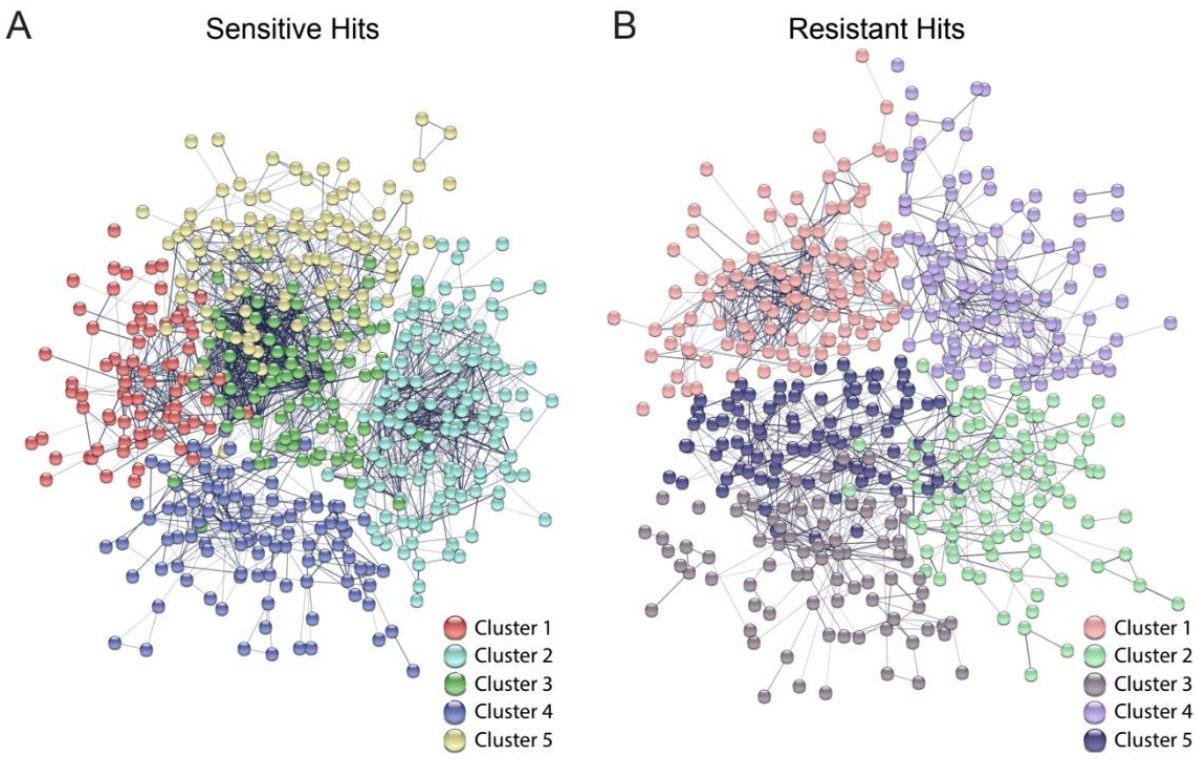

Figure 2: Network cluster maps of interacting genes. Network maps were generated using STRING for the synthetic negative / suppressors of *ded1-ΔCT* (A) and the synthetic positive / enhancers of *ded1-ΔCT* (B) hits that exceeded the 1.5 standard deviation threshold below and above the mean interaction score, respectively. Thickness of the edges between genes signifies the strength of data support for the interaction. Disconnected nodes / genes are not shown. Clusters were generated via k-means clustering. The identity of each cluster (#1-5) is labeled below, and corresponding colors were used in Tables 1 and 2.

Table 1: Enriched GO-terms in cluster analysis of suppressors

	GO-Term	# of Proteins	Strength	False Discovery Rate
Cluster 1	Tricarboxylic acid metabolic process	3	1.5	0.0357
	Re-entry into mitotic cell cycle after pheromone arrest	3	1.45	0.0439
	Branched-chain amino acid biosynthetic process	4	1.32	0.0133
	Alpha-amino acid metabolic process	21	0.98	1.26×10^{-11}
	Dicarboxylic acid metabolic process	5	0.97	0.0399
	Mitochondrial translation	8	0.77	0.0142
Cluster 2	Phosphatidylinositol-3-phosphate biosynthetic process	4	1.55	0.0018
	Intralumenal vesicle formation	4	1.41	0.0041
	ATP export	8	1.32	2.05×10^{-5}
	Protein retention in Golgi apparatus	4	1.21	0.0135
	Vacuolar acidification	8	1.12	0.00011
	Retrograde transport, endosome to Golgi	8	0.98	0.00044
	Phosphatidylinositol metabolic process	10	0.87	0.00025
	Vesicle organization	15	0.83	2.05×10^{-5}
	Late endosome to vacuole transport	9	0.83	0.0012
	Vacuole organization	13	0.82	5.59×10^{-5}
Cluster 3	Heme transport	3	1.7	0.0108
	De novo co-translational protein folding	3	1.55	0.0214
	Structural constituent of ribosome	19	0.86	3.00×10^{-8}
	Translation	29	0.81	1.19×10^{-12}
	Ribosome biogenesis	17	0.55	0.0009
	RNA binding	26	0.51	2.06×10^{-5}
	ncRNA processing	15	0.51	0.0081
Cluster 4	Regulation of conjugation with cellular fusion	8	0.82	0.0465
	Carbohydrate metabolic process	19	0.74	1.23×10^{-5}
Cluster 5	Sucrose catabolic process	3	1.35	0.0186
	Peptidyl-histidine modification	3	1.3	0.0238
	Histone H3 acetylation	3	1.3	0.0238
	Nucleosome disassembly	6	1.26	0.0001
	Telomere tethering at nuclear periphery	5	1.22	0.001
	Histone deacetylation	7	1.19	5.00×10^{-5}

	Posttranscriptional tethering of RNA polymerase II gene DNA at nuclear periphery	4	1.13	0.012
	Double-strand break repair via nonhomologous end joining	6	1.11	0.0006
	DNA-templated transcription, elongation	12	1.06	2.12×10^{-7}
	Regulation of transcription by RNA polymerase I	6	0.96	0.0031

Table 2: Enriched GO-terms in cluster analysis of enhancers

	GO-Term	# of Proteins	Strength	False Discovery Rate
Cluster 1	Ribosome	16	0.51	0.0358
Cluster 2	Hydrolase activity, hydrolyzing O-glycosyl compounds	8	1.01	0.0036
Cluster 3	Regulation of transcription from RNA polymerase II promoter in response to oxidative stress	3	1.39	0.0449
	Peptidyl-tyrosine dephosphorylation	4	1.17	0.0293
	Regulation of MAPK cascade	5	1.04	0.0216
	Negative regulation of signal transduction	6	1	0.0119
	Regulation of signal transduction	12	0.83	0.00032
	Protein glycosylation	7	0.83	0.0194
	Cellular response to abiotic stimulus	6	0.8	0.0449
	Establishment or maintenance of cell polarity	9	0.76	0.0096
Cluster 4	Aerobic respiration	11	0.81	0.0083
Cluster 5	AP-type membrane coat adaptor complex	5	1.39	0.0045
	Late endosome	5	0.87	0.0499
	Vesicle	12	0.53	0.0366
	Bounding membrane of organelle	20	0.38	0.0366

Table 3: Enriched GO-terms in previously-annotated hits

	GO-Term	# of Proteins	Strength	P-value
Known rapamycin-resistant enhancers	Positive regulation of GTPase activity	4	1.08	0.0005
	Negative regulation of transcription by RNA polymerase II	6	0.64	0.0026
	Response to oxidative stress	5	0.63	0.0066
	Regulation of intracellular signal transduction	4	0.62	0.0167
	Ribosomal large subunit biogenesis	4	0.51	0.0360
	Telomere organization	4	0.51	0.0360
	Chromatin organization	9	0.50	0.0022
	Positive regulation of transcription by RNA polymerase II	9	0.50	0.0022
Known rapamycin-sensitive enhancers	Positive regulation of DNA-templated transcription elongation	4	0.85	0.0029
	Dephosphorylation	4	0.77	0.0054
	Endocytosis	6	0.67	0.0021
	Protein localization to membrane	5	0.52	0.0188
	Regulation of translation	6	0.49	0.0137
	Autophagy	5	0.42	0.0419
	DNA repair	8	0.41	0.0136
	Vesicle-mediated transport	11	0.38	0.0059
Known rapamycin-resistant suppressors	Negative regulation of transcription by RNA polymerase II	9	0.90	2.03×10^{-6}
	RNA catabolic process	5	0.64	0.0058
	Protein ubiquitination	4	0.62	0.0168
	Positive regulation of transcription by RNA polymerase II	8	0.53	0.0024
	Cellular ion homeostasis	4	0.49	0.0423
Known rapamycin-sensitive suppressors	Intralumenal vesicle formation	4	1.25	0.0003
	ATP export	9	1.22	4.63×10^{-8}
	Protein localization to Golgi apparatus	8	1.07	1.91×10^{-6}
	Maintenance of DNA trinucleotide repeats	4	1.05	0.0010
	Positive regulation of TOR signaling	4	0.98	0.0016
	Homoserine metabolic process	4	0.92	0.0025
	Retrograde transport, endosome to Golgi	11	0.89	7.47×10^{-7}
	Vacuolar acidification	7	0.89	8.31×10^{-5}

APPENDIX B

YEAST CELL CYCLE WITH SYTOX GREEN

1. Grow cells under the desired conditions to 0.5-1x10^7 cells/mL. Collect up to 1-2x10^7 cells per sample. All the following steps can be performed in a single 1.7mL microfuge tube per sample.
2. Pellet the cells (a few seconds in a microfuge). Resuspend the cells in 300µl H_2O. Be sure the pellets have been dispersed before the next step.
3. Add 0.7mL 100% ethanol and vortex; incubate at 4°C for at least 30 minutes.
4. Pellet the cells as before and resuspend in 1mL of 50mM sodium citrate, pH 7.4.
5. Sonicate the cells (10 pulses of 0.9 seconds each, setting of –32 to –40).
6. Pellet the cells again and resuspend them in 1mL Na-citrate containing 0.25mg/mL RNase A. Incubate at 50-55°C for 1 hour.
7. Add 25µL of 20mg/mL Proteinase K and continue the incubation for an additional hour.
8. Pellet the cells again and resuspend the pellets in 500µl of 50mM Na-citrate. *[But go instead to "Alternative" in Step 10 if your cell concentration is not very high.]*
9. Prepare a batch of 1x Sytox Green (= 1µM) in 50mM Na-citrate. The stock solution provided by the vendor is 5mM = 5000x, in DMSO. Note: the manufacturer recommends wearing two pairs of gloves when handling the stock solution. The Sytox stock solution takes a while to thaw, so plan ahead.
10. Pipette out 1 ml aliquots of the 1x Sytox solution into FACS analysis tubes (Falcon 2054). Add 50µL of the cell sample (or enough to get ~1-2x10^6cells; the goal is to have 100-200 events per second within the gated region when the samples are being read). Incubate 1 hour to overnight at 4°C; stained samples can be stored at 4°C for several weeks. *[Alternative: If your sample is low-concentration, you can simply add 1 ml of 2x Sytox to the cell sample immediately after step 7, and you'll be good to go.]*
11. Use FL1 on the FACSCAN instrument. Sytox Green fluoresces more strongly than propidium iodide, so the voltage/gain won't have to be set as high as with propidium iodide.

Sytox Green: Invitrogen, catalog # S7020

APPENDIX C

Translational control by helicases during cellular stress

Sara B. Carey[1] and Timothy A. Bolger[1#]

[1] Department of Molecular and Cellular Biology, University of Arizona, Tucson, Arizona, USA.

[#] Address correspondence to TAB, tbolger@email.arizona.edu

Key words: helicase, translation, stress, yeast, growth curve, polysome profile, metabolic labeling, luciferase

Running title: Translation during stress

Abstract

Stress is inevitable, so all organisms have developed response mechanisms to allow for their survival during times of stress. Regulation of gene expression is a critical part of these responses, which allows for the appropriate cohort of proteins to be produced to counter the stress while downregulating others in order to conserve resources. Translation is both highly energy intensive and able to rapidly shift the proteome, thus making it a key target for regulation during stress. Numerous stress pathways converge on translation, and examining the regulatory mechanisms that underlie these pathways is essential for understanding the initial and long-term effects of stress on cells. A number of RNA helicases, including eIF4A, Ded1/DDX3X, and Dhh1/DDX6, have been previously linked to translation, and given their ability to dramatically alter RNA-protein interactions, they are well-positioned to play critical roles in translation regulation during stress. Therefore, assessing the role of helicases in these conditions is vital to the overall understanding of stress. Outlined below are key assays focusing on two areas: assessing cellular phenotypes in growth and survival during stress conditions, and analyzing cellular translation in the presence and absence of stress. The combination of these two approaches will begin to establish the function(s) of a given helicase in the overall stress response.

Contents

iii. Notes

4.3 Polysome profiles and fractionation

i. Equipment and reagents

ii. Procedure

iii. Notes

5. Other general protocols
6. Summary and conclusions
7. Acknowledgments
8. References

1. Introduction

Whether single-celled microbes or higher eukaryotes, cells frequently face a variety of environmental stresses, and they mount a variety of responses to these stresses in order to continue to proliferate and survive. In particular, adverse conditions, such as nutrient deprivation, osmotic shifts, or temperature shock, induce highly coordinated changes in gene expression at all levels so that the proper cohort of proteins is produced to allow for maintenance of critical cell functions and viability. (Albig & Decker, 2001; B. Liu & Qian, 2014; Saavedra, Tung, Amberg, Hopper, & Cole, 1996). The extensive regulatory mechanisms governing gene expression in the cellular stress response ensure that these changes are implemented with high fidelity (Y. Liu, Beyer, & Aebersold, 2016; Mitchell & Parker, 2014). Although vital for cellular response and organismal survival, many of these mechanisms and their connections to signaling hubs, such as the Target-of-Rapamycin (TOR) pathway, are poorly understood.

Changes in translation play a particularly large role in stress responses. Translation is one of the most energy intensive cellular processes; therefore, in energy limiting conditions, general downregulation of translation is required in order to conserve cellular resources for responding to the stress (B. Liu & Qian, 2014). Supporting this idea, ribosome footprinting (Ribo-Seq) studies have indicated that massive translational reprogramming occurs under stress with changes in translational efficiency of a third or more of all mRNAs (Gerashchenko, Lobanov, & Gladyshev, 2012; Ingolia, Ghaemmaghami, Newman, & Weissman, 2009). However, this regulation is specific and complex, wherein bulk translation is down-regulated, but translation of some mRNAs is up-regulated (e.g. those that encode proteins needed to respond to the stress) (Crawford & Pavitt, 2019; B. Liu & Qian, 2014). While some of the regulatory mechanisms controlling translation in stress are relatively well-defined, such as the canonical Integrated

Stress Response (ISR) that results in phosphorylation and inhibition of the translation factor eIF2α (Costa-Mattioli & Walter, 2020), others remain much more poorly defined. Underscoring the importance of this research, stress response pathways are often misregulated in disease, including cancer and aging (Gonskikh & Polacek, 2017; Robichaud, Sonenberg, Ruggero, & Schneider, 2019).

In addition to the ISR, another major signaling hub for controlling stress responses is the Target-Of-Rapamycin (TOR) pathway. When active the TOR pathway is responsible for cell proliferation, protein synthesis, and ribosome synthesis, while stresses such as nutrient starvation cause inhibition of TOR and repression of these processes, including translation (Gonzalez & Rallis, 2017; Saxton & Sabatini, 2017). Inhibition of TOR leads to inactivation of a number of translation factors through a variety of mechanisms, including dephosphorylation of ribosomal protein S6, inhibition of eIF4E through 4E-BPs, and degradation of eIF4G and other factors (Berset, Trachsel, & Altmann, 1998; Kelly & Bedwell, 2015; Spriggs, Bushell, & Willis, 2010). We and others have also found that at least two members of the DEAD-box RNA helicase family, eIF4A and Ded1, are part of the translational response to TOR inhibition. The DEAD-box proteins are the largest family of RNA helicases, and they play multiple, critical roles in gene expression, acting to remodel both RNA secondary structures and RNA-protein binding in a largely non-processive manner (Valentini & Linder, 2021). PDCD4, which is downregulated by the TOR-dependent S6 Kinase, is a well-established inhibitor of eIF4A, and eIF4B, a binding partner of eIF4A, is also regulated by TOR (Roux & Topisirovic, 2018; Yang et al., 2003). More recently, we showed that Ded1 appears to switch from promoting translation initiation in pro-growth conditions to down-regulating translation following TOR inactivation, at least in part by promoting dissociation and degradation of eIF4G (Aryanpur et al., 2019). In addition to these

direct roles in translation, eIF4A, Ded1 and its human ortholog DDX3X, and Dhh1/DDX6 all play roles in the assembly and disassembly of stress granules and processing bodies, cytoplasmic accumulations of RNA and protein that form in response to stresses (Beckham et al., 2008; Carroll, Munchel, & Weis, 2011; Hilliker, Gao, Jankowsky, & Parker, 2011; Tauber et al., 2020).

Because these regulatory mechanisms are vital for adequate translation of proteins and for coordinated and effective response to stress, understanding how to evaluate RNA helicases for translation abnormalities is crucial for understanding the total cellular response to stress. Outlined in this chapter are specific assays for understanding differences in translation between wild-type cells and genetically altered cells both in normal, pro-growth conditions and during stress. Two sets of assays are described. The first set (Section 2) allow for characterization of growth phenotypes during stress. These growth phenotypes indirectly assess translation but can provide reliable insight into helicase function. For instance, mutating a relevant helicase, such as Ded1, could affect cells' ability to continue to grow and/or survive during stress. Such a result alone does not provide definitive evidence that the helicase is promoting this resistance via a translational response. Assays in the second set (Section 3) can then address this hypothesis more directly by examining cellular translation status under the same conditions as the first set of assays. Combining the results from both sets of assays would thus build confidence that the helicase (or other factor) has an important function in the translational stress response. In essence, the protocols described here provide a roadmap for the initial characterization of a specific factor hypothesized to play a role in these responses.

2. General reagents and conditions

Throughout this chapter are general protocols for assessing the function of a helicase regarding translational control during cellular stress. These protocols are meant to serve as guidelines to assess any helicase in any type of stress but were optimized using the specific conditions and yeast strains that are detailed below.

2.1 Media

i. YEPD

1. Dextrose stock: 40% dextrose (w/v) in dH_2O. Autoclave.
2. Liquid media (1 L): 10 g yeast extract, 20 g peptone, 200 µl 10N NaOH in 950 ml dH_2O.
    i. Aliquot media (237.5 ml is a convenient stock volume) as desired and autoclave.
    ii. Add dextrose to media to final concentration of 2% (12.5 ml in 237.5 ml media).
3. Plate media (1 L): 10 g yeast extract, 20 g peptone, 20 g agar, 200 µl 10N NaOH in 950 ml dH_2O in a suitable Erlenmeyer flask.
    i. Add a stir bar to media and autoclave.
    ii. Place media on stir plate and stir until mixture has cooled enough to comfortably touch the glass.
    iii. Add dextrose to media to final concentration of 2% (50 ml for 1 L media). Add to side of flask to reduce bubbles.

iv. Pour plates: add 20 to 25 ml of media to each 10 cm petri plate. We recommend wrapping the neck of the flask in paper towels to catch drips. A Bunsen burner can be used to pop bubbles.

ii. Minimal/selective media

1. Amino acid drop-out mix: 100 g yeast nitrogen base (YNB) w/o amino acids and w/o ammonium sulfate, 293.11 g ammonium sulfate, 1.2 g adenine sulfate, 1.2 g L-arginine sulfate, 1.2 g L-histidine-HCl, 1.8 g L-isoleucine, 3.6 g L-leucine, 1.8 g L-lysine-HCl, 1.2 g L-methionine, 3.0 g L-phenylalanine, 1.2 g L-tryptophan, 1.8 g L-tyrosine, 1.2 g L-uracil, 9.0 g L-valine, 1.5 g L-aspartic acid, 1.5 g L-glutamic acid, 1.5 g L-threonine, 1.5 g L-serine, 1.5 g L-proline
    i. The above list contains all necessary amino acids. If selective media is required, leave that amino acid out of the mix.
    ii. Thoroughly mix amino acids, then gradually mix in YNB and ammonium sulfate. We recommend a blender if possible.
2. Dextrose stock: 40% dextrose (w/v) in dH_2O. Autoclave.
3. Liquid media (1 L): 7.1 g amino acid drop-out mix, 200 µl 10N NaOH in 950 ml dH_2O.
    i. If adjustments to the drop-out mix are needed, the desired amino acid can be added in the following amounts (per L): 20 mg histidine, 60 mg leucine, 20 mg uracil, 20 mg tryptophan, 30 mg lysine, 20 mg methionine, 20 mg adenine.
    ii. Aliquot media (237.5 ml is a convenient stock volume) as desired and autoclave.

iii. Add dextrose to media to final concentration of 2% (12.5 ml in 237.5 ml media).

4. Plate media (1 L): 7.1 g amino acid drop-out mix, 20 g agar, 200 µl 10N NaOH in 950 ml dH_2O in a suitable Erlenmeyer flask.
    i. If adjustments to the drop-out mix are needed, add the desired amino acid as above.
    ii. Add a stir bar to media and autoclave.
    iii. Place media on stir plate and stir until mixture has cooled enough to comfortably touch the glass.
    iv. Add dextrose to media to final concentration of 2% (50 ml for 1 L media). Add to side of flask to reduce bubbles.
    v. Pour plates: add 20 to 25 ml of media to each 10 cm petri plate. We recommend wrapping the neck of the flask in paper towels to catch drips. A Bunsen burner can be used to pop bubbles.

2.2 Stress conditions

Table 1 lists several potential stressors along with the treatment conditions that we have tested previously. The user may find that they require further optimization in their hands, however. Of course, other stressors (e.g. DNA damage agents, heavy metal toxicity, etc.) can also be used as the user finds appropriate.

2.3 Strains previously used

Table 2 contains a list of several yeast strains that we have previously tested in many of the above stress conditions (Aryanpur, Mittelmeier, & Bolger, 2022; Aryanpur et al., 2019; Bolger & Wente, 2011; Takahara & Maeda, 2012; Thomas & Rothstein, 1989). We have generally used the W303 yeast background in our studies. Many stress responses (particularly TOR dependent ones) seem to be more pronounced in this background compared to, for example, the S288C / Research Genetics strains used to generate many of the available yeast libraries.

3. Growth assays to assess stress phenotypes

Yeast growth assays are routinely used to assess growth phenotypes of mutant strains. Perhaps the most well-known qualitative method to assess yeast growth phenotypes is the spot titer method (yeast serial dilution growth assay). Advantages of this method include ease of setup and the ability to qualitatively assess differences in growth between several different strains. However, this method is not well suited for capturing smaller but still significant differences in yeast growth rate and cannot accurately differentiate between different phases of yeast growth (lag, exponential, diauxic, stationary). Furthermore, it is not a good method for screening a larger number of strains in different growth conditions, as making serial dilutions is time-consuming and becomes limiting. Liquid culture methods that measure optical density of cultures (at 600 nm) over a time-course are a more quantitative way to assess yeast growth and can capture more subtle differences in growth rate of yeast strains. Ultimately, this can lead to a more nuanced understanding of how different gene mutations affect yeast growth rate and determine whether specific growth phases are affected. Additionally, liquid growth methods can easily be adapted to

screen many yeast strains under different growth conditions and/or drug treatments using 96-well plate micro-cultures. Both protocols have their advantages and disadvantages depending on the nature of the question being addressed.

A central consideration in assessing stress phenotypes is the nature of the stress, as different stressors induce multiple different pathways as part of the stress response. Examples of these include sugar or amino acid deprivation, temperature shock, oxidative stress, and osmotic shock, all of which have been shown to be mediated by helicases (Aryanpur et al., 2022; Aryanpur et al., 2019; Beck et al., 2014; Carroll et al., 2011; Hilliker et al., 2011; Iserman et al., 2020; Seok, Nguyen, Van Nguyen, Lee, & Moon, 2020). Growth assays may be designed for chronic stress, where cells are grown at constant semi-permissive conditions (e.g. <1 mM hydrogen peroxide), for survival/recovery, where cells are subjected to intense stress where no growth occurs followed by incubation in pro-growth conditions (e.g. 50 °C for 1 hr followed by 30 °C recovery), or for pharmacological inhibition of specific stress pathways (e.g. 200 ng / ml rapamycin). If a general analysis of phenotypes during cellular stress is desired, we recommend assaying a panel of these different conditions.

3.1 Spot titer growth analysis

The spot titer method is one of the simplest methods for growth analysis of yeast strains. Cells at a pre-determined range of concentrations are “spotted” in a small droplet onto the desired agar media, then incubated until grown sufficiently to discern differences amongst strains. This protocol is for 5 spots of 1:5 dilutions with 100000, 20000, 4000, 800, 160 cells per spot. Other dilutions, numbers of cells, and number of spots can also be used; the math and preparation will need to be adjusted to reflect these changes. As mentioned above, the media

used will depend on the stress condition tested. General controls will include media lacking the stress (or cells that have not been exposed to it) and ideally, positive and negative control yeast strains.

i. Equipment and Reagents

1. Spectrophotometer or hemacytometer (depending how cell concentration will be calculated)
2. Microcentrifuge
3. Benchtop vortexer
4. Incubator(s)
5. Flatbed scanner with associated software (EPSON Perfection V500)
6. Sterile 1.5 ml tubes
7. Plates with desired media (see section 2.1 and Table 1)
8. Sterile dH_2O or liquid media
9. Desired yeast strains (see Table 2)

ii. Procedure

1. Grow yeast cultures overnight in 3 ml of appropriate media.
2. Back-dilute cultures and grow to log phase growth (OD_{600} = 0.2 to 0.8)
3. Set up tubes for serial dilutions:
    a. For each sample to be analyzed collect 5 x 1.5 ml Eppendorf tubes.
    b. Add 400 µl sterile water (or liquid media, see notes) to 4 of the 5 sets of tubes, leaving the 5^{th} tube empty. The 5^{th} tube will be used for step 5.

c. Warm up plates for 30 to 60 min prior to plating (see notes for plate suggestion).

4. Determine the number of cells / ml for each strain by:
    a. Counting with hemacytometer: follow standard directions, but generally, the average number of cells in the large squares (4x4 or 5x5) is multiplied by 10^5 cells / ml.
    b. Measuring OD_{600} (Note: this is obviously faster but may be inaccurate if one or more of the strains are irregular in shape or size). Multiply OD_{600} values by 50 x 10^6 cells / ml.
5. Calculate volume of culture needed for the initial spot (see below). Pipet appropriate number of cells into the empty tube from tube setup (#3).
    a. If plating on YEPD plates, use 6.25 x 10^6 cells.
    b. For selective plates, use 5 x 10^6 cells.
6. Equalize sample volumes and cell concentration:
    a. If volumes of <u>all</u> samples are less than 250 μl, add sterile water (or liquid media) up to 250 μl.
    b. If not, centrifuge samples at full speed for 1 min and aspirate supernatant. (See notes about selective media.) Add 250 μl sterile water or liquid media and vortex briefly.
7. Add 100 μl of cell suspensions from this set of tubes to the next set of tubes (with 400 μl water or media already in them).
8. Vortex briefly.

9. Repeat by adding 100 µl of the diluted cells to the next set of tubes to make successive dilutions.
10. Tape down plates on top of pattern template (Figure 1A).
11. Spot cell suspensions: Take 4 µl (5 µl if selective media) from 1st dilution, pipet onto plate(s) as a circular spot. Repeat for rest of dilutions, arranging the serially diluted spots in a line for each strain. Be sure to briefly vortex each dilution before spotting.
12. Wait for spots to dry/absorb into plate, then incubate at desired temperature.
13. Take out plates, allow to equilibrate to room temperature (to avoid condensation during imaging), and use a flatbed scanner to image as desired (Figure 1B; also see notes for information on growth period).

iii. Notes

1. Unlike liquid phase growth assays, spot titer assays are less sensitive to whether the cells are in early-, mid-, or late-log phase when plated, although the cell concentrations of the strains tested should be relatively close to each other.
2. Diluting in sterile water versus media: while yeast cells can tolerate a temporary suspension in water, it is both nutrient deprivation and an osmotic shock. The user may therefore wish to consider diluting the cells in liquid media similar to that used to induce the stress.
3. Warming up plates: 6 to 8 strains can fit on one plate, depending on how tightly packed the spots are. Use this as a basic metric to determine the number of plates needed.
4. Centrifuging with selective media: cells will spin down more easily in selective media if water or YPD is added to the tubes prior to centrifugation.

5. Pipeting: if dilutions are made in 96-well plates instead of 1.5 ml tubes, a multichannel pipet can be used for making the dilutions and for spotting cells. Extra care must be taken that equal volumes are pipetted for each channel, so normal micropipets are preferred unless a large number of strains are to be assayed.
6. Growth period: Wild-type cells on dextrose at 30 °C or 37 °C usually take ~1 day, at 25 °C takes ~2 days. Other sugars, drug treatments, or growth at 16 °C can require 5 to 10 days. Once the colonies have grown sufficiently, the apparent colony size will increase more slowly. Strains that grow more slowly can then "catch up", making differences in growth less apparent. Thus, the ideal imaging time must be determined empirically and is before growth has begun to slow.

3.2 96-Well Plate Growth Analysis

This protocol describes the use of 96-well plate micro-cultures and a plate reader to measure OD_{600} over a time course, followed by curve fitting to generate growth curves that can be used for comparison of growth rates of different strains in specific growth phases. This assay has the advantages of allowing comparison between a large number of different combinations of strains and conditions, which is highly useful for stress studies, and providing quantitative measurements of both growth rate and the extent of lag phase. A disadvantage is that the range of concentrations that can be accurately measured (and therefore the potential length of incubations) is fairly small compared to the spot titer assay described above.

i. Equipment and Reagents

1. Visible light plate reader (We use the Molecular Devices VersaMax)

2. Plate reader software (SoftMax Pro)
3. Data analysis software (Excel and Graphpad Prism)
4. Shaking incubator
5. Multi-channel pipet (recommended)
6. Toothpicks (sterile)
7. 96-well plates (flat-bottom)
8. Plates with desired media (see section 2.1)
9. Liquid media and any desired treatments (see Table 1)
10. Desired yeast strains (see Table 2)

ii. Procedure

1. Preparing strains for inoculation:
    a. Streak out strains of interest for single colonies on either YEPD or selective plates.
    b. Pick individual colonies with toothpick and streak a "strain track" for each strain onto a fresh YEPD or selective plate using the serial dilution plate template as a guide for spacing (see Figure 2A for reference). A small amount of yeast on the toothpick is sufficient. Larger amounts may cause uneven growth for later steps.
    c. Incubate plate overnight at 30 °C
    d. The next morning, check the plates to see if there is a relatively even array of strain-tracks corresponding to the different strains.
2. Inoculating the 96-well plate micro-cultures:

a. Using proper sterile technique, use a multichannel pipet to dispense 250 µl of liquid media into the wells of a flat-bottom 96-well plate.
b. Inoculate wells of 96-well plate by picking a small amount of yeast from strain tracks (see notes for suggestions). Inoculate a minimum of 5 replicates per strain track. See Figure 2B for reference.
c. Set shaking incubator to 30 °C and 350 rpm. Put plate with lid on shaker and tape it securely to the shaker. Let the cultures grow overnight.

3. Back diluting the cultures and allowing them to reach exponential growth:
    a. The next morning check the plate to see that each well has grown. The overnight micro-cultures should all be overgrown (in stationary phase) at this point with visible cells settled at the bottom of the plate.
    b. Increase the shaker speed to 450 rpm, re-tape the plate and let it shake for ~5 min to resuspend the cells.
    c. Obtain a new 96-well flat-bottom plate and use multichannel pipet to dispense 200 µl of fresh media per well.
    d. Inoculate wells of new plate with 25 µl of the overnight micro-culture. Pipet up-and down ~10X to mix.
    e. Turn on the plate reader and ready it to take readings. If using a VersaMax, turn on and open SoftMax Pro software. Set wavelength to 600 nm.
    f. Measure OD_{600} using plate reader.

g. Check OD_{600} readings. Each back-diluted culture should have an OD_{600} between 0.2 and 0.3. If cultures are not within this range, adjust accordingly with more cells or more media as needed.

h. Incubate at 30 °C while shaking at 400rpm.

i. Check OD_{600} after 4 to 6 hours using plate reader. ODs should be between 0.4 and 0.7. Adjust volume with appropriate media so all micro-cultures are at a similar density.

j. Dispense 200 μl fresh media into wells of new 96-well flatbottom plate. See notes and Figure 2C for reference on the well arrangement. Add drug treatment/stress at this stage if doing so.

k. Calculate the volume of cultures to add to each well for and OD_{600} of 0.07 to 0.1. This should be approximately 20 μl of a mid-log culture.

l. Inoculate calculated amount to each well in the new plate. Mix well by pipetting up and down 10X with multichannel pipet. Make sure to mix well without generating bubbles.

m. Check that OD_{600} values are 0.07-0.1 using plate reader. At this stage the volume of each micro-culture should be the same and OD_{600} measurements should be within 0.02 OD_{600} units from one another.

n. Set shaking incubator to desired temperature and 350 rpm. Put plate with lid on shaker and tape it to the shaker.

4. Time-course OD_{600} measurements:

a. Measure OD_{600} of wells using the plate reader at pre-determined time-points. At a minimum it is recommended to take one OD_{600} measurement per cell doubling for exponentially growing cultures.
b. Before taking an OD_{600} measurement, set shaker to 450 rpm for 5 minutes to make sure cells are resuspended.
c. Take care to get rid of bubbles with pipet or by tapping on counter before measurement.
d. Continue taking OD_{600} measurements until all strains reach stationary phase (OD_{600} of ~1.4)

5. Data analysis and curve fitting:
    a. Compile all data into a spreadsheet program (e.g. Excel).
    b. Calculate average of all background (media only) OD_{600} readings. Subtract background average from values for experimental wells for each time point.
    c. Use a graphing/curve fitting program to generate an XY graph using background subtracted measurements. We recommend Graphpad Prism as it has many options but is optimized for biological data sets.
    d. It may be helpful to perform a Q test to identify true outliers at this stage. The small scale coupled with exponential growth can result in substantial amplification of small errors. We recommend that exclusion of any outliers be applied to the entire replicate rather than individual time-points.

e. Fit a curve to each strain/condition with a re-parameterized version of the Gompertz growth equation, which has the following form (Zwietering, Jongenburger, Rombouts, & van 't Riet, 1990):

$$OD_{600} = Ae^{-e^{\frac{\mu_{max} \cdot e}{A}(\lambda - t)+1}}$$

Here, *t* is the incubation time, *A* represents the asymptotic maximum value (the maximum OD_{600} in stationary phase), μ_{max} represents the maximum growth rate (the tangent of the inflection point), and λ is a measure of the lag time (technically, the x-axis intercept of μ_{max}). See notes for further discussion.

f. If the curve fitting does not seem to describe the data, consider:
    i. Judiciously adding constraints, such as setting all *A* parameters to the same value. Try to avoid overfitting.
    ii. Repeating experiments with more time points and/or replicates.

g. Compare curves between different strains and conditions. Following stress treatments, cells will often display a long lag time (λ) before beginning significant growth. The growth rate itself (μ_{max}) may also differ between strains or before/after treatment. Use appropriate statistical tests, such the extra sum-of-squares F test, to determine significance between parameters.

iii. Notes

1. Before starting experiment:
    a. Plan the timing of experiment beforehand to minimize the need to perform measurements at odd hours. For long drug treatments or stress conditions

the timing of the experiment becomes more important. It may take some trial and error.

b. Pre-plan the layout of the 96-well plate with strains, replicates and experimental conditions. It is helpful to make a template for each experiment (see Figure 2C). Leave blank wells on the outer edges of the plate; these wells tend to have higher evaporation than the inner wells, throwing off the growth measurements.

c. Always make sure 96-well plate is taped securely onto the shaking incubator.

d. Minimize/eliminate bubbles in micro-cultures prior to OD_{600} measurement, as they can interfere with accurate measurements.

2. For initial inoculation of colonies, single colonies can be hand-picked using a toothpick or sterile pipet tip, or multiple colonies can be selected at once using the multi-channel pipet. The latter is not easy and is dependent on accurate spacing of strain tracks.

3. The Gompertz growth equation is one of several described in microbiology literature (Zwietering et al., 1990). For stress treatments, it has the advantage of including a variable-length lag phase as well as a maximal growth rate, both useful measurements. The usual form of the Gompertz equation is:

$$f(t) = ae^{-e^{b-ct}}$$

However, in this form, the parameters are purely mathematical and do not correspond to biologically-relevant values. It is unlikely that any curve-fitting software on hand will have the re-parameterized form as a default (Prism does

not); therefore, it will likely need to be input as a custom equation. A linear version of the re-parameterized form that may be helpful for software entry is:

$$y = A \cdot \exp\left(-\exp\left(((u \cdot \exp(1))/A) \cdot (l - x) + 1\right)\right)$$

4. In general, this protocol is described using software and equipment common to our lab, but equipment and software of your preference can be substituted.

4. Translation assays to assess stress phenotypes

As discussed above, translation regulation is a key part of stress responses, resulting in massive reprogramming of translation and the redistribution of cellular resources (Crawford & Pavitt, 2019; B. Liu & Qian, 2014). In general, protein synthesis is repressed during stress with translation of most mRNAs, especially those encoding proteins with pro-growth or "housekeeping" functions, being down-regulated. Despite this bulk inhibition, select mRNAs, including those encoding "stress response genes" such as protein chaperones, are translationally upregulated, while others are particularly sensitive to down-regulation, indicating that the translational response is specific and complex (Gerashchenko et al., 2012; Ingolia et al., 2009). Furthermore, after cells adapt to the stress or it is removed, the renewed growth is accompanied by a resumption of bulk translation, which requires an additional layer of regulation (Advani & Ivanov, 2019; Aryanpur et al., 2022). Several mechanisms have been identified that regulate various aspects of this specificity, including the action of RNA helicases such as eIF4A and Ded1/DDX3X, but much remains poorly understood (Aryanpur et al., 2019; Guenther et al., 2018; Tauber et al., 2020; Tsokanos et al., 2016).

In this section, several assays are described that indicate the status of cellular translation: ^{35}S-methionine labeling, luciferase reporters, and polysome profiles/fractionation. One

consideration is that ^{35}S-methionine labeling and polysome profiles themselves are read-outs for general/bulk translation, especially for the most abundant and highly translated mRNAs, so regulation of specific mRNAs, such as stress response genes, will likely not be represented (in some cases such as heat shock, expression of individual heat shock proteins can sometimes be observed using ^{35}S-methionine labeling). In contrast, luciferase reporter translation is specific for the particular construct design; thus, different reporters can be used as "generic" indicators for translation or for translation of mRNAs with very specific regulatory mechanisms. Additionally, as described below, fractionation of polysome profiles can be performed to examine the association of proteins and RNAs with ribosomal complexes, which can also be used as a proxy for the translation status of specific mRNAs. The most comprehensive way to examine translation of individual mRNAs is using ribosome footprinting (Ribo-seq), which is discussed elsewhere (e.g. see (McGlincy & Ingolia, 2017; Powers & Brar, 2021)). However, it is worth noting that the normalization procedures for Ribo-seq are often optimized for examining relative differences between mRNAs rather than absolute levels of translation, and so, this method may not be ideal when bulk translational changes are expected.

A general caveat with these assays is that it can be difficult to distinguish between changes in translation and effects on upstream gene expression processes such as transcription. Especially if characterizing a novel factor or condition, it may be helpful to include additional controls to show that the observed translational effect is not due to indirect effects, for example in the form of mutants in the transcription and/or mRNA export machinery. Additionally, for luciferase assays, RT-PCR can be performed to ensure that reporter mRNA levels are similar, and in polysome profiles, analysis of the profile pattern can sometimes suggest if indirect effects are present.

4.1 Translation status via ^{35}S–methionine labeling

This protocol is used to observe *in vivo* biosynthesis of proteins. The addition of radioactively labeled methionine allows newly formed proteins to be observed via polyacrylamide gel. It also allows the visualization of translation during stress conditions by displaying all new proteins synthesized after stress conditions have been added. A limitation of this method is that it does not innately allow for characterization of the individual proteins being actively translated other than their apparent molecular weight, and therefore cannot be used to examine specific proteins. It is also important to note that before attempting this protocol, the proper certification must be acquired to handle radioactive materials, although alternative formulations of methionine labeled with fluorescent tags or biotin are also available.

i. Equipment and Reagents

1. Shaking incubator
2. Spectrophotometer
3. Benchtop centrifuge
4. Microcentrifuge
5. Power supply and gel apparatus for SDS-PAGE
6. Gel dryer
7. Film and developer/dark room
8. Desired yeast strains (see Table 2)
9. Liquid media and any desired treatments (see Table 1)
10. Minimal media lacking methionine (see section 2.1)

11. ^{35}S-methionine, 1000 Ci / mmol (recommend using within one half-life)
12. Lysis buffer: 1.85 M NaOH, 7.4% β-mercaptoethanol
13. 50% Trichloroacetic acid (TCA)
14. 1 M Tris Base (do not adjust pH)
15. SDS sample buffer: 100 mM Tris pH 6.8, 5% SDS, 0.1 M DTT, 0.02% bromophenol blue, 15% glycerol
16. Fixing solution: 40% methanol, 10% acetic acid, 3% glycerol
17. Fluoro-Hance autoradiography enhancer
18. Reagents for SDS-PAGE gels
19. Safe work space, storage, and waste disposal for radioactive materials

ii. Procedure

1. Inoculate 20 ml yeast cultures in a 125 ml flask and grow to mid-log phase. If stresses, drug treatments, etc. are to be used, perform these at this stage and have the cultures ready for step 2.
2. Measure and record OD_{600} of cultures with spectrophotometer
3. Transfer cells to 50-ml conical tubes and spin down cells in centrifuge for 5 min at 4000 rpm.
4. Discard supernatants.
5. Methionine starvation (see also notes for alternative method):
    a. Re-suspend cells in 10 ml of minimal media lacking methionine.
    b. Pellet cells again by centrifugation and discard supernatant.

c. Resuspend cells in 3 ml of minimal medial lacking methionine.

6. Add 25 μCi of ^{35}S-methionine per OD_{600} unit (the OD_{600} measurement times the amount of culture (~20 ml) spun down) to each culture. Make sure to follow proper radioactivity safety protocols from this point forward.
7. Incubate cells for 30 to 60 minutes in 30 °C while shaking. Stress treatments should also be repeated for this incubation if possible.
8. Record OD_{600} of samples.
9. Pellet the cells via centrifugation for 5 min at 4000 rpm.
10. Discard supernatant.
11. Lyse cells (if needed cells can be frozen and stored at this step). Multiple methods can be used, and here we briefly describe an adapted version of the crude cell lysate protocol of Yaffe & Schatz (Yaffe & Schatz, 1984) (also see notes):
    a. Resuspend cells in 1 ml H_2O and transfer to 1.5 ml tubes. Spin 30 sec in microcentrifuge and discard supernatant.
    b. Resuspend in 160 μl of freshly prepared lysis buffer. Mix and incubate on ice 10 min.
    c. Add 160 μl 50% TCA. Mix and incubate on ice 10 min.
    d. Spin 2 min in microcentrifuge. Wash pellet (don't resuspend) with 0.5 ml 1M Tris base.
    e. Resuspend in 150 μl of SDS sample buffer per OD_{600} unit (OD_{600} x culture volume). Alternate heating at 95 °C and vortexing to resuspend the pellet.
    f. Briefly centrifuge to bring all liquid to the bottom of the tube before loading.

12. Load as much sample as possible on a polyacrylamide gel (10% or 4-15% gradient). Run samples as standard SDS-PAGE (see notes).
13. Fix and dry gel:
    a. Remove gel from electrophoresis apparatus and add to fixing solution. Gel should be completely submerged in solution for a minimum of 1 hour.
    b. Decant fixing solution and add sufficient Fluoro-Hance to submerge gel. Incubate 20 minutes.
    c. Dry gel using a gel dryer.
14. Visualize ^{35}S-labeled bands by exposing dried gel to autoradiography film. Exposure times can vary from one day to a full week, and the proper exposure time should be determined empirically. Develop film (see Figure 3 for example).
15. For quantitation, scan film and perform band densitometry using ImageJ (or a similar application) to measure total ^{35}S signal in each lane.

iii. Notes

1. Alternative to methionine starvation: skip this step and just re-suspend cells in 3 ml of YEPD or minimal complete media. Since unlabeled methionine will be present, this will reduce the labeling of proteins and produce a lower signal, but in many cases the signal will still be sufficient to visualize.
2. Once the ^{35}S-methionine is added in step 6, all samples, reagents, and equipment used are considered radioactively contaminated. Please plan accordingly and follow all appropriate safety protocols.
3. Other extract preparation protocols can be used if preferred.

4. Standard SDS-PAGE conditions are recommended. Details are not described here but can be found in many laboratory protocols.

4.2 Translation status via luciferase reporter

This protocol describes the use of a luciferase assay as a reporter for intracellular translation status. *In vitro* translation systems with luciferase mRNA are also available, although they are not described here (see (Wu, Amrani, Jacobson, & Sachs, 2007)). Such systems can be of great utility in studying translation (e.g. (Balagopal & Parker, 2011)); however, it is not straightforward to study stress-specific functions *in vitro*, so here we focus on the reporter assays in cells. In these assays, the amount of luciferase signal is dependent on the design of the reporter construct. In theory, any highly expressed promoter and 5' UTR fused to the luciferase coding region could serve as a baseline reporter, and reporters can then be altered to add secondary structure, mutate the start codon, or other changes to test more specific aspects of translation. We recommend pFJZ342 (*CEN/URA3*), which contains the promoter and 5' UTR of *RPL41A* with an insertion of 23 CAA repeats fused to the firefly luciferase coding sequence (Sen, Zhou, Ingolia, & Hinnebusch, 2015). This is part of a set of reporters with 5' UTRs of different lengths and secondary structures, which have been used to characterize the RNA helicases Ded1 and eIF4A (Brown, Vergara, Whelan, Guerra, & Bolger, 2021; Sen et al., 2015).

i. Equipment and Reagents

1. Spectrophotometer
2. Shaking incubator
3. Mini bead-beater (Biospec)

4. Luminometer (Promega Glomax)
5. 1.5 ml screw top tubes
6. 1.5 ml microfuge tubes
7. Acid-washed glass beads (425 – 600 μm)
8. 1 ml syringes with small gauge needles (recommend 23G or higher)
9. Luciferase lysis buffer (25 mM Tris phosphate (pH 7.8), 0.5% Triton, 2 mM EGTA, 2 mM DTT, 10% Glycerol)
10. Luciferase assay reagent (luciferin). If using Promega reagents, add suggested volume of buffer to lyophilized reagent. If custom-made, resuspend luciferin at 150 μg / ml in buffer containing 15 mM $MgSO_4$, 15 mM K_2HPO_4, 4 mM EGTA, 1 mM ATP, 1 mM DTT). Protect from light. Can aliquot and freeze at -80 °C.
11. Yeast strains transformed with luciferase reporters (see Table 2)

ii. Procedure

1. Sample Preparation:
    a. Inoculate yeast cultures and grow overnight.
    b. Dilute cultures and split into triplicate (3-5 ml each). Grow cultures to mid-log phase (OD_{600} = ~0.5).
    c. If stresses and/or drug treatments are to be performed, dilute cultures back to OD_{600} of 0.05 to 0.2 depending on length of treatment. Add drug/stress and incubate.
    d. Recover samples and record OD_{600} of each sample.

e. Transfer up to 1.5 ml of culture to microfuge tubes and spin down in microcentrifuge for 1 min.

f. Aspirate media and resuspend in 200 μl luciferase lysis buffer.

g. Add ~100 μl glass beads to screw top tubes, then transfer samples into them.

h. Shake in mini-bead beater at 4 °C twice for 2.5 min each, with 1 min on ice in between runs (or 4 x 1.25 min with 30 sec on ice in between).

i. Spin 6 min in microcentrifuge at 4 °C.

j. Using a 1 mL syringe with small-gauge needle or a thin gel-loading tip, transfer supernatants from screw cap tubes to 1.5 ml tubes.

k. Keep on ice or at -20°C.

2. Luciferase Assay

a. Turn on luminometer to warm up at least 15 min before use and thaw luciferase assay reagent. Protect the reagent from light.

b. Set luminometer to a single injection of 100 μl, minimal delay, and 10 sec (or more) integration time.

c. Prime luciferase assay reagent in injector.

d. If desired, insert an empty tube in the luminometer and run as a “blank” to check that the injector and detector are working properly (see notes).

e. Add 5 to 50 μl of sample to a 1.5 ml microfuge tube (or appropriate container for luminometer).

f. Run each sample in the luminometer and record result.

g. Flush the luminometer with water after use.

h. Normalize each sample by dividing the luciferase value by the OD_{600}, and compare values.

iii. Notes

1. This assay is a measure of the amount of luciferase protein present in the cells, so when performing a time-course, residual luciferase may still be present even if translation is repressed. Therefore, we recommend choosing time points on the order of hours rather than minutes.
2. The luciferase value for the blank may be subtracted from the sample values as background, but in our experience, the blanks give a negligible value compared to samples.
3. Luciferase assays have a large dynamic range, eight orders of magnitude or more. The amount of sample added to the assay can be adjusted if needed, however.

4.3 Polysome profiles and fractionation

Polysome profiling utilizes centrifugation of cellular extracts over a sucrose gradient to separate the different types of ribosomal complex (40S, 60S, 80S, and polysomes) by relative density. These profiles can potentially give several different kinds of outputs that provide information on cellular translational status. First, a trace of the absorbance (at 255 nm, a measurement of RNA concentration) along the gradient is generated, marking each of the ribosomal complexes and their relative abundances. By measuring the area under the curve of each peak, the relative amount of translation that is occurring globally can be quantified. With this information, mutations, drug treatments, or stress conditions can be evaluated as to what

extent they are able to alter global, or bulk, translation (e.g. (Chuang, Weaver, Liu, & Chang, 1997)). Generally, profiles would be expected to show translation repression during stress responses, which is then restored as the cells adapt and recover (Aryanpur et al., 2022; Aryanpur et al., 2019; Shenton et al., 2006). Second, fractions can be collected from the gradients and immunoblotted for specific translation factors or other proteins. These results can help reveal the effects of changes in ribosomal complexes as a result of stress or mutations. An additional crosslinking step (see notes) is recommended when performing in-depth protein analysis. A method to use fluorescently-tagged proteins to generate continuous traces of protein signal, similar to the RNA absorbance trace, has also recently been described (Shaffer & Rollins, 2020). Third, RNA can be isolated from the gradient fractions, and quantitative RT-PCR can be performed in order to examine the association of individual mRNAs with more or less active translation complexes (see notes). However, this method is technically challenging and requires additional equipment; thus, other methods may be more accessible for examining translation of individual mRNAs.

i. Equipment and Reagents

1. Small gradient mixer (Hoefer SG30)
2. Stir plate
3. Small peristaltic pump (Fisher mini-pump is sufficient)
4. Small-diameter (~2 mm) tubing, connectors, ~12 cm stainless steel tube (interior diameter ~2 mm) and rubber stopper
5. Shaking incubator
6. Spectrophotometer

7. Benchtop centrifuge
8. Vortexer with lid (Turbo-Mix)
9. Microcentrifuge
10. Standard balance
11. Ultracentrifuge (Beckman)
12. SW-41TI ultracentrifuge rotor
13. Density gradient fractionation system (Brandel). See Figure 4 and notes.

i. Syringe pump with 50 ml glass syringe (Brandel)
ii. Gradient separator (Brandel)
iii. Absorbance detector (Teledyne-ISCO UA-6 with Type 11 Optical Unit)
iv. Fraction collector (Teledyne-ISCO Foxy R1)
v. Data capture software (Brandel PeakChart)

14. Thinwall polypropylene tubes (recommend Beckman #331372, 14 x 89 mm)
15. 50 ml conical tubes
16. 1.5 ml tubes
17. Acid-washed glass beads (425 – 600 μm)
18. Cycloheximide (10 mg / ml)
19. Low salt (LS) buffer (20 mM HEPES-KOH**,** 100 mM KOAc**,** 5 mM MgOAc**,** 1 mM EDTA) in RNase-free water (see notes). Add fresh day of**:** 1 mM DTT**,** 100 μM PMSF**,** 1X protease inhibitor cocktail, 100 μg / ml cycloheximide.

20. 7% sucrose (w/v) solution in LS buffer (add DTT and cycloheximide but other additives not needed). See notes.
21. 47% sucrose (w/v) solution in LS buffer (add DTT and cycloheximide but other additives not needed). See notes.
22. Fluorinert FC-40 chase solution
23. RNase-free water
24. Liquid media and any desired treatments (see section 2.1 and Table 1)
25. Desired yeast strains (see Table 2)
26. Ice-cold ethanol (optional)
27. SDS sample buffer (optional): 100 mM Tris pH 6.8, 5% SDS, 0.1 M DTT, 0.02% bromophenol blue, 15% glycerol

ii. Procedure

1. Pour gradients (can be done one day prior and stored at 4 °C, also see notes):
    a. Set up gradient prep apparatus (see Figure 5A). Place gradient mixer on stir plate and add a micro stir bar to the front well. Attach tubing from gradient mixer to pump and from pump to stainless tube. Insert tube through rubber stopper and place stopper on top of a polypropylene ultracentrifuge tube so that stainless tube extends inside. Make sure the ultracentrifuge tube is securely held in a vertical position, and position the stainless tube so it does not quite touch the bottom of the ultracentrifuge tube.

b. Move the stainless tube/stopper to empty into a beaker. Add RNase-free water to gradient mixer wells and turn on cartridge pump and stir plate (stir bar should be spinning cleanly). Wash system with water, ethanol, and water again. Run until all liquid has drained.
c. Close valves on gradient mixer.
d. Add 5.7 ml of 47% sucrose solution to rear well of mixer, and 5.7 ml of 7% to front well.
e. Open valve between wells of mixer, then front valve, then turn on pump (use a low setting; it should take 5 to 10 minutes to pour each gradient). The solution should flow smoothly between the wells and should start moving into the tubing.
f. The progress of the sucrose solution can be tracked through the tubing. When it approaches the stainless tube/stopper, move it so it empties into the pre-positioned polypropylene ultracentrifuge tube.
g. When the solution in the mixer is nearly empty, air bubbles will form in the line. Continue running the pump until bubbles are near/within the stainless tube, then stop it. The gradient solution should be near (but not at) the top of the polypropylene tube (if it is not, discard the gradient and pour again). In one smooth, continuous motion, remove the stainless tube from the ultracentrifuge tube (this minimizes mixing of the gradient in the tube) and place in waste beaker.
h. Restart the pump to run out any last bits. Reset for the next gradient. Washing between each gradient is not usually necessary.

i. When finished, be very gentle moving gradients around to minimize mixing. Wash system extensively (as in step b); the sucrose solutions can leave significant residue if not cleaned.

2. Harvest cells:
    a. Culture 30 to 50 ml of desired yeast strains to mid-log phase in desired conditions. Add drugs and/or stress conditions and treat as desired (see notes). Measure OD_{600} and multiply by culture volume to get "OD units". Protocol works best with 8 to 15 OD units. Generally, this protocol is limited to 6 samples at a time due to the ultracentrifuge rotor.
    b. Add cycloheximide at 100 μg / ml directly to cultures and incubate on ice 5 min. Transfer to 50 ml conical tube.
    c. Spin down cells for 5 min at 3000 g.
    d. Decant media and add 5 ml of LS buffer (+cycloheximide).
    e. Spin down again and remove all supernatant. Can freeze cell pellets overnight at this step if needed.
    f. Resuspend pellets in LS buffer (+additives) at 13.3 μl per OD unit and transfer to 1.5 ml tubes.
    g. Add an approximately equal volume of glass beads to each tube.
    h. Vortex at 4 °C for 5 min. Spin in microcentrifuge at 4 °C for 5 min.
    i. Transfer extracts (supernatants) to fresh tubes.
3. Lyse cells, load gradients, and spin:
    a. Carefully load extracts on the top of each gradient by layering along the side of the tube. We recommend 100 μl (7.5 OD units) per sample.

b. Gently place gradients into the buckets for SW-41 rotor. Balance them as closely as possible: weigh each pair of buckets, and add extra LS Buffer to the top of the lighter sample. Ideally each pair is within 0.02 g.

c. Carefully transport buckets to ultracentrifuge, hang buckets on rotor, and set up ultracentrifuge. Make sure rotor is mounted properly in ultracentrifuge and that vacuum is working properly. Spin at 38,000 rpm for 2.5 hrs at 4°C.

4. Polysome fractionator operation protocol (This protocol is specific to using the Brandel density gradient fractionation system, but equivalent steps will need to be performed in other systems):

    a. Turn on the absorbance detector and let warm up for at least 15 minutes. Open the data collection software application (PeakChart).

    b. Turn on the fraction collector. If desired, set up to collect fractions, and place the appropriate number of open 1.5 ml tubes in the collector (see notes).

    c. Assemble the gradient separator apparatus (see Figure 5B).

    d. As needed, rinse lines with RNAse-free water, ethanol, and water again, followed by clearing the lines out with air. We recommend adding a three-way valve between the syringe pump and the bottom of the gradient separator and inserting a spare polypropylene tube into the separator. The third outlet of the three-way valve can then be used for pushing water, ethanol, or air through the system via a syringe. Please note that the fraction collector must be started in order to push anything through.

e. If needed, add Fluorinert to the glass syringe in the syringe pump: Disconnect the tubing to the gradient separator and place in Fluorinert stock. Filling the syringe to 40-50 ml is preferable. Avoid bubbles since they will disturb the gradient if they are pumped through it. The pump can be turned on its side to remove excess air from the system. Reconnect tubing to separator.

f. Prime the system with Fluorinert: if present, remove the spare tube from the separator. Extend tube piercing needle until the outlet hole is visible, then turn on syringe pump (forward, 1.5 ml per min). Watch Fluorinert travel through tubing until it starts coming out of the needle, then stop pump. Wipe up excess Fluorinert. Retract needle below gasket.

g. When ultracentrifuge spin is complete, open each bucket and remove the gradients with forceps. Keep at 4 °C until analyzed.

h. Insert a gradient into the gradient separator: Loosen the upper collar in the separator and carefully insert the gradient tube into the collar. Push firmly upwards and tighten the collar until the tube is securely held. Raise the lower separator assembly so that the gradient tube is centered and tight between the top and bottom of the separator, and tighten in place. Extend the needle until it pierces the tube and both black lines are visible in the tube. See Figure 5B.

i. Set syringe pump to remote start/stop, 1.5 ml per min, forward.

j. Start the pump via the software. In PeakChart, click the green trace button - looks like a marker tip. The fraction collector should start, and the

absorbance trace should start in the software (if it does not, stop and troubleshoot, otherwise sample may be lost). Immediately switch fraction collector to waste (trash can icon).

k. Fluorinert should start coming out of the needle hole and filling the bottom of the gradient tube. The gradient should be slowly pushed up into the top of the separator and the UV detector in the optical unit.

l. Adjust baseline of the absorbance trace ("Baseline Adjust" knob on the optical unit) as needed. We find that the baseline reading at the beginning of a trace (in air) should be 0.2 to 0.25 V to avoid bottoming out later in the run.

m. If collecting fractions, when the detector begins detecting sample (trace jumps upward), switch collector back to run (arrow icon) if delay is set. If delay is not used, wait to switch collector until sample is about to come out of the fractionator.

n. Run entire profile (~10 min). At the end, the trace will often spike, then begin acting erratically. Run sample all the way through fractionator and wait until Fluorinert begins dripping out (Fluorinert has less cohesion than an aqueous sample, so the drops are smaller and faster).

o. Stop trace in application (red "x" button in PeakChart). Manually switch the syringe pump to reverse at 6 ml per min, and pump Flourinert back into glass syringe. There may still be some sample at the Fluorinert/air interface, so stop the pump before the Fluorinert reaches the needle hole.

p. Remove the gradient tube from the separator and discard. Close used fraction tubes, remove from fractionator, and store at 4 °C until ready to precipitate protein. Reset the system for the next sample. It is usually not necessary to clean the lines between each sample, but this can be done if lines appear dirty/blocked.

q. When finished, rinse lines as in step (d) with RNAse-free water, ethanol, and water again, followed by clearing the lines out with air. We recommend also disassembling the separator and wiping down its components to minimize sucrose residue.

5. Analysis of profiles (see Figure 6):

   a. To assess the general translation status of samples, first calculate the area under the curve for the peaks from the UV absorbance trace. PeakChart has a tool for calculating this, but instead, we recommend opening the image file in ImageJ/Fiji. Draw a baseline underneath the trace; a common practice is to draw a horizontal line at the lowest point on the trace, usually between the 80S and the disome peak. Draw vertical lines to separate the peaks as needed, and use the measurement tool to calculate the area.

   b. The most important comparison is the relative area of the 80S monosome peak versus the polysome peaks. A larger polysome to monosome ratio indicates more active translation, and a lower ratio indicates lower bulk translation. Note that translation repression generally leads to an increased 80S peak and not substantial increases in the “free” 40S and 60S.

However, for long time points in stress conditions, ribophagy, degradation of ribosomes, can also occur, resulting in a general loss of signal from the trace. Other types of effects have also been observed on the absorbance traces, such as defects in ribosome biogenesis, which can manifest as changes in the relative amounts of 40S and 60S complexes and/or the appearance of "halfmers", shoulders that appear on each monosome and polysome peak. However, we caution users that these differences are not always reliable and can vary from sample to sample.

c. If fractions have been collected, then the association of proteins with the various complexes can be examined. To do so, first precipitate proteins from the fractions by addition of 0.8 ml ice-cold ethanol to each 0.5 ml fraction, followed by vortexing and incubation overnight at -20 °C. Spin samples in microcentrifuge at 4 °C for 10 min, and remove supernatant. Wash the pellets once with 75% ethanol and then resuspend in SDS sample buffer. Proteins can then be separated by SDS-PAGE and blotted for the desired factors. Association of the target protein with translation complexes can be observed as well as shifts to more or less actively translated mRNAs in different conditions.

d. Fractions can also be examined for individual mRNAs. RNA extraction can be performed via phenol or with a commercial kit as desired. Depending on the technique, the fractions may need to be diluted with additional LS buffer before extraction to decrease the sucrose concentration. Fractions may also be pooled (for example, into "non-

translated", "low translated", and "highly translated" pools) for simplicity. Relative RNA levels can then be determined via qPCR or Northern blot and then compared to the absorbance trace, where association with heavier polysomes is evidence of higher translation levels.

iii. Notes

1. This protocol is designed around the Brandel Density Gradient Fractionation system, the only complete system available of which we are aware. However, systems can also be constructed out of the individual components listed. A syringe pump is highly recommended, as other types, such as peristaltic pumps, do not provide the same levels of smooth, continuous action. The gradient separator is fairly specialized but is available from Brandel and others. If accessible to the user, HPLC or FPLC systems may be able to provide the necessary flow cell, UV absorbance readings, and data capture, while fraction collectors are available from multiple suppliers. If using a custom-assembled system, the operation section of the protocol will need to be modified to fit the system, but generally the same steps will need to be included.
2. Given that this protocol relies on intact RNA-protein complexes, degradation due to RNases is a concern, although ribosomal RNA itself is somewhat RNase-resistant. Therefore, all buffers, tubes, and other reagents that come into contact with the samples

following lysis should be RNAse-free. This includes the interior spaces of the fractionation system, so RNase-free water should be used for rinsing the lines. Water can be either DEPC-treated or purchased as RNAse-free.

3. When preparing sucrose solutions, please note that the percentages listed are (solute) weight by (solution) volume. Given the high sucrose percentages, the volume of the sucrose will need to be accounted for, i.e. much less than 100 ml of LS buffer will be needed for 100 ml of 47% sucrose solution.
4. Other methods of generating sucrose gradients exist and can be used if desired, such as layering a step gradient and allowing it to equilibrate overnight. We have found that using a gradient mixer is a more reliable and user-friendly method.
5. When examining translation during stress conditions (or indeed in mutant cells), the user should carefully consider the appropriate time course. Translation is repressed fairly quickly in stress (in minutes rather than hours), and this is reflected in the polysome profiles in 15 minutes or less of rapamycin treatment, for example (Aryanpur et al., 2019). However, our studies and others have shown that the extent of repression continues to increase for a number of hours, depending on the severity of the stress, while eventually slower processes such as ribophagy can affect the profiles (Aryanpur et al., 2019; Kelly & Bedwell, 2015).

6. If fractions are to be collected, the fraction collector unit must be set up correctly. With the Brandel system collector, the user can choose between collecting each fraction through an equal number of drops (droplet icon) or through an equal time of collection (clock icon). We generally find the timer method to be more consistent. The number of drops or amount of time for each fraction will need to be determined empirically, depending on the number of desired fractions. With either method, a delay (hourglass icon) should be set before the counter/timer begins. The delay will synchronize the fraction collecting with the absorbance measurement, reflecting the time it takes for the sample to travel from the detector to the fraction collector outlet. The length of the delay will need to be empirically determined but is ~30 sec for a typical Brandel setup. Programming in the delay will also locate the fraction markers in the PeakChart software at the correct points on the trace. When using this method, remember to switch the collector to waste immediately after starting the trace and to switch it back to the run once the sample reaches the detector.
7. If in-depth analysis of protein association with translation complexes, particularly pre-initiation complexes, is desired, consider adding a crosslinking step. Formaldehyde crosslinking has been shown to aid in retention of associated proteins during profiling (see (Valasek, Szamecz, Hinnebusch, & Nielsen, 2007)).

We modified this protocol slightly to treat cells with 0.25% formaldehyde for 15 min on ice, followed by quenching with 0.5 mM glycine (Aryanpur et al., 2019). Note that this is a significantly lower formaldehyde concentration, as we found that higher levels introduced artifacts into the profiles.

5. Other general protocols

Above are specific instructions for several protocols associated with analyzing helicases for translation functions in stress. These protocols are essential for understanding the complex phenotypes that are associated with stress in cells, but there are, of course, other assays that may be useful in examining translation during stress that complement the above approaches. Two of these approaches are described in general form below: stress granule analysis and protein half-life evaluation.

The formation of stress granules is another common response to cellular stress. Stress granules are membrane-less cytoplasmic foci of RNA and proteins that form under conditions of translation repression (Buchan & Parker, 2009; Protter & Parker, 2016). They are thought to be sites for the storage of repressed mRNAs that can later be degraded or shifted back into active translation, although their precise function has remained somewhat unclear. Stress granule analysis is immensely useful when analyzing a stress condition that is known to trigger stress granule formation. Given the association of translation repression and stress granules, effects on stress granule dynamics can be evidence of translational changes, changes in stress granules themselves, or both. It should be noted that rapamycin treatment is not known to induce stress granule formation, although many other stresses, such as glucose deprivation and oxidative

stress, are great candidates for this type of analysis. In brief, stress granules can be assessed by growing *S. cerevisiae* cells (or others) containing fluorescent stress granule markers to mid-log phase. The most common of these markers is *PAB1* fused to *GFP* or *mCherry* (Buchan, Kolaitis, Taylor, & Parker, 2013). At this point, depending on the type of stress being analyzed, either an addition of drug or a change of media needs to be completed. For most assays there is a time requirement to induce stress granules and this time can vary between types of stress from a few minutes to several hours. Cells can then be collected and concentrated for evaluation using a fluorescence microscope over the appropriate time course. Added attention should be given to the concentration portion of the sample preparation since centrifugation has been shown to induce stress phenotypes independent of initial cell conditions. For more detailed protocols, there are several available (e.g. (Aulas et al., 2017; Buchan, Nissan, & Parker, 2010)), but in essence the user should follow basic fluorescence microscopy protocols.

Another generalized approach to analyzing phenotypes of stress is to evaluate changes in protein levels. As cells are subjected to stress conditions, particularly for prolonged periods, subsets of proteins, including ribosomes and certain translation factors, begin to be degraded, possibly as a scavenging response in scarce resources (Berset et al., 1998; Kelly & Bedwell, 2015; Kraft, Deplazes, Sohrmann, & Peter, 2008). These degradation mechanisms can be studied through examining protein levels during stress, including in cells with mutations in the factors that promote degradation. Using basic methods of cell collection, cell lysis, and western blotting for specific factors an apparent protein "half-life" in stress can be determined. For example, the apparent half-life of eIF4G1 in rapamycin-treated yeast cells was about 1 hour in our hands, but it increased over two-fold in cells with mutations in *DED1*, which helps control its degradation (Aryanpur et al., 2019). Understanding how the half-life of proteins change over the course of

stress can elucidate basic functions of those proteins and even help to clarify whether those proteins have an active, passive, or non-existent role in the stress response.

These are just two of the many assays that can be used, alongside the more detailed protocols provided, to evaluate stress in cells. It is highly recommended that when evaluating a DEAD-box helicase or other protein for a role in stress responses, effects on basic functions are considered before more complex methods are undertaken. This will help ensure that adequate information is known about the protein before committing to time- and labor-intensive assays.

6. Summary and Conclusion

As discussed above, gene expression processes are not static, but rather they flexibly respond to changes in cellular conditions, particularly during stresses like a lack of nutrients or extreme environmental conditions. Translational control is critical during stress both because of the immense energy requirements of translation and because it allows relatively quick alterations to the proteome. Furthermore, given their ability to modulate RNA-RNA and RNA-protein interactions, RNA helicases are a natural regulatory node in these conditions. Described above are two different complementary approaches to addressing helicase (or any protein) function in translation during stress. First, growth assays (Section 2) are a straightforward way to associate a given gene with a stress function. Once growth phenotypes have been identified under stress, more specific assays can be designed. These could include examining not only different stress conditions, but also address whether the phenotypes are due to effects on cell growth, survival, and/or recovery during stress. However, it is difficult to conclude that a factor is specifically affecting translation from growth assays alone. In contrast, translation assays (Section 3) carried out in stress conditions can address whether the translational stress response is affected. It should

be noted, however, that it is possible that effects in other processes (e.g. transcription) can have indirect effects on translation. More specific translation assays (e.g. reporters that test a particular aspect of translation) and/or analysis of association with translation complexes can provide additional confidence that the observed translation phenotypes are, in fact, direct. Furthermore, assays that examine a detailed mechanism can also add to our understanding of the complex regulation of the translational response to cellular stress.

7. Acknowledgments

The authors would like to thank Michael Trakselis, Frederico Paulo Mendoza, and other editors at *Methods in Enzymology* for this opportunity. We would also like to thank current and former members of the Bolger lab for helpful advice and discussion. This work was partly supported by a grant from the National Institute of General Medical Sciences (R01-GM136827).

8. References

Advani, V. M., & Ivanov, P. (2019). Translational Control under Stress: Reshaping the Translatome. *Bioessays, 41*(5), e1900009.

Albig, A. R., & Decker, C. J. (2001). The target of rapamycin signaling pathway regulates mRNA turnover in the yeast Saccharomyces cerevisiae. *Mol Biol Cell, 12*(11), 3428-3438.

Aryanpur, P. P., Mittelmeier, T. M., & Bolger, T. A. (2022). The RNA Helicase Ded1 Regulates Translation and Granule Formation during Multiple Phases of Cellular Stress Responses. *Mol Cell Biol, 42*(1), e0024421.

Aryanpur, P. P., Renner, D. M., Rodela, E., Mittelmeier, T. M., Byrd, A., & Bolger, T. A. (2019). The DEAD-box RNA helicase Ded1 has a role in the translational response to TORC1 inhibition. *Mol Biol Cell, 30*(17), 2171-2184.

Aulas, A., Fay, M. M., Szaflarski, W., Kedersha, N., Anderson, P., & Ivanov, P. (2017). Methods to Classify Cytoplasmic Foci as Mammalian Stress Granules. *J Vis Exp*(123).

Balagopal, V., & Parker, R. (2011). Stm1 modulates translation after 80S formation in Saccharomyces cerevisiae. *Rna, 17*(5), 835-842.

Beck, Z. T., Cloutier, S. C., Schipma, M. J., Petell, C. J., Ma, W. K., & Tran, E. J. (2014). Regulation of glucose-dependent gene expression by the RNA helicase Dbp2 in Saccharomyces cerevisiae. *Genetics, 198*(3), 1001-1014.

Beckham, C., Hilliker, A., Cziko, A. M., Noueiry, A., Ramaswami, M., & Parker, R. (2008). The DEAD-box RNA helicase Ded1p affects and accumulates in Saccharomyces cerevisiae P-bodies. *Mol Biol Cell, 19*(3), 984-993.

Berset, C., Trachsel, H., & Altmann, M. (1998). The TOR (target of rapamycin) signal transduction pathway regulates the stability of translation initiation factor eIF4G in the yeast Saccharomyces cerevisiae. *Proc Natl Acad Sci U S A, 95*(8), 4264-4269.

Bolger, T. A., & Wente, S. R. (2011). Gle1 is a multifunctional DEAD-box protein regulator that modulates Ded1 in translation initiation. *J Biol Chem, 286*(46), 39750-39759.

Brown, N. P., Vergara, A. M., Whelan, A. B., Guerra, P., & Bolger, T. A. (2021). Medulloblastoma-associated mutations in the DEAD-box RNA helicase DDX3X/DED1 cause specific defects in translation. *J Biol Chem*, 100296.

Buchan, J. R., Kolaitis, R. M., Taylor, J. P., & Parker, R. (2013). Eukaryotic stress granules are cleared by autophagy and Cdc48/VCP function. *Cell, 153*(7), 1461-1474.

Buchan, J. R., Nissan, T., & Parker, R. (2010). Analyzing P-bodies and stress granules in *Saccharomyces cerevisiae*. *Methods Enzymol, 470*, 619-640.

Buchan, J. R., & Parker, R. (2009). Eukaryotic stress granules: the ins and outs of translation. *Mol Cell, 36*(6), 932-941.

Carroll, J. S., Munchel, S. E., & Weis, K. (2011). The DExD/H box ATPase Dhh1 functions in translational repression, mRNA decay, and processing body dynamics. *J Cell Biol, 194*(4), 527-537.

Chuang, R. Y., Weaver, P. L., Liu, Z., & Chang, T. H. (1997). Requirement of the DEAD-Box protein Ded1p for messenger RNA translation. *Science, 275*(5305), 1468-1471.

Costa-Mattioli, M., & Walter, P. (2020). The integrated stress response: From mechanism to disease. *Science, 368*(6489).

Crawford, R. A., & Pavitt, G. D. (2019). Translational regulation in response to stress in Saccharomyces cerevisiae. *Yeast, 36*(1), 5-21.

Gerashchenko, M. V., Lobanov, A. V., & Gladyshev, V. N. (2012). Genome-wide ribosome profiling reveals complex translational regulation in response to oxidative stress. *Proc Natl Acad Sci U S A, 109*(43), 17394-17399.

Gonskikh, Y., & Polacek, N. (2017). Alterations of the translation apparatus during aging and stress response. *Mech Ageing Dev, 168*, 30-36.

Gonzalez, S., & Rallis, C. (2017). The TOR Signaling Pathway in Spatial and Temporal Control of Cell Size and Growth. *Front Cell Dev Biol, 5*, 61.

Guenther, U. P., Weinberg, D. E., Zubradt, M. M., Tedeschi, F. A., Stawicki, B. N., Zagore, L. L., . . . Jankowsky, E. (2018). The helicase Ded1p controls use of near-cognate translation initiation codons in 5' UTRs. *Nature, 559*(7712), 130-134.

Hilliker, A., Gao, Z., Jankowsky, E., & Parker, R. (2011). The DEAD-Box Protein Ded1 Modulates Translation by the Formation and Resolution of an eIF4F-mRNA Complex. *Mol Cell, 43*(6), 962-972.

Ingolia, N. T., Ghaemmaghami, S., Newman, J. R., & Weissman, J. S. (2009). Genome-wide analysis in vivo of translation with nucleotide resolution using ribosome profiling. *Science, 324*(5924), 218-223.

Iserman, C., Desroches Altamirano, C., Jegers, C., Friedrich, U., Zarin, T., Fritsch, A. W., . . . Alberti, S. (2020). Condensation of Ded1p Promotes a Translational Switch from Housekeeping to Stress Protein Production. *Cell, 181*(4), 818-831 e819.

Kelly, S. P., & Bedwell, D. M. (2015). Both the autophagy and proteasomal pathways facilitate the Ubp3p-dependent depletion of a subset of translation and RNA turnover factors during nitrogen starvation in Saccharomyces cerevisiae. *Rna, 21*(5), 898-910.

Kraft, C., Deplazes, A., Sohrmann, M., & Peter, M. (2008). Mature ribosomes are selectively degraded upon starvation by an autophagy pathway requiring the Ubp3p/Bre5p ubiquitin protease. *Nat Cell Biol, 10*(5), 602-610.

Liu, B., & Qian, S. B. (2014). Translational reprogramming in cellular stress response. *Wiley Interdiscip Rev RNA, 5*(3), 301-315.

Liu, Y., Beyer, A., & Aebersold, R. (2016). On the Dependency of Cellular Protein Levels on mRNA Abundance. *Cell, 165*(3), 535-550.

McGlincy, N. J., & Ingolia, N. T. (2017). Transcriptome-wide measurement of translation by ribosome profiling. *Methods, 126*, 112-129.

Mitchell, S. F., & Parker, R. (2014). Principles and properties of eukaryotic mRNPs. *Mol Cell, 54*(4), 547-558.

Powers, E. N., & Brar, G. A. (2021). Performing Ribosome Profiling to Assess Translation in Vegetative and Meiotic Yeast Cells. *Methods Mol Biol, 2252*, 89-125.

Protter, D. S. W., & Parker, R. (2016). Principles and Properties of Stress Granules. *Trends Cell Biol, 26*(9), 668-679.

Robichaud, N., Sonenberg, N., Ruggero, D., & Schneider, R. J. (2019). Translational Control in Cancer. *Cold Spring Harb Perspect Biol, 11*(7).

Roux, P. P., & Topisirovic, I. (2018). Signaling Pathways Involved in the Regulation of mRNA Translation. *Mol Cell Biol, 38*(12).

Saavedra, C., Tung, K. S., Amberg, D. C., Hopper, A. K., & Cole, C. N. (1996). Regulation of mRNA export in response to stress in Saccharomyces cerevisiae. *Genes Dev, 10*(13), 1608-1620.

Saxton, R. A., & Sabatini, D. M. (2017). mTOR Signaling in Growth, Metabolism, and Disease. *Cell, 168*(6), 960-976.

Sen, N. D., Zhou, F., Ingolia, N. T., & Hinnebusch, A. G. (2015). Genome-wide analysis of translational efficiency reveals distinct but overlapping functions of yeast DEAD-box RNA helicases Ded1 and eIF4A. *Genome Res, 25*(8), 1196-1205.

Seok, H. Y., Nguyen, L. V., Van Nguyen, D., Lee, S. Y., & Moon, Y. H. (2020). Investigation of a Novel Salt Stress-Responsive Pathway Mediated by Arabidopsis DEAD-Box RNA Helicase Gene AtRH17 Using RNA-Seq Analysis. *Int J Mol Sci, 21*(5).

Shaffer, D., & Rollins, J. A. (2020). Fluorescent Polysome Profiling in Caenorhabditis elegans. *Bio Protoc, 10*(17), e3742.

Shenton, D., Smirnova, J. B., Selley, J. N., Carroll, K., Hubbard, S. J., Pavitt, G. D., . . . Grant, C. M. (2006). Global translational responses to oxidative stress impact upon multiple levels of protein synthesis. *J Biol Chem, 281*(39), 29011-29021.

Spriggs, K. A., Bushell, M., & Willis, A. E. (2010). Translational regulation of gene expression during conditions of cell stress. *Mol Cell, 40*(2), 228-237.

Takahara, T., & Maeda, T. (2012). Transient sequestration of TORC1 into stress granules during heat stress. *Mol Cell, 47*(2), 242-252.

Tauber, D., Tauber, G., Khong, A., Van Treeck, B., Pelletier, J., & Parker, R. (2020). Modulation of RNA Condensation by the DEAD-Box Protein eIF4A. *Cell, 180*(3), 411-426 e416.

Thomas, B. J., & Rothstein, R. (1989). The genetic control of direct-repeat recombination in Saccharomyces: the effect of rad52 and rad1 on mitotic recombination at GAL10, a transcriptionally regulated gene. *Genetics, 123*(4), 725-738.

Tsokanos, F. F., Albert, M. A., Demetriades, C., Spirohn, K., Boutros, M., & Teleman, A. A. (2016). eIF4A inactivates TORC1 in response to amino acid starvation. *Embo J, 35*(10), 1058-1076.

Valasek, L., Szamecz, B., Hinnebusch, A. G., & Nielsen, K. H. (2007). In vivo stabilization of preinitiation complexes by formaldehyde cross-linking. *Methods Enzymol, 429*, 163-183.

Valentini, M., & Linder, P. (2021). Happy Birthday: 30 Years of RNA Helicases. *Methods Mol Biol, 2209*, 17-34.

Wu, C., Amrani, N., Jacobson, A., & Sachs, M. S. (2007). The use of fungal in vitro systems for studying translational regulation. *Methods Enzymol, 429*, 203-225.

Yaffe, M. P., & Schatz, G. (1984). Two nuclear mutations that block mitochondrial protein import in yeast. *Proc Natl Acad Sci U S A, 81*(15), 4819-4823.

Yang, H. S., Jansen, A. P., Komar, A. A., Zheng, X., Merrick, W. C., Costes, S., . . . Colburn, N. H. (2003). The transformation suppressor Pdcd4 is a novel eukaryotic translation initiation factor 4A binding protein that inhibits translation. *Mol Cell Biol, 23*(1), 26-37.

Zwietering, M. H., Jongenburger, I., Rombouts, F. M., & van 't Riet, K. (1990). Modeling of the bacterial growth curve. *Appl Environ Microbiol, 56*(6), 1875-1881.

Tables and Figure Legends

Table 1: Stressors and recommended conditions

Stressor	**Details of treatment**
Rapamycin (TOR inhibition)	200 ng / ml added to (plates or liquid) media
Hydrogen peroxide (oxidative stress)	0.75 mM in (liquid) media. Usage in plates appears to have inconsistent effects. Note that H_2O_2 degrades fairly rapidly, even at 4°C. Consider replacing stock every 2 to 3 months.
Sodium azide (oxidative stress)	0.5% in (liquid) media. Best used for stress granule induction. Usage in plates appears to have inconsistent effects.
Heat shock	Incubate at 42°C if performing an assay such as polysome profiles. Cells will not grow appreciably at that temperature, however. If a survival assay is desired, incubate at 50°C in liquid culture for 1 hour and then spread on plates at 30°C.
Nitrogen withdrawal	Pre-grow cells in minimal media (as in 2.1.ii) until mid-log phase, then switch into a minimal media without ammonium sulfate or any amino acids added.
Glucose withdrawal	Pre-grow cells in minimal media with 2% glucose until mid-log phase, then switch to a minimal media lacking glucose. Low concentrations of glucose (e.g. 0.2%, 0.05%) can also be used.
Stationary phase	Grow cells to mid-log phase. Spin down and resuspend in minimal media to an OD_{600} of 0.2, and grow at 30°C (3 to 14 days).
High salt (osmotic shock)	Add 1 M NaCl to (plates or liquid) media

Table 2: A selection of previously used strains

Strain Name	Genotype	Source
W303	*MATα ade2-1 ura3-1 his3-11,15 leu2-3,112 trp1-1 can1-100*	(Thomas & Rothstein, 1989)
TS161	*MATα ura3-52*	(Takahara & Maeda, 2012)
TS184	*MATα ura3-52 TOR1^{L2134M}*	(Takahara & Maeda, 2012)
TBY52	*MATα ded1::KAN ade2-1 ura3-1 his3-11,15 leu2-3,112 trp1-1 can1-100 +pCEN/LEU2/DED1*	(Aryanpur et al., 2019)
TBY121	*MATα ded1::KAN ade2-1 ura3-1 his3-11,15 leu2-3,112 trp1-1 can1-100 +pCEN/LEU2/ded1-ΔCT*	(Aryanpur et al., 2019)
TBY108	*MATα ded1::KAN ade2-1 ura3-1 his3-11,15 leu2-3,112 trp1-1 can1-100 +pCEN/LEU2/ded1-Δ591-604*	(Aryanpur et al., 2019)
SWY4277	*MATα ded1::KAN ade2-1 ura3-1 his3-11,15 leu2-3,112 trp1-1 can1-100 +pCEN/LEU2/ded1-120*	(Bolger & Wente, 2011)
TBY159	*MATα tif4631::HYG ded1::KAN ade2-1 ura3-1 his3-11,15 leu2-3,112 trp1-1 can1-100 +pCEN/LEU2/DED1*	(Aryanpur et al., 2022)
TBY165	*MATα tif4631::HYG ded1::KAN ade2-1 ura3-1 his3-11,15 leu2-3,112 trp1-1 can1-100 +pCEN/LEU2/ded1-Δ536-604*	(Aryanpur et al., 2022)
TBY118	*MATα ded1::KAN NIP1-PROTA::spHIS5 ade2-1, ura3-1, his3-11,15 leu2-3,112 trp1-1 can1-100 +pCEN/LEU2/DED1*	(Aryanpur et al., 2019)
TBY130	*MATα ded1::KAN NIP1-PROTA::spHIS5 ade2-1 ura3-1 his3-11,15 leu2-3,112 trp1-1 can1-100 +pCEN/LEU2/ded1-ΔCT*	(Aryanpur et al., 2019)

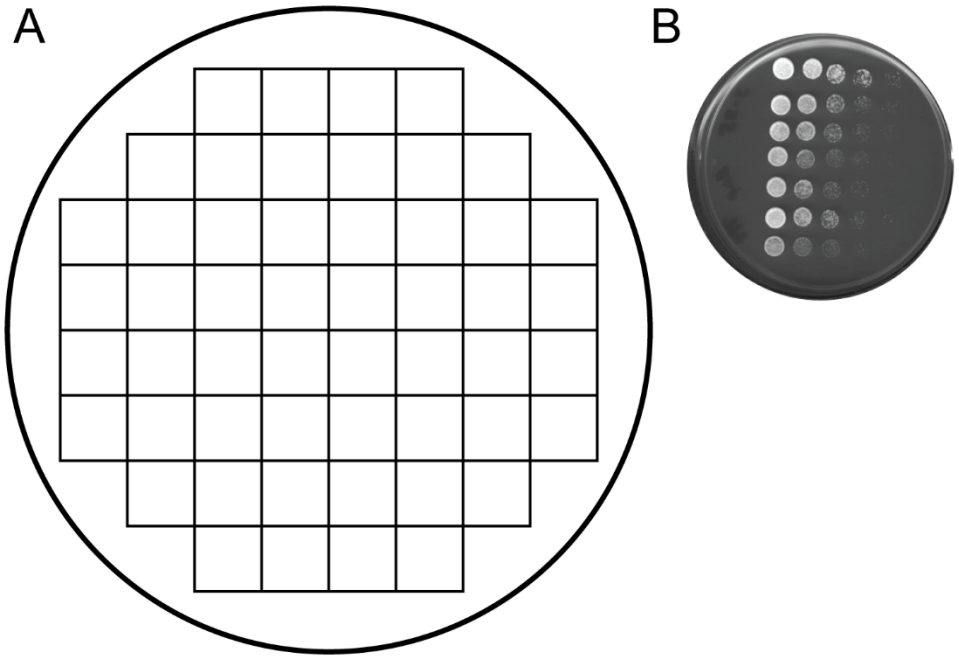

[Please maintain original size of this figure if possible. Part (A) is intended as a template that can be printed out for use in the procotol.]

Figure 1: Spot titer growth analysis. (A) Template for spot titer assay for a standard 10 cm plate (to scale). (B) Example of a spot titer assay result.

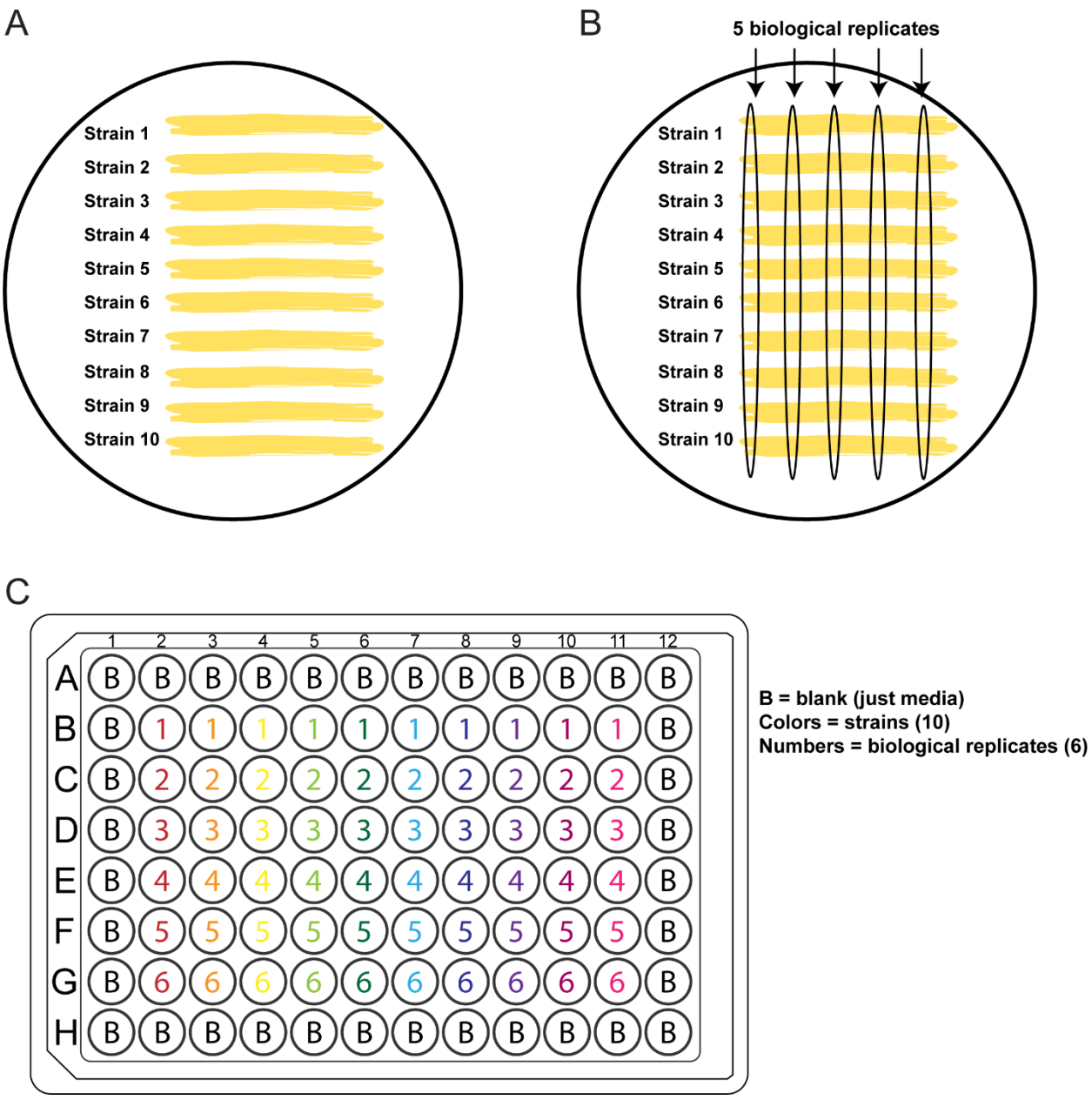

Figure 2: 96-well plate growth analysis. (A) Layout for streaking individual strains ("strain-tracks") onto a standard 10 cm plate for generating growth curves. (B) Diagram for selecting five biological replicates from a "strain-tracks" stock plate. (C) Sample layout for 96-well plate for six biological replicates of 10 strains/conditions. Note that the perimeter is reserved for buffer-only controls to reduce edge effects.

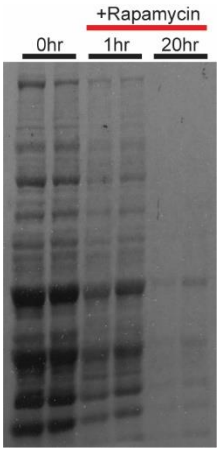

Figure 3: ^{35}S-methionine labeling. Representative ^{35}S-methionine autoradiogram displaying newly translated proteins 0, 1 hr, and 20 hr after treatment with rapamycin. Film exposed for 4.5 days and loaded with 10 µl sample.

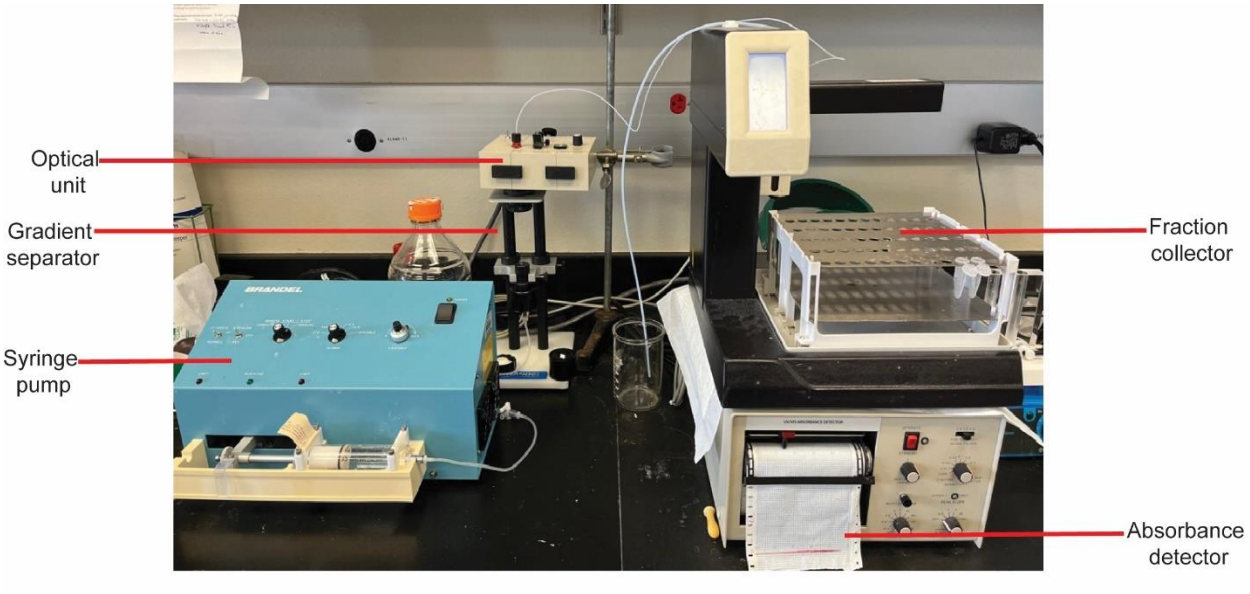

Figure 4: Density gradient fractionation system (Brandel). Major components are labeled. Flow moves from left to right: Fluorinert is pushed from syringe pump through tubing to gradient separator, pushing sample in gradient tube (not shown) up into optical unit of absorbance detector, through tubing to fraction collector, and into 1.5 ml tubes or waste beaker.

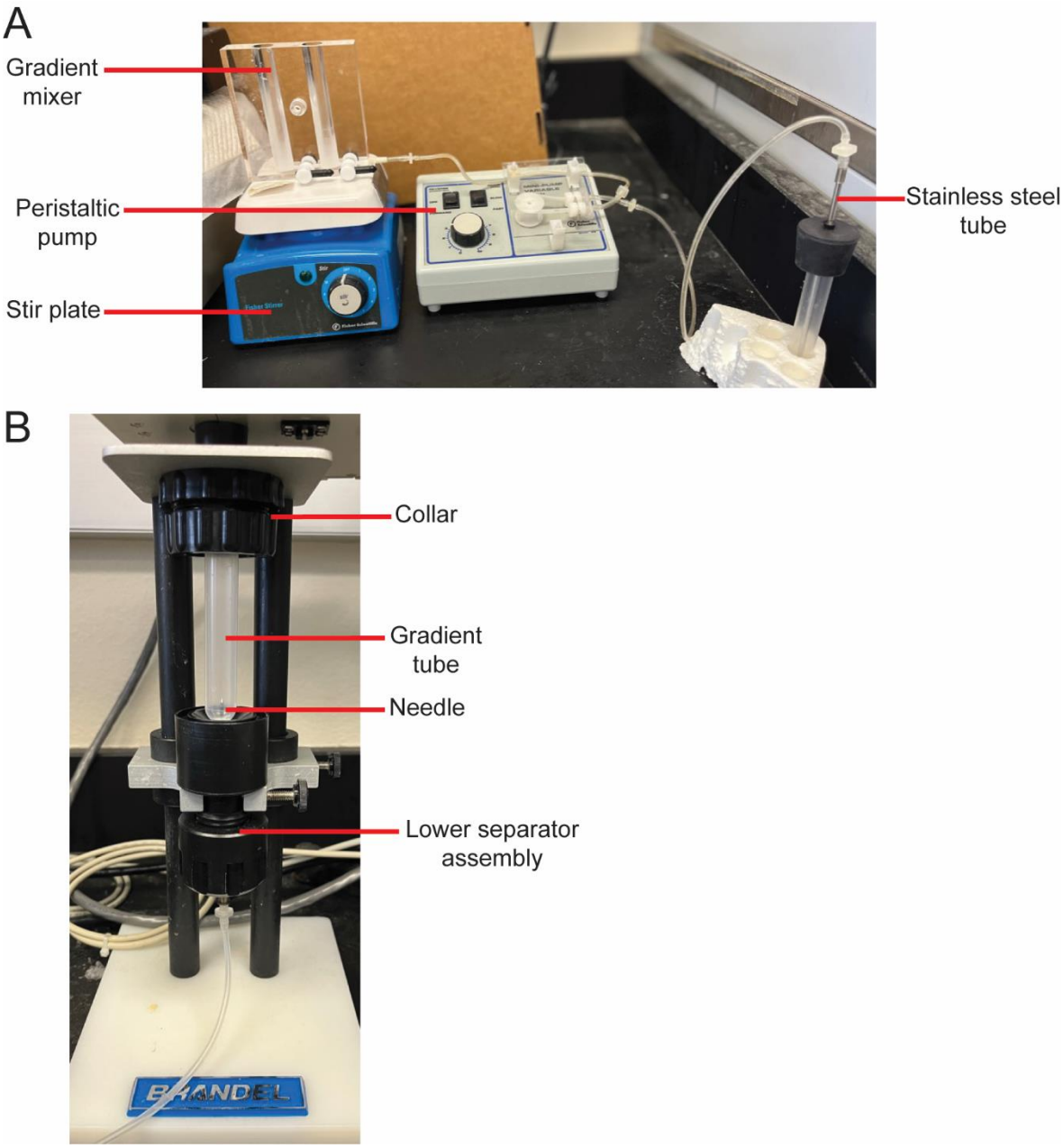

Figure 5: Gradient pouring setup and gradient separator. (A) Setup for pouring gradients with components labeled. Sucrose solutions are added to the mixer; then are pulled into the tubing, through the pump, and out of the stainless steel tube into the gradient tube. (B) Close-up of the gradient separator with gradient tube and other relevant parts labeled.

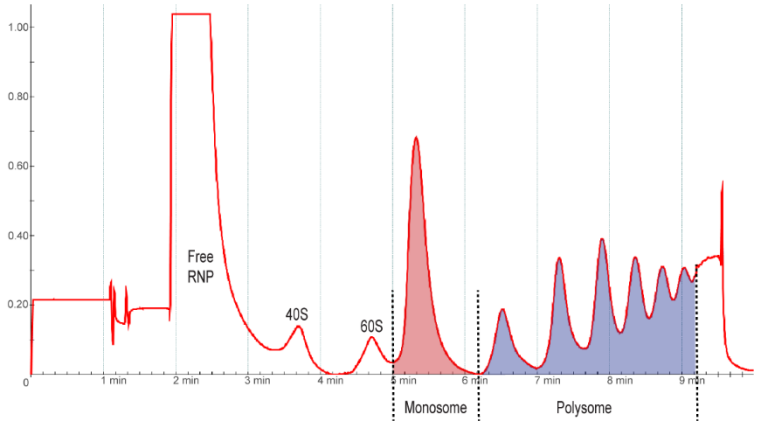

Figure 6: Sample polysome profile. Output absorbance trace from PeakChart showing a sample profile (of unstressed wild-type yeast cells) with peaks for free RNPs, 40S, 60S, monosome (80S), and polysomes labeled. Note that the sample reaches the detector about 2 min after starting the trace, and the bottom of the gradient is reached after slightly more than 9 min. Shaded regions display the area under the curve that would be calculated for the polysome (blue) to monosome (red) ratio. The baseline (see 3.3.ii.5.a) is not specifically labeled since it would overlay the x-axis for this profile.

REFERENCES

1. Henn, A., Bradley, M. J., and De La Cruz, E. M. (2012) ATP Utilization and RNA Conformational Rearrangement by DEAD-Box Proteins. Annu. Rev. Biophys. 41, 247–267
2. Woodson, S. A. (2010) Taming free energy landscapes with RNA chaperones. RNA Biol. 7, 677–686
3. Mitchell, S. F., and Parker, R. (2014) Principles and Properties of Eukaryotic mRNPs. Mol. Cell. 54, 547–558
4. Fairman-Williams, M. E., Guenther, U.-P., Jankowsky, E., Puglisi, J., and Williamson, J. (2010) SF1 and SF2 helicases: family matters This review comes from a themed issue on Nucleic acids Edited. Curr. Opin. Struct. Biol. 20, 313– 324
5. Corbalenya, A. E., and Koonin, E. V (1993) Helicases: amino acid sequence comparisons and structure-function relationships. Curr. Opin. Struct. Biol. 3, 419– 429
6. Singleton, M. R., Dillingham, M. S., and Wigley, D. B. (2007) Structure and Mechanism of Helicases and Nucleic Acid Translocases. Annu. Rev. Biochem. 76, 23–50
7. Linder, P., and Jankowsky, E. (2011) From unwinding to clamping - the DEAD box RNA helicase family. Nat. Rev. Mol. Cell Biol. 12, 505–516
8. Linder, P., and Fuller-Pace, F. V. (2013) Looking back on the birth of DEAD-box RNA helicases. Biochim. Biophys. Acta - Gene Regul. Mech. 1829, 750–755
9. Jarmoskaite, I., and Russell, R. (2011) DEAD-box proteins as RNA helicases and chaperones. Wiley Interdiscip. Rev. RNA. 2, 135–152

10. Gilman, B., Tijerina, P., and Russell, R. (2017) Distinct RNA-unwinding mechanisms of DEAD-box and DEAH-box RNA helicase proteins in remodeling structured RNAs and RNPs. Biochem. Soc. Trans. 45, 1313–1321
11. Henn, A., Bradley, M. J., and De La Cruz, E. M. (2012) ATP Utilization and RNA Conformational Rearrangement by DEAD-Box Proteins. Annu. Rev. Biophys. 41, 247–267
12. Hilbert, M., Karow, A. R., and Klostermeier, D. (2009) The mechanism of ATP-dependent RNA unwinding by DEAD box proteins. Biol. Chem. 390, 1237–1250
13. Liu, F., Putnam, A., and Jankowsky, E. (2008) ATP hydrolysis is required for DEAD-box protein. PNAS. 51, 20209–20214
14. Del Campo, M., and Lambowitz, A. M. (2009) Structure of the Yeast DEAD Box Protein Mss116p Reveals Two Wedges that Crimp RNA. Mol. Cell. 35, 598–609
15. Bono, F., Ebert, J., Lorentzen, E., and Conti, E. (2006) The Crystal Structure of the Exon Junction Complex Reveals How It Maintains a Stable Grip on mRNA. Cell. 126, 713–725
16. Yang, Q., Del Campo, M., Lambowitz, A. M., and Jankowsky, E. (2007) DEAD- Box Proteins Unwind Duplexes by Local Strand Separation. Mol. Cell. 28, 253– 263
17. Horn, M., Collingro, A., Schmitz-Esser, S., Beier, C. L., Purkhold, U., Fartmann, B., Brandt, P., Nyakatura, G., Droege, M., Frishman, D., Rattei, T., Mewes, H. W., and Wagner, M. (2004) Protein Displacement by DExH/D “RNA Helicases” Without Duplex Unwinding. Science. 304, 728–730
18. Sharma, D., and Jankowsky, E. (2014) The Ded1/DDX3 subfamily of DEAD-box RNA helicases. Crit. Rev. Biochem. Mol. Biol. 49, 343–360

19. Foresta, C. (2000) Deletion and expression analysis of AZFa genes on the human Y chromosome revealed a major role for DBY in male infertility. Hum. Mol. Genet. 9, 1161–1169

20. Northcott, P. A., Jones, D. T. W., Kool, M., Robinson, G. W., Gilbertson, R. J., Cho, Y. J., Pomeroy, S. L., Korshunov, A., Lichter, P., Taylor, M. D., and Pfister, S. M. (2012) Medulloblastomics: The end of the beginning. Nat. Rev. Cancer. 12, 818–834

21. Kool, M., Jones, D. T. W., Jäger, N., Northcott, P. A., Pugh, T. J., Hovestadt, V., Piro, R. M., Esparza, L. A., Markant, S. L., Remke, M., Milde, T., Bourdeaut, F., Ryzhova, M., Sturm, D., Pfaff, E., Stark, S., Hutter, S., Sxeker-Cin, H., Johann, P., Bender, S., Schmidt, C., Rausch, T., Shih, D., Reimand, J., Sieber, L., Wittmann, A., Linke, L., Witt, H., Weber, U. D., Zapatka, M., König, R., Beroukhim, R., Bergthold, G., Van Sluis, P., Volckmann, R., Koster, J., Versteeg, R., Schmidt, S., Wolf, S., Lawerenz, C., Bartholomae, C. C., Von Kalle, C., Unterberg, A., Herold- Mende, C., Hofer, S., Kulozik, A. E., Von Deimling, A., Scheurlen, W., Felsberg, J., Reifenberger, G., Hasselblatt, M., Crawford, J. R., Grant, G. A., Jabado, N., Perry, A., Cowdrey, C., Croul, S., Zadeh, G., Korbel, J. O., Doz, F., Delattre, O., Bader, G. D., McCabe, M. G., Collins, V. P., Kieran, M. W., Cho, Y. J., Pomeroy, S. L., Witt, O., Brors, B., Taylor, M. D., Schüller, U., Korshunov, A., Eils, R., Wechsler-Reya, R. J., Lichter, P., and Pfister, S. M. (2014) Genome sequencing of SHH medulloblastoma predicts genotype-related response to smoothened inhibition. Cancer Cell. 25, 393–405

22. He, Y., Zhang, D., Yang, Y., Wang, X., Zhao, X., Zhang, P., Zhu, H., Xu, N., and Liang, S. (2018) A double-edged function of DDX3, as an oncogene or tumor suppressor, in cancer progression (Review). Oncol. Rep. 39, 883–892

23. Chen, H. H., Yu, H. I., Yang, M. H., and Tarn, W. Y. (2018) DDX3 Activates CBC-eIF3–Mediated translation of uORF-containing oncogenic mRNAs to promote metastasis in HNSCC. Cancer Res. 78, 4512–4523

24. Lai, M.-C., Chang, W.-C., Shieh, S.-Y., and Tarn, W.-Y. (2010) DDX3 regulates cell growth through translational control of cyclin E1. Mol. Cell. Biol. 30, 5444–53

25. Shih, J.-W., Wang, W.-T., Tsai, T.-Y., Kuo, C.-Y., Li, H.-K., and Wu Lee, Y.-H. (2012) Critical roles of RNA helicase DDX3 and its interactions with eIF4E/PABP1 in stress granule assembly and stress response. Biochem. J. 441, 119–29

26. Chuang, A. R., Weaver, P. L., Liu, Z., Chang, T.-H., and Chuang, R.-Y. (2012) Requirement of the DEAD-Box Protein Dedi p for Messenger RNA Translation. Science. 275, 1468–1471

27. De, J. J., Cruz, L. A., Iost, I., Kressler, D., and Linder, P. (1997) The p20 and Ded1 proteins have antagonistic roles in eIF4E-dependent translation in Saccharomyces cerevisiae (RNA helicaseDEAD-box familycap-dependent initiationyeast4E-BP). PNAS. 94, 5201–5206

28. Struhl, K. (1985) Nucleotide sequence and transcriptional mapping of the yeast pet56-his3-ded1 gene region. Nucleic Acids Res. 13, 8587–601

29. Gao, Z., Putnam, A. A., Bowers, H. A., Guenther, U. P., Ye, X., Kindsfather, A., Hilliker, A. K., and Jankowsky, E. (2016) Coupling between the DEAD-box RNA helicases Ded1p and eIF4A. Elife. 10.7554/eLife.16408

30. Gupta, N., Lorsch, J. R., and Hinnebusch, A. G. (2018) Yeast Ded1 promotes 48S translation pre-initiation complex assembly in an mRNA-specific and eIF4F- dependent manner. Elife. 10.7554/eLife.38892

31. Yang, Q., and Jankowsky, E. (2005) ATP- and ADP-dependent modulation of RNA unwinding and strand annealing activities by the DEAD-box protein DED1. Biochemistry. 44, 13591–13601

32. Putnam, A. A., and Jankowsky, E. (2013) AMP Sensing by DEAD-Box RNA Helicases. J. Mol. Biol. 425, 3839–3845

33. Sharma, D., Putnam, A. A., and Jankowsky, E. (2017) Biochemical Differences and Similarities between the DEAD-Box Helicase Orthologs DDX3X and Ded1p. J. Mol. Biol. 429, 3730–3742

34. Hilliker, A., Gao, Z., Jankowsky, E., and Parker, R. (2011) The DEAD-Box Protein Ded1 Modulates Translation by the Formation and Resolution of an eIF4F- mRNA Complex. Mol. Cell. 43, 962–972

35. Senissar, M., Le Saux, A., Belgareh-Touze, N., Adam, C. C., Banroques, J., Tanner, N. K., Belgareh-Touzé, N., Adam, C. C., Banroques, J., and Tanner, N. K. (2014) The DEAD-box helicase Ded1 from yeast is an mRNP cap-associated protein that shuttles between the cytoplasm and nucleus. Nucleic Acids Res. 42, 10005–10022

36. Sen, N. D., Zhou, F., Ingolia, N. T., and Hinnebusch, A. G. (2015) Genome-wide analysis of translational efficiency reveals distinct but overlapping functions of yeast DEAD-box RNA helicases Ded1 and eIF4A. Genome Res. 25, 1196–205

37. Guenther, U. P., Weinberg, D. E., Zubradt, M. M., Tedeschi, F. A., Stawicki, B. N., Zagore, L. L., Brar, G. A., Licatalosi, D. D., Bartel, D. P., Weissman, J. S., and Jankowsky, E. (2018) The helicase Ded1p controls use of near-cognate translation initiation codons in 5′ UTRs. Nature. 559, 130–134

38. Sen, N. D., Zhou, F., Harris, M. S., Ingolia, N. T., and Hinnebusch, A. G. (2016) eIF4B stimulates translation of long mRNAs with structured 5′ UTRs and low closed-loop potential but weak dependence on eIF4G. Proc. Natl. Acad. Sci. 113, 10464–10472

39. Beckham, C., Hilliker, A., Cziko, A.-M., Noueiry, A., Ramaswami, M., and Parker, R. (2008) The DEAD-box RNA helicase Ded1p affects and accumulates in Saccharomyces cerevisiae P-bodies. Mol. Biol. Cell. 19, 984–93

40. Firczuk, H., Kannambath, S., Rgen Pahle, J., Claydon, A., Beynon, R., Duncan, J., Westerhoff, H., Mendes, P., and Mccarthy, J. E. (2012) An in vivo control map for the eukaryotic mRNA translation machinery. Mol. Syst. Biol. 9, 635

41. Loewith, R., and Hall, M. N. (2011) Target of rapamycin (TOR) in nutrient signaling and growth control. Genetics. 189, 1177–1201

42. Loewith, R., Jacinto, E., Wullschleger, S., Lorberg, A., Crespo, J. L., Bonenfant, D., Oppliger, W., Jenoe, P., and Hall, M. N. (2002) Two TOR Complexes, Only One of which Is Rapamycin Sensitive, Have Distinct Roles in Cell Growth Control. Mol. Cell. 10, 457–468

43. Heitman, J., Movva, N. R., Hiestand, P. C., and Hall, M. N. (1991) FK 506- binding protein proline rotamase is a target for the immunosuppressive agent FK 506 in Saccharomyces cerevisiae. Proc. Natl. Acad. Sci. U. S. A. 88, 1948–52

44. Urban, J., Soulard, A., Huber, A., Lippman, S., Mukhopadhyay, D., Deloche, O., Wanke, V., Anrather, D., Ammerer, G., Riezman, H., Broach, J. R., De Virgilio, C., Hall, M. N., and Loewith, R. (2007) Sch9 Is a Major Target of TORC1 in Saccharomyces cerevisiae. Mol. Cell. 26, 663–674

45. Huber, A., Bodenmiller, B., Uotila, A., Stahl, M., Wanka, S., Gerrits, B., Aebersold, R., and Loewith, R. (2009) Characterization of the rapamycin-sensitive phosphoproteome reveals that Sch9 is a central coordinator of protein synthesis. Genes Dev. 23, 1929–1943
46. Hardwick, J. S., Kuruvilla, F. G., Tong, J. K., Shamji, A. F., and Schreiber, S. L. (1999) Rapamycin-modulated transcription defines the subset of nutrient-sensitive signaling pathways directly controlled by the Tor proteins. Proc. Natl. Acad. Sci. U. S. A. 96, 14866–70
47. Barbet, N. C., Schneider, U., Helliwell, S. B., Stansfield, I., Tuite, M. F., and Hall, M. N. (1996) TOR controls translation initiation and early G1 progression in yeast. Mol. Biol. Cell. 7, 25–42
48. Hughes Hallett, J. E., Luo, X., and Capaldi, A. P. (2014) State transitions in the TORC1 signaling pathway and information processing in Saccharomyces cerevisiae. Genetics. 198, 773–786
49. Liu, B., and Qian, S. B. (2014) Translational reprogramming in cellular stress response. Wiley Interdiscip. Rev. RNA. 5, 301–305
50. Hinnebusch, A. G. (2005) Translation regulation of GCN4 and the general amino acid control of yeast. Annu. Rev. Microbiol. 59, 407–450
51. Ryoo, H. D., and Vasudevan, D. (2017) Two distinct nodes of translational inhibition in the Integrated Stress Response. BMB Rep. 50, 539–545
52. Pakos-Zebrucka, K., Koryga, I., Mnich, K., Ljujic, M., Samali, A., and Gorman, A. M. (2016) The integrated stress response. EMBO Rep. 17, 1374 LP-1395
53. Simpson, C. E., and Ashe, M. P. (2012) Adaptation to stress in yeast: to translate or not? Biochem. Soc. Trans. 40, 794–799

54. Dever, T. E., Feng, L., Wek, R. C., Cigan, A. M., Donahue, T. F., and Hinnebusch, A. G. (1992) Phosphorylation of initiation factor 2α by protein kinase GCN2 mediates gene-specific translational control of GCN4 in yeast. Cell. 68, 585–596

55. Mueller, P. P., and Hinnebusch, A. G. (1986) Multiple upstream AUG codons mediate translational control of GCN4. Cell. 45, 201–7

56. Hinnebusch, A. G. (1997) Translational regulation of yeast GCN4. A window on factors that control initiator-trna binding to the ribosome. J. Biol. Chem. 272, 21661–4

57. Gonskikh, Y., and Polacek, N. (2017) Alterations of the translation apparatus during aging and stress response. Mech. Ageing Dev. 168, 30–36

58. Cosentino, G. P., Schmelzle, T., Haghighat, A., Helliwell, S. B., Hall, M. N., and Sonenberg, N. (2000) Eap1p, a novel eukaryotic translation initiation factor 4E-associated protein in Saccharomyces cerevisiae. Mol. Cell. Biol. 20, 4604–13

59. Arndt, N., Ross-Kaschitza, D., Kojukhov, A., Komar, A. A., and Altmann, M. (2018) Properties of the ternary complex formed by yeast eIF4E, p20 and mRNA. Sci. Rep. 8, 6707

60. Aryanpur, P. P., D. M. Renner, E. Rodela, T. M. Mittelmeier, A. Byrd, and T. A. Bolger, "The DEAD-box RNA helicase Ded1 has a role in the translational response to TORC1 inhibition.", Mol Biol Cell, vol. 30, issue 17, pp. 2171-2184, 2019 08 01

61. Sengoku, T., Nureki, O., Nakamura, A., Kobayashi, S., and Yokoyama, S. (2006) Structural Basis for RNA Unwinding by the DEAD-Box Protein Drosophila Vasa. Cell. 125, 287–300.

62. Bishop, Anthony C.; Ubersax, Jeffrey A.; Petsch, Dejah T.; Matheos, Dina P.; Gray, Nathanael S.; Blethrow, Justin; Shimizu, Eiji; Tsien, Joe Z.; Schultz, Peter G.; Rose,

Mark D.; Wood, John L. (September 2000). "A chemical switch for inhibitor-sensitive alleles of any protein kinase". Nature. 407 (6802): 395–401

63. Murray, A. & Hunt, T. (1993) *The Cell Cycle* (Oxford Univ. Press, New York).

64. De Souza CP, Osmani SA (September 2007). "Mitosis, not just open or closed". *Eukaryotic Cell*. **6** (9): 1521–7.

65. Wenzel ES, Singh ATK. *Cell-cycle Checkpoints and Aneuploidy on the Path to Cancer*. In Vivo. 2018 Jan-Feb;32(1):1-5.

66. Baserga R (2008). *"Biochemistry of the Cell Cycle: A Review"*. *Cell Proliferation*. ***1*** *(2): 167–191*D

67. Wei W, Nurse P, Broek D. *Yeast cells can enter a quiescent state through G1, S, G2 or M phase of the cell cycle*. Cancer Res. 1993 Apr 15;53(8):1867-70

68. Rodgers JT, King KY, Brett JO, Cromie MJ, Charville GW, Maguire KK, Brunson C, Mastey N, Liu L, Tsai CR, Goodell MA, Rando TA (June 2014). "mTORC1 controls the adaptive transition of quiescent stem cells from G0 to G(Alert)". *Nature*. **510** (7505): 393–6.

69. Gupta N, Lorsch JR, Hinnebusch AG. Yeast Ded1 promotes 48S translation pre-initiation complex assembly in an mRNA-specific and eIF4F-dependent manner. Elife. 2018 Oct 3;7:e38892. doi: 10.7554/eLife.38892. PMID: 30281017; PMCID: PMC6181565.

70. Suna Gulay, Neha Gupta, Jon R Lorsch, Alan G Hinnebusch (2020) Distinct interactions of eIF4A and eIF4E with RNA helicase Ded1 stimulate translation in vivo eLife 9:e58243

71. Aryanpur PP, Mittelmeier TM, Bolger TA. The RNA Helicase Ded1 Regulates Translation and Granule Formation during Multiple Phases of Cellular Stress Responses.

Mol Cell Biol. 2022 Jan 20;42(1):e0024421. doi: 10.1128/MCB.00244-21. Epub 2021 Nov 1. PMID: 34723653; PMCID: PMC8773058.

72. Wei W, Nurse P, Broek D. Yeast cells can enter a quiescent state through G1, S, G2, or M phase of the cell cycle. Cancer Res. 1993 Apr 15;53(8):1867-70. PMID: 8467507.